Copyright Warning & Restrictions

The copyright law of the United States (Title 17, United States Code) governs the making of photocopies or other reproductions of copyrighted material.

Under certain conditions specified in the law, libraries and archives are authorized to furnish a photocopy or other reproduction. One of these specified conditions is that the photocopy or reproduction is not to be "used for any purpose other than private study, scholarship, or research." If a, user makes a request for, or later uses, a photocopy or reproduction for purposes in excess of "fair use" that user may be liable for copyright infringement,

This institution reserves the right to refuse to accept a copying order if, in its judgment, fulfillment of the order would involve violation of copyright law.

Please Note: The author retains the copyright while the New Jersey Institute of Technology reserves the right to distribute this thesis or dissertation

Printing note: If you do not wish to print this page, then select "Pages from: first page # to: last page #" on the print dialog screen

CONSTITUTIVE MODELING OF GLASSY SHAPE MEMORY POLYMERS

by

Mahesh Khanolkar

The aim of this research is to develop constitutive models for non-linear materials. Here, issues related for developing constitutive model for glassy shape memory polymers are addressed in detail. Shape memory polymers are novel material that can be easily formed into complex shapes, retaining memory of their original shape even after undergoing large deformations. The temporary shape is stable and return to the original shape is triggered by a suitable mechanism such heating the polymer above a transition temperature. Glassy shape memory polymers are called glassy because the temporary shape is fixed by the formation of a glassy solid, while return to the original shape is due to the melting of this glassy phase.

The constitutive model has been developed to capture the thermo-mechanical behavior of glassy shape memory polymers using elements of nonlinear mechanics and polymer physics. The key feature of this framework is that a body can exist stress free in numerous natural configurations, the underlying natural configuration of the body changing during the process, with the response of the body being elastic from these evolving natural configurations. The aim of this research is to formulate a constitutive model for glassy shape memory polymers (GSMP) which takes in to account the fact that the stress-strain response depends on thermal expansion of polymers. The model developed is for the original amorphous phase, the temporary glassy phase and transition between these phases. The glass transition process has been modeled using a framework that was developed recently for studying crystallization in polymers and is based on the

theory of multiple natural configurations. Using the same frame work, the melting of the glassy phase to capture the return of the polymer to its original shape is also modeled. The effect of nanoreinforcement on the response of shape memory polymers (GSMP) is studied and a model is developed. In addition to modeling and solving boundary value problems for GSMP's, problems of importance for CSMP, specifically a shape memory cycle (Torsion of a Cylinder) is solved using the developed crystallizable shape memory polymer model. To solve complex boundary value problems in realistic geometries a user material subroutine (UMAT) for GSMP model has been developed for use in conjunction with the commercial finite element software ABAQUS. The accuracy of the UMAT has been verified by testing it against problems for which the results are known.

CONSTITUTIVE MODELING OF GLASSY SHAPE MEMORY POLYMERS

by

Mahesh Khanolkar

A Dissertation
Submitted to the Faculty of
New Jersey Institute of Technology
in Partial Fulfillment of the Requirements for the Degree of
Doctor of Philosophy in Mechanical Engineering

Department of Mechanical Engineering

May 2010

APPROVAL PAGE

CONSTITUTIVE MODELING OF GLASSY SHAPE MEMORY POLYMERS

Mahesh Khanolkar

Dr. I. J. Rao, Dissertation Advisor — Date
Associate Professor of Mechanical & Industrial Engineering, NJIT

Dr. Rajpal S. Sodhi, Committee Member — Date
Professor of Mechanical & Industrial Engineering, NJIT

Dr. Zhiming Ji, Committee Member — Date
Associate Professor of Mechanical & Industrial Engineering, NJIT

Dr. Bernard Koplik, Committee Member — Date
Professor of Mechanical & Industrial Engineering, NJIT

Dr. Thomas Juliano, Committee Member — Date
Associate Professor of Engineering Technology, NJIT

BIOGRAPHICAL SKETCH

Author: Mahesh Khanolkar

Degree: Doctor of Philosophy

Date: May 2010

Undergraduate and Graduate Education:

- Doctor of Philosophy in Mechanical Engineering,
  New Jersey Institute of Technology, Newark, NJ, 2010
- Master of Science in Mechanical Engineering,
  New Jersey Institute of Technology, Newark, NJ, 2003
- Bachelor of Science in Mechanical Engineering,
  Karnataka University, India, 2000

Major: Mechanical Engineering

Publications and Presentations:

Mahesh Khanolkar and I. J. Rao
"Modeling of glassy Shape Memory Polymers", in preparation.

Mahesh Khanolkar and I. J. Rao
"Application of the Constitutive Model for Crystallizable Shape Memory Polymers: Torsion of a cylinder", Submitted.

Mahesh Khanolkar, Jaskirat Sodhi and I. J. Rao
"Shape Memory Polymers: Modeling and Mechanics," *The Dana Knox Student Research Showcase* New Jersey Institute of Technology, April 2009.

Mahesh Khanolkar, G. Barot and I. J. Rao
"Constitutive Modeling and Simulation of Shape Memory Polymers, Society of Engineering Science 2008," *45th Annual Technical Meeting University of Illinois at Urbana-Champaign.*

To,

Dr. I.J Rao, Dr. Rajpal Sodhi, Dr. Gautam Barot & Mr. Amit Khanolkar

"Who has first thought of the task and wished for successful completion before it started"

My parents: Mr. Anant Khanolkar and Mrs. Snehal Khanolkar

"For their love, support and encouragement"

ACKNOWLEDGMENT

The completion of my dissertation and subsequent Ph.D has been a long journey. I could not have succeeded without the invaluable support of several people. To start with, I would like to express my deepest gratitude to Dr. I Joga Rao and his family, who not only served as my research advisor, providing valuable and countless resources, but also constantly gave me support, encouragement, and reassurance. It has been my privilege to benefit from his patience, kindness and a genuine interest in my welfare.

Special thanks are given to Dr. Rajpal Sodhi, Dr. Bernard Koplik, Dr. Zhiming Ji, Dr. Thomas Juliano and Dr. Gautam Barot for taking interest in my research, contributing to its success and actively participating in my committee.

My gratitude is also extended to Ms. Clarisa Gonzalez-Lenahan who has known the answer to every question regarding the details of the language and structure of the dissertation write up. I am also thankful to the staff of mechanical engineering department for helping me out in various activities for GAMES and other clerical works.

My heartfelt thanks extend to my colleagues: Jaskirat Sodhi, Sai Chaitanya Nudurpati, Mansoor Muhammud Janjua, and Bhavin Dalaal for providing numerous technical and computing help. My friends Anupam Makhija, Kalpesh Patel, Abhishek Jaintilal Rana, Arvind Ramanujam, Mathew Jacob and Shubhadeep Mukherji have played a very important role in my life. They have been a constant source of encouragement and I have learnt a lot from interacting with them. We have lived together or studied together and experienced the various trials and tribulations of graduate life and/or international student life. They all have been great source of emotional support throughout my journey

TABLE OF CONTENTS

TABLE OF CONTENTS
(Continued)

TABLE OF CONTENTS
(Continued)

LIST OF TABLES

LIST OF FIGURES

LIST OF FIGURES
(Continued)

LIST OF FIGURES
(Continued)

CHAPTER 1

INTRODUCTION

1.1 Motivation & Research Objective

Since the inception of shape memory polymers as smart, active materials most of the research been done is experimental. Relatively little work has addressed the constitutive modeling of the unique thermomechanical coupling in SMP's. Constitutive models are critical for predicting the deformation and recovery of SMP's under a range of different constraints. Rao et al. 2006 have developed a model for the thermo mechanics and phase change occurring in crystallizable shape memory polymers (CSMP). The model developed was for large deformations and is based on the theory of evolving natural configurations. The key feature of this framework is that a body can exist stress free in numerous natural configurations, the underlying natural configuration of the body changing during the process, with the response of the body being elastic from these evolving natural configurations.

The aim of this research is to formulate a constitutive model for glassy shape memory polymers (GSMP) which takes in to account the fact that the stress-strain response depends on thermal expansion of polymers. A framework within the context of continuum mechanics to predict the glass transition of shape memory polymer is presented. The model captures the amorphous rubbery phase, the cooling process, the shape fixity and melting to return to its original shape. The effect of nanoreinforcement on the response of shape memory polymers (GSMP) is studied and a model is developed. In addition to modeling and solving boundary value problems for GSMP's we also solve

problems of importance for CSMP specifically a shape memory cycle (Torsion of a Cylinder) is solved using the crystallizable shape memory polymer model.

1.2 Introduction to Shape Memory Polymers

A polymer is a large molecule (macromolecule) composed of repeating structural units typically connected by covalent chemical bonds. While polymer in popular usage suggests plastic, the term actually refers to a large class of natural and synthetic materials with a variety of properties. Due to the extraordinary range of properties accessible in polymeric materials [1], they have come to play an essential and ubiquitous role in everyday life [2] from plastics and elastomers on the one hand to natural biopolymers such as DNA and proteins that are essential for life on the other.

A simple example is polyethylene, whose repeating unit is based on ethylene (IUPAC name ethene) monomer. Most commonly, as in this example, the continuously linked backbone of a polymer used for the preparation of plastics consists mainly of carbon atoms. However, other structures do exist; for example, elements such as silicon form familiar materials such as silicones, examples being silly putty and waterproof plumbing sealant. The backbone of DNA is in fact based on a phosphodiester bond, and repeating units of polysaccharides (e.g. cellulose) are joined together by glycosidic bonds via oxygen atoms.

Natural polymeric materials such as shellac, amber, and natural rubber have been in use for centuries. Biopolymers such as proteins and nucleic acids play crucial roles in biological processes. A variety of other natural polymers exist, such as cellulose, which is the main constituent of wood and paper. The list of synthetic polymers includes synthetic

rubber, Bakelite, neoprene, nylon, PVC, polystyrene, polyethylene, polypropylene, polyacrylonitrile, PVB, silicone, and many more. Polymers are studied in the fields of polymer chemistry, polymer physics, and polymer science.

SMP's belong to a large family of shape memory materials which are defined by their capacity to store a deformed (temporary) shape and recover an original (parent) shape [3]. Shape memory materials have the ability to change size and shape in response to changes in temperature, moisture, pH, or electric and magnetic fields; and for SMP's it is temperature. Using a temperature-dependent process, these polymers can be deformed into any shape, and when stimulated, regain a previously memorized shape to achieve its function. These materials have variable structure or composition depending on the application.

A polymer engineered with shape memory characteristics provides a unique set of material qualities and capabilities that enhance the traits inherent in the polymer system itself. SMP changes between rigid and elastic states by way of thermal stimuli. The change takes place at what is referred to as the glass transition temperature (T_g). SMP can be formulated with a T_g that matches an application need. Current SMP systems have been demonstrated with T_gs from –30 °C to 260 °C (–20 °F to 500 °F).

SMP materials have several advantages over alternative active materials such as shape memory alloys (SMAs). The low density of shape memory polymers is a benefit for lightweight structural applications. Another advantage is their controllable activation temperature that is linked to the glass transition temperature and can be manipulated by changing the co-polymer composition or the degree of cross-linking.

1.3 Thermo Responsive Shape Memory Polymers

Thermo responsive shape memory material can be classified in to two groups: shape memory alloys and shape memory polymers. The mechanism of memory function of shape memory alloys (SMAs) is based on the rearrangement of the position of the atoms within the crystal lattice of the metal.

As shown in Figure 1.1, below the transition temperature, SMA is in the *martensite state*, in which the molecular structure is soft and can be easily deformed into various shapes. To revert back to its original shape, the alloy must be held in position and heated up. The heat transferred to the alloy allows it to arrange the atoms into the most compact and regular lattice pattern, resulting in a rigid cubic arrangement known as the *austenite phase*. The cubic austenite phase is the same size and shape as the undeformed martensite phase on a macroscopic scale, so that no change in size or shape is visible in shape memory alloys during cooling and heating until the martensite is deformed. SMA can exert tremendous force during their transformation usually exceeding 400 MPa against a resistance. This attribute makes SMA suitable for military, medical, safety, and robotics applications. However, the high cost, poor fatigue properties, and low recoverable tensile strain of SMAs, in the order of 10%, limit their applications, especially where large deformation is encountered. SMP's on the other hand withstand large deformation making them more flexible.

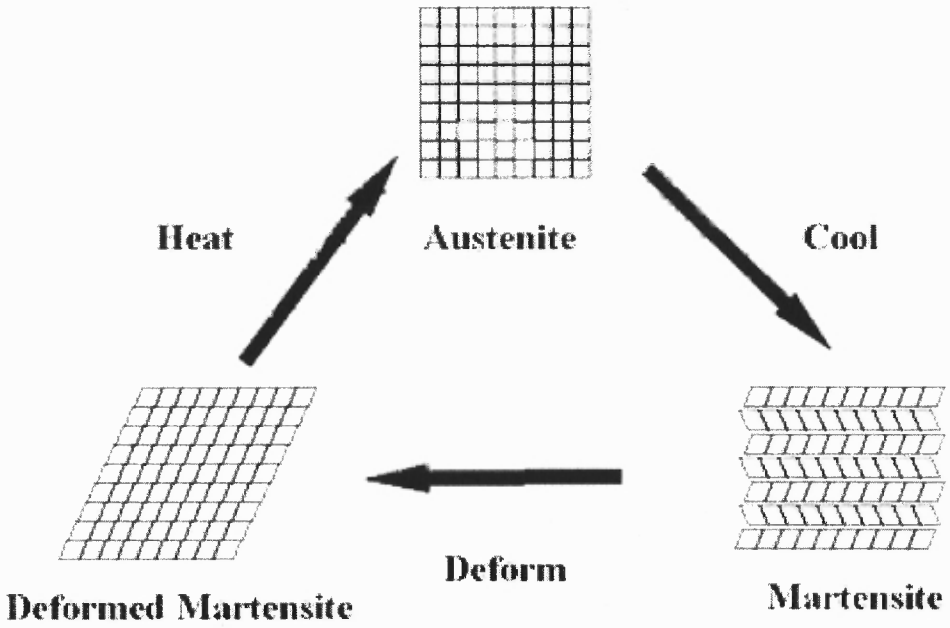

Figure 1.1 Schematic representation of the mechanism of the shape memory effect for metallic alloys based on a martensitic phase transformation.

Source: www.mrsec.wisc.edu/.../memmetal/index.html

1.4 Physical Process (Shape Memory Cycle)

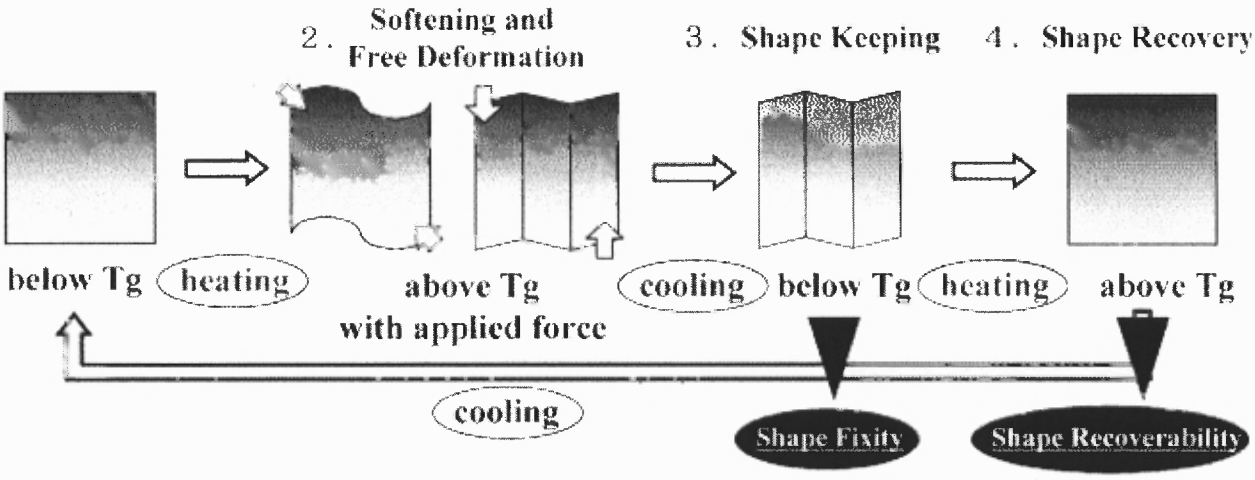

Figure 1.2 Typical shape memory polymer cycle.

Source: Takeru Ohki, Qing-Qing Ni, Norihito Ohsako and Masaharu Iwamoto "Mechanical and shape memory behavior of composites with shape memory polymer Composites" Part A: Applied Science and Manufacturing Volume 35, Issue 9, September 2004, Pages 1065-1073.

Traditionally, a shape recovery thermo-mechanical cycle for SMP [4] material consists of the following steps:

1. Deform the polymer at a temperature above the glass transition temperature, T_g.
2. Fix the deformed polymer shape and cool below T_g.
3. Upon the completion of cooling, remove the constraint from the polymer.
4. Heat the polymer above T_g to recover original shape.

The polymer must first be processed (molded and cured) to the desired shape. In Step 1, the as-processed material is deformed at a temperature above T_g. In Step 2, the polymer is held in its final deformed shape and cooled below T_g. Removal of the constraint required to bend the polymer at the higher temperature is performed in Step 3. Generally, the polymer can hold the deformed shape in Step 3 indefinitely, until recovery

is necessary. In Step 4, the polymer is heated above T_g to recover the original undeformed as-processed shape.

1.5 Illustration of Shape Memory Effect in Crystallizable/Glassy Shape Memory Polymers

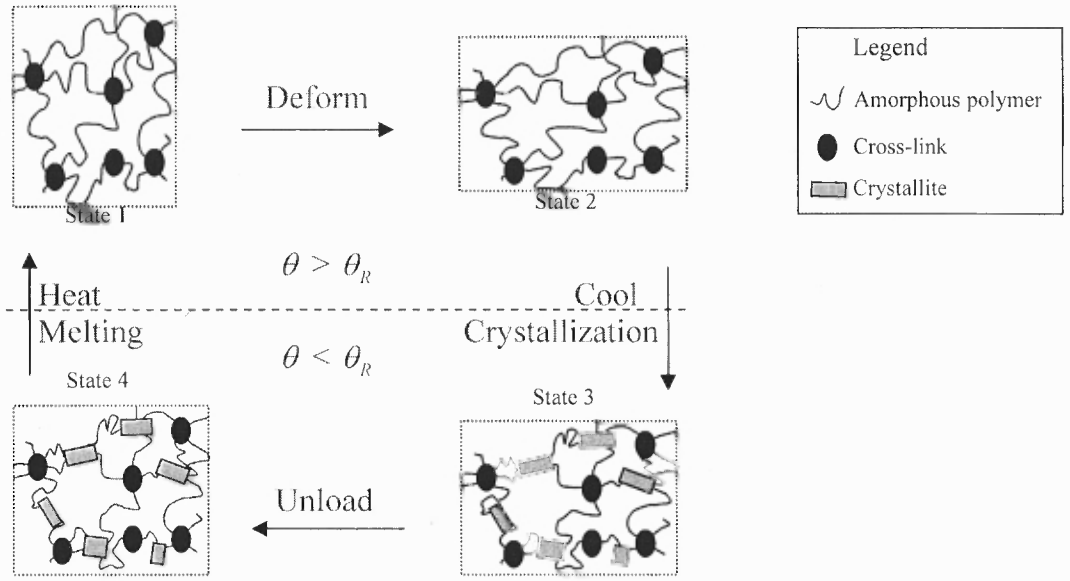

Figure 1.3 Schematic illustration of the shape memory effect in crystallizable shape memory polymers.

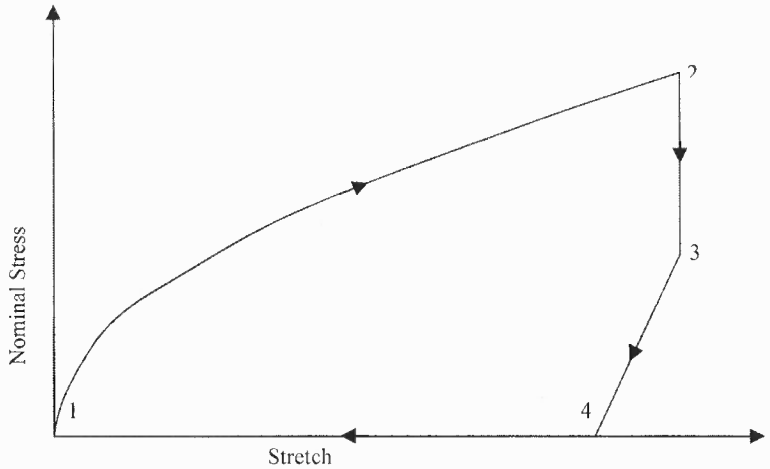

Figure 1.4 Typical stress versus strain curve for crystallizable shape memory polymer.

Figure 1.3 shows a schematic illustration of the shape memory effect in Crystallizable Shape Memory polymers [4,5]. Crystallizable shape memory polymers can be either thermosets or thermoplastics. Thermoplastic crystallizable shape memory polymers are block copolymers consisting of alternating chains of two different polymers (A and B) linked end to end. The polymers A and B are chosen so that the copolymer exhibits shape memory behavior. One of the constituent polymers, say A, is chosen to have a high melting or glass transition temperature, which is denoted by θ_h while the other polymer, represented by B, has a lower melting temperature, which for reasons to be made apparent shortly, by θ_R (for recovery temperature). When the polymer is cooled from a melt like state the polymer with the higher melting / glass transition temperature, here polymer A, solidifies first forming segregated hard domains. These hard domains are linked together by polymer B, which crystallizes at a lower temperature (θ_R). *Between these two temperatures ($\theta_R < \theta < \theta_h$) the materials behavior is rubber-like, with the hard domains acting as cross-links due to which the polymer returns to its original shape even after undergoing large deformations.* If the polymer is cooled below θ_R, polymer B *partially crystallizes* and the material stiffens, losing its rubber like behavior. If the material is cooled while it is in a deformed configuration, polymer B crystallizes in this deformed configuration, and these newly formed crystallites act as temporary cross-links which prevent the shape memory polymer from returning to its original shape. On unloading the specimen below θ_R a small amount of recovery is observed as the polymer has its original cross-links still in place. On subsequent heating above θ_R the crystalline phase associated polymer B melts and the shape memory polymer returns to its original

shape. On further heating above θ_R the hard domains also melt and the material returns to the melt-like state.

Thermoset shape memory polymers also show similar behavior, except the permanent shape is a result of chemically cross-linking a crystallizable polymer and not due to the presence of hard domains. Vulcanization of rubber is a common example of such a process, wherein the introduced Sulphur reacts with natural rubber forming a network structure. Above the melting temperature of the polymer, which is again denoted by θ_R, the SMP has a rubber like behavior due to the presence of chemical cross-links, however upon cooling below θ_R, polymer crystallization takes place. These newly formed crystals act to stiffen the SMP with the crystallites acting as cross-links. If the polymer is deformed prior to cooling, the crystallites, which act as temporary cross-links are formed in the deformed configuration and as a result the polymer retains its transient shape. The original shape is recovered on heating above the melting temperature. The behavior of these two types of SMPs, i.e., thermosets and thermoplastic SMPs is hence, very similar.

In Figure 1.3, the filled circles represent the cross-links (they could be the hard domains or chemical cross-links), the wavy line connecting the cross-links represents the crystallizable polymer in its amorphous state while the rectangular blocks represent the crystallizable polymer in a crystalline state. State 1 in both figures denotes the undeformed configuration. Above the recovery temperature θ_R the polymers behavior is rubber-like and its elastic behavior is driven by changes in entropy. On deforming above θ_R, the polymer molecules between the cross-links stretch (state 2). If the polymer is now cooled to a temperature below θ_R, crystallization takes place and the crystals are formed

in this deformed configuration. The onset of crystallization is accompanied by a sharp drop in the stress (from state 2 to state 3). *After unloading (state 3 to state 4) the polymer remains in a deformed configuration with a small amount of recovery. This recovery is due to the presence of two components (amorphous and crystalline) each with their own stress-free states.* The amorphous part has a tendency to retract to its original configuration while the crystalline part prefers the deformed configuration. As the crystalline part is a lot stiffer, the recovery strain is small (see Figure 1.4). The mechanical response of the polymer in this state is similar to that of a semi-crystalline polymer with oriented crystallites, i.e., it is relatively stiff and the mechanical behavior is anisotropic. Usually when this semi-crystalline polymer is subject to small deformations it exhibits elastic behavior, energetic in origin. If however, the polymer is subject to large deformations, inelastic behavior caused by reorientation of the crystallites and secondary crystallization takes place. During these inelastic processes degradation of the original cross-links can occur reducing the ability of the polymer to return to its original shape on heating. When the polymer is heated to above θ_R, (from state 4 to state 1) the crystallites melt returning to their original amorphous state, if the cross-links originally present in the polymer remain the polymer retracts to its original shape. This retractive force depends on the extent to which the polymer was deformed prior to cooling and is an important parameter when shape memory polymers are used in actuators.

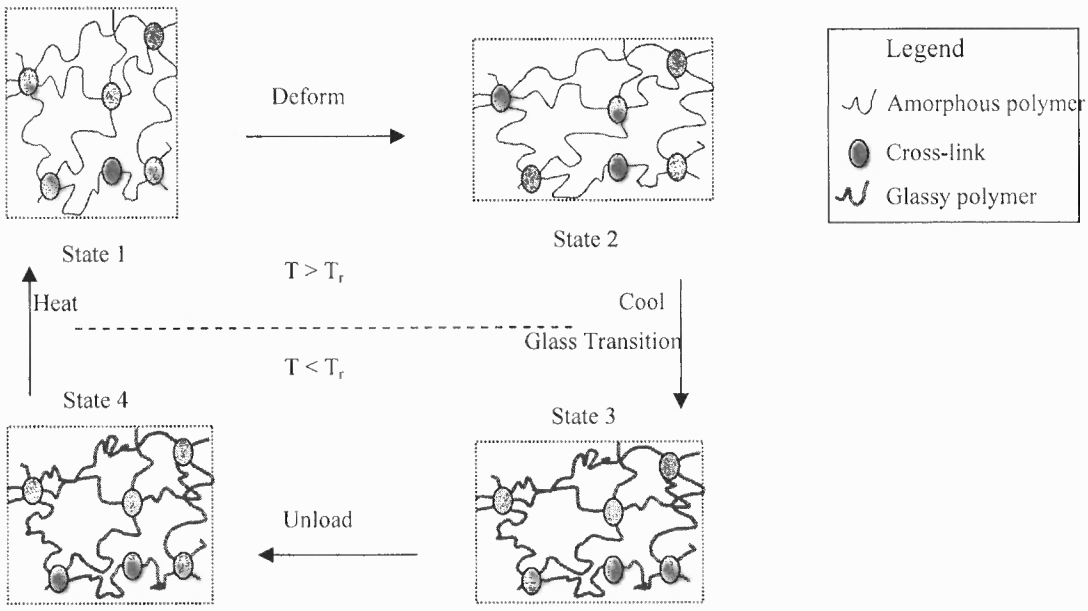

Figure 1.5 Schematic illustration of the shape memory effect in glassy shape memory polymers.

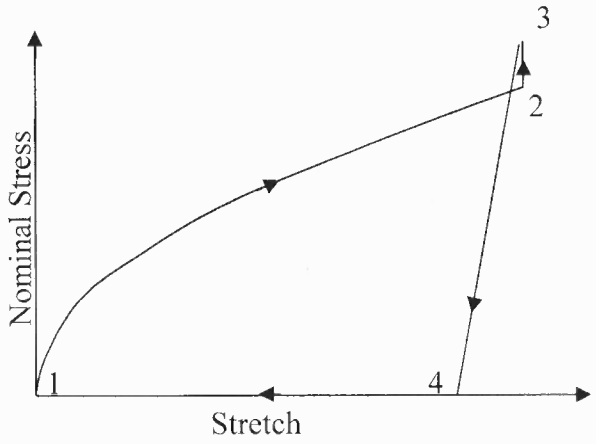

Figure 1.6 Typical stress versus strain curve for glassy shape memory polymer.

Glassy shape memory polymers are mostly thermoset and the cycle is analogus to crystallizable SMP's. Thus the temporary shape is due to the chemical crosslinks. After cooling below the glass transition temperature a glassy or amorphous solid is formed. Since the amorphous solid is formed in a stressed state the stress increases (Figure 1.6) [3]. Upon unloading the temporary shape is fixed and heating above the glass transition temperature takes the SMP to its original shape.

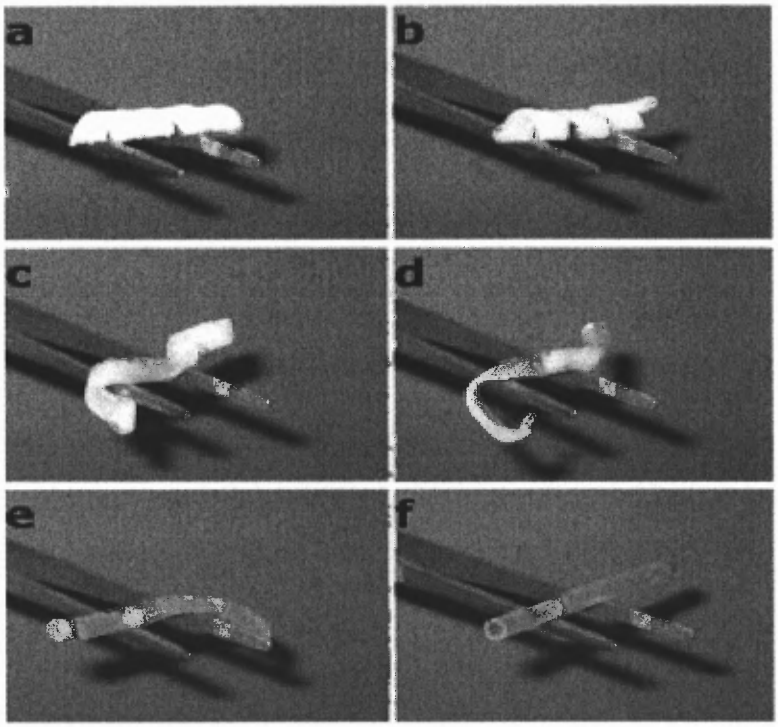

Figure 1.7 Time series photographs that show the recovery of a shape-memory tube. (a)-(f) Start to finish of the process takes a total of 10 s at 50°C.

Source: Marc Behl and Andreas Lendlein " Shape-memory polymers" Materials Today, Volume 10, Issue 4, April 2007, Pages 20-28.

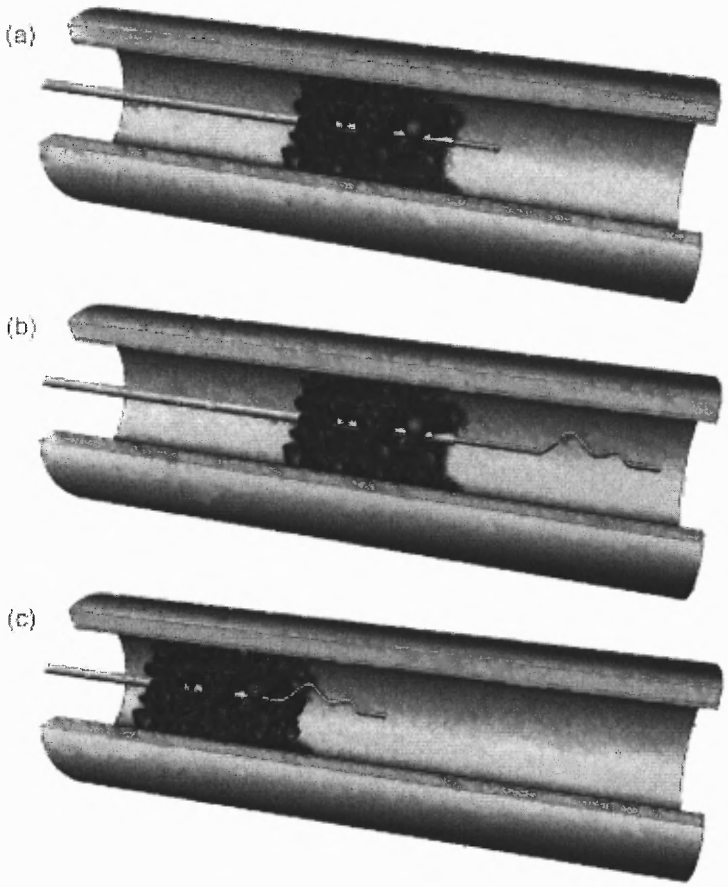

Figure 1.8 Removing a blood clot with SMP- the delivery of an shape-memory-polymer corkscrew device to remove a blood clot occurs in three distinct phases. (a) In its secondary straight shape, the device is delivered through a catheter to pierce the clot. (b) The device is then heated with a diode laser, transforming it back to its primary corkscrew shape. (c) Finally, the device captures and removes the clot as it is retracted.

Source: https://www.llnl.gov/str/MayJune08/maitland.html

1.6 Classification of Shape Memory Polymers

SMP's are classified in to Crystallizable SMP's and Glassy SMP's. In Crystallizable SMP's entanglement of the molecules or crosslink's are used to remember the permanent shape and the formation of the crystalline phase is used to retain the transient shape with the polymer returning to its original shape on melting of the crystalline phase [5]. On the other hand Glassy SMP's are characterized by the presence of polymer segments that undergo glass transition [3]. The present study will focus mainly on glassy SMP's.

Glassy SMP's are classified as Thermoplastics, Elastomers and Thermosets. Thermosets which are heavy cross linked polymers are studied here. Thermoset glassy SMP's have glass transition above room temperature and cannot melt of flow upon heating (they decompose at high temperature). Thus only the glass transition needs to be considered during the thermomechanical cycle. The rubbery elasticity, glass transition viscoelasticity and yield phenomena in the glassy state of amorphous polymers will be considered.

The properties of a polymer near T_g account for the shape memory behavior during a thermo mechanical cycle. At temperatures well below T_g the polymer is in the glassy state and behaves as elastic solid at small strains. The low temperature elasticity is due to primary bond stretching, which causes a change in internal energy. At temperatures above T_g the polymer is in rubbery state. The stiffness of the polymer is low and the deformation energy is converted in conformational entropy change. In both the glassy and rubbery state, the energy can be stored instantaneously and released instantaneously upon removal of the applied strain and stress.

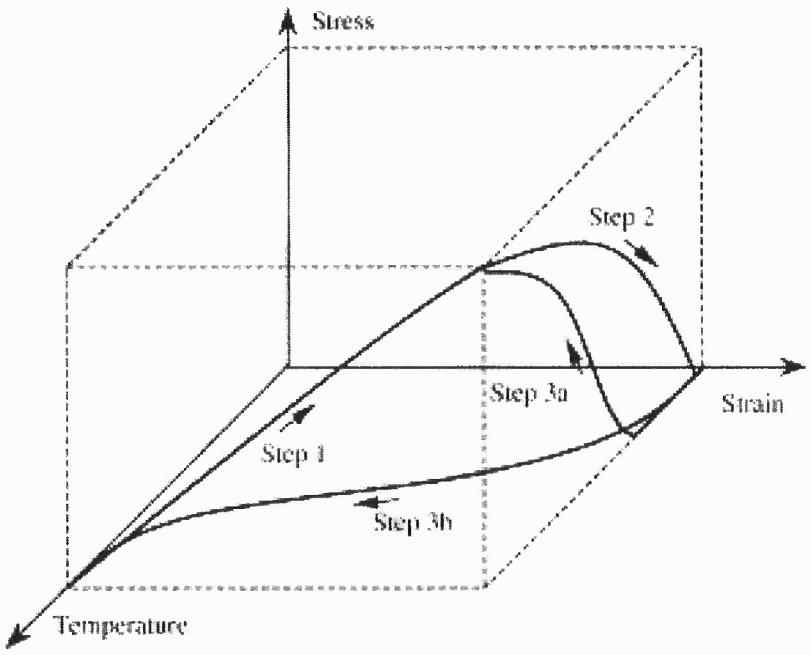

Figure 1.9 Schematic of the stress–strain–temperature behavior during typical thermo mechanical cycle in flexure.

Source: Y Liu, K Gall, ML Dunn, P McCluskey "Thermomechanical recovery couplings of shape memory polymers in flexure" Smart materials and structures, 2003

A typical pre-deformation and recovery cycle for SMPs in three-point flexure loading can be described in three steps (Figure 1.7) [6]. To start the thermo mechanical cycle, the SMP is heated to an elevated temperature near T_g. The first step of the cycle (Step 1) involves a high-strain deformation to a desired shape. The second step (Step 2) is a constraining procedure whereby the SMP is cooled while maintaining the fixed shape. The stress needed to maintain the shape gradually diminishes as the temperature decreases. At a lower temperature, SMP chain segments are frozen in a temporary position by thermally reversible interactions between the molecular chains. At this point, the constraint is removed and the induced shape is fully retained. In the final step, the SMP is subjected to a prescribed constraint level and heated towards T_g. The two limiting cases of constraint are constrained recovery and unconstrained recovery. Constrained

recovery implies the fixing of the pre-deformation strain and the generation of a gradually increasing recovery stress (Step 3a). Unconstrained recovery implies the absence of external stresses and the free recovery of the induced strain (Step 3b). With the increase of temperature, the strain is gradually recovered.

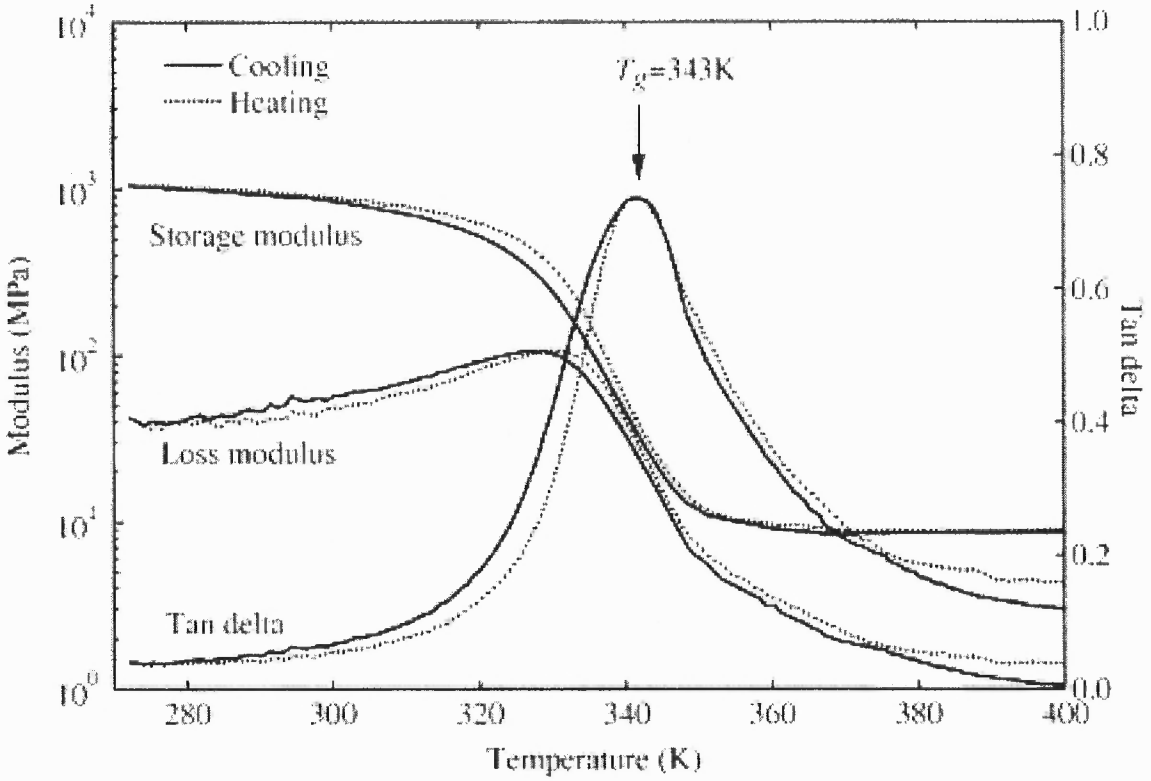

Figure 1.10 Storage modulus, loss modulus and tangent delta of a shape memory epoxy resin.

Source: Yiping Liu, Ken Gall, Martin L. Dunn, Alan R. Greenberg and Julie Diani "Thermomechanics of shape memory polymers: Uniaxial experiments and constitutive modeling" International Journal of Plasticity, Volume 2, Issue 2, February 2006, Page 279-313.

The characteristic of amorphous polymers with appropriate cross-linking density is shown in Figure 1.10. Since the mechanical properties of polymeric materials are strongly temperature dependent an amorphous polymer that is stiff at room temperature can become compliant and behave in a ductile, rubbery manner at higher temperatures.

1.7 Advantages and Applications of SMP's

SMP materials have several advantages over alternative active materials such as shape memory alloys. The low density of unreinforced or reinforced SMPs is an advantage for lightweight structural applications [6]. Another benefit of SMPs is their controllable activation temperature range that is linked to the glass transition temperature T_g and can be manipulated by changing co-polymer composition or the degree of cross-linking [7], [8]. Low temperature curing and molding process for SMP fabrication yield additional advantages for creating complex geometries at a reasonable cost. SMP structures can be fabricated by casting, injection molding, extrusion or blow molding methods.

SMP materials are predominantly used in deployable space structures, medical devices and in Biological Microelectro Mechanical Systems (Bio MEMS) [9], [10], [11], [12]. The strong temperature dependence of the elastic modulus can be utilized to make temperature sensor. The shape fixity and recoverability can be used to make utensil parts e.g., handles. Another common application of shape memory polymers is shrinkable tubes and connectors. The biocompatible and biodegradable implant shape memory polymers have become extremely attractive in the biomedical field. The biodegradable suture made of hydrosylable shape memory polymer thermoplastics has been use for wound closure. The suture that is initially in a loose shape tightens after heating to high temperature.

CHAPTER 2

LITERATURE REVIEW

2.1 Shape Memory Polymer Thermomechanical Behavior and Modeling Efforts

Shape memory materials include physically cross-linked polymers and chemically cross-linked polymers. Physical cross-linking is formed by chain entanglements while chemical cross linking is created by covalent bonds. The earliest research work on the characterization on the shape memory polymer mechanical properties has been published in [13], [14], [15]. (Tobushi et al. 1992) studied deformation resistance for rubbery state polyurethane in cyclic tensile test with a strain of 50%. It was found that the deformation resistance rises with the cycling number.

In 1997 the same research group (Tobushi et al. 1997) published a constitutive model for the shape memory polymer thermomechanical cycle. A slip mechanism due to internal friction was added to the standard linear viscoelastic model and is responsible for the irreversible strain.

$$\dot{\varepsilon} = \frac{\dot{\sigma}}{E} + \frac{\sigma}{\mu} - \frac{(\varepsilon - \varepsilon_s)}{\lambda} + \alpha \dot{T} \tag{2.1}$$

In the above equation, the slip strain was $\varepsilon_s = C(\varepsilon_{creep} - \varepsilon_0)$ where ε_0 the threshold strain is. The relationship between the non-recoverable slip strain and the creep strain was obtained through isothermal creep tests. If the creep strain was larger than a threshold value, the slip strain increased in proportion to the creep strain minus the threshold value. The slip ratio increased with decreasing temperature. Thermal expansion effect which

was assumed to be independent of the shape memory polymer mechanical behavior was considered in the model. This constitutive model can predict the overall trends of shape fixity, shape recovery and stress recovery under strain constraint for deformation strain level lower than 10%.

In the work of Jeong and Kim [16], [17], [18], [19], [20] detail description of both phases of shape memory polymer namely: amorphous phase and crystalline phase can be found. Optimized ratio of both co-polymers is essential for maximizing the crystallinity and with the increasing crystallinity, hysterisis can also be increased. Transition temperature of shape memory polymer can also be adjusted using proper combination of the copolymer used.

In a review article of shape memory polymers [21], the mechanism, chemical and thermomechanical aspects of the materials are discussed. An improved nonlinear constitutive model (Tobushi et al. 2001) was developed by modifying the previous model (Tobushi et al. 1997). Additional nonlinear elastic and nonlinear viscoelastic stress terms were added to the previous constitutive equation. The nonlinear strain level up to 20% was considered.

$$\dot{\varepsilon} = \frac{\dot{\sigma}}{E} + m\left(\frac{\sigma - \sigma_y}{k}\right)^{m-1}\frac{\dot{\sigma}}{k} + \frac{\sigma}{\mu} + \frac{1}{b}\left(\frac{\sigma}{\sigma_c} - 1\right)^{n} - \left(\frac{\varepsilon - \varepsilon_s}{\lambda}\right) + \alpha\dot{T}, \qquad (2.2)$$

Based on the thermodynamic concepts of entropy and internal energy, it is possible to interpret the thermo mechanical behavior of SMPs from a macroscopic viewpoint without explicitly incorporating details of the molecular interactions. Liu et al. (2006) developed model using the same concept for amorphous shape memory polymers. The model quantified the storage and release of the entropic deformation during thermo-mechanical processes. The fraction of the material freezing a temporary entropy state was

a function of temperature, which was determined by fitting the free strain recovery response. A free energy function for the model was formulated and thermodynamic consistency was ensured.

However, as the model was for amorphous shape memory polymers both phases were considered as isotropic, hyperelastic solid and transition from rubbery phase to glassy phase were done my increasing shear modulus only. The main difference between modeling amorphous shape memory polymers and crystalline shape memory polymer is the modeling phase transition. Phase transition in CSMP involves crystallization. Properties of the semi crystalline phase or temporary shape depend on what happens during the crystallization.

Yiping Liu et al. 2006 developed a one-dimensional for glassy shape memory polymer.

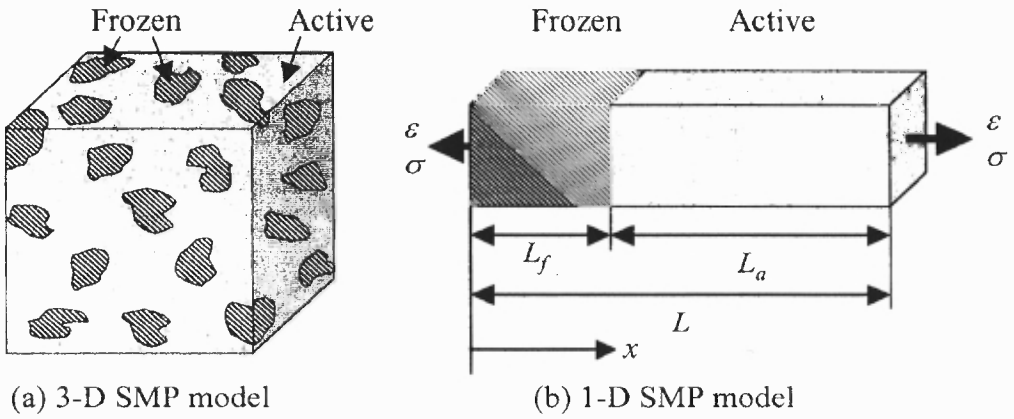

Figure 2.1 Schematic diagram of the micromechanics foundation of the shape memory polymer constitutive model.

Source: Yiping Liu, Ken Gall, Martin L. Dunn, Alan R. Greenberg and Julie Diani "Thermomechanics of shape memory polymers: Uniaxial experiments and constitutive modeling" International Journal of Plasticity, Volume 2, Issue 2, February 2006, Pages 279-313

The overall constitutive equation for the shape memory polymer in a thermomechanical cycle was obtained as follows.

$$\sigma = \frac{\varepsilon - \varepsilon_S - \int_{T_h}^{T} \alpha dT}{\frac{1}{E_i} + \frac{1 - f_f}{E_s}} \tag{2.3}$$

The rate evolution for stored strain was obtained as follows:

$$\frac{d\varepsilon_s}{dT} = \frac{\varepsilon - \varepsilon_s - \int_{T_h}^{T} \alpha dT}{E_s\left(\frac{1}{E_i} + \frac{1 - f_f}{E_s}\right)}\left(\frac{df_f}{dT}\right) \tag{2.4}$$

The modeling results demonstrated that the constitutive model could capture the overall thermomechanical behavior of shape memory polymers. They could be validate the experimental results as shown in the following figures. In Figure 2.1, the material is formed in a stress stated and when it undergoes the glass transition completely, constrained cooling produces thermal stress which results in increased total stress. Figure 2.2, shows that the stress begins to recover once the polymer is heated above the glass transition temperature. Figure 2.4, shows the stress recovery under different strain conditions.

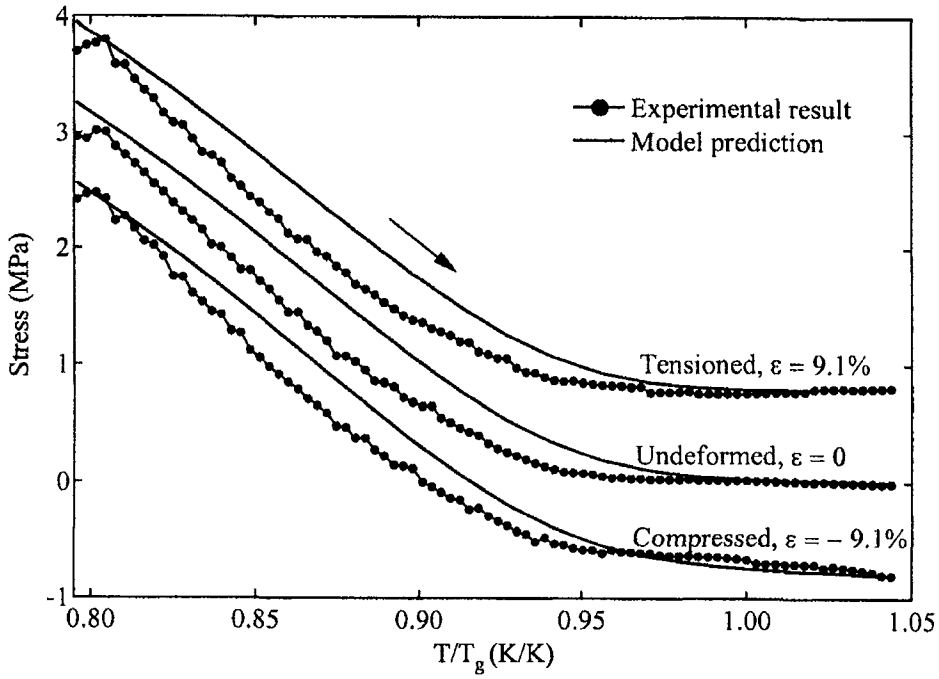

Figure 2.3 Predictions of stress strain responses of the polymer during heating under different strain conditions.

Source: Yiping Liu, Ken Gall, Martin L. Dunn, Alan R. Greenberg and Julie Diani "Thermomechanics of shape memory polymers: Uniaxial experiments and constitutive modeling" International Journal of Plasticity, Volume 2, Issue 2, February 2006, Pages 279-313.

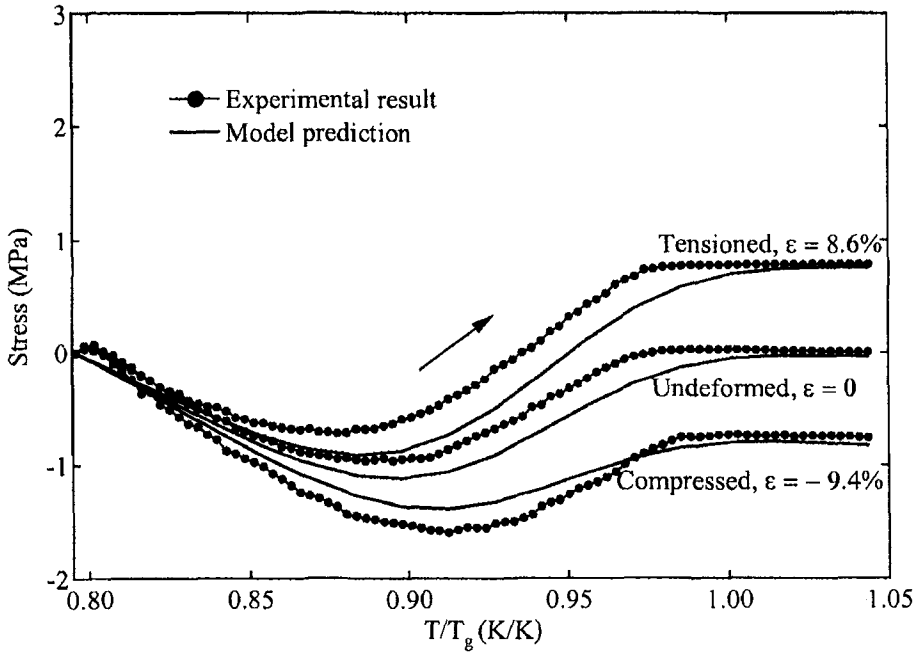

Figure 2.4 Prediction of the stress recovery responses during heating for polymers under different fixed-strain constraint conditions.

Source: Yiping Liu, Ken Gall, Martin L. Dunn, Alan R. Greenberg and Julie Diani "Thermomechanics of shape memory polymers: Uniaxial experiments and constitutive modeling" International Journal of Plasticity, Volume 2, Issue 2, February 2006, Pages 279-313.

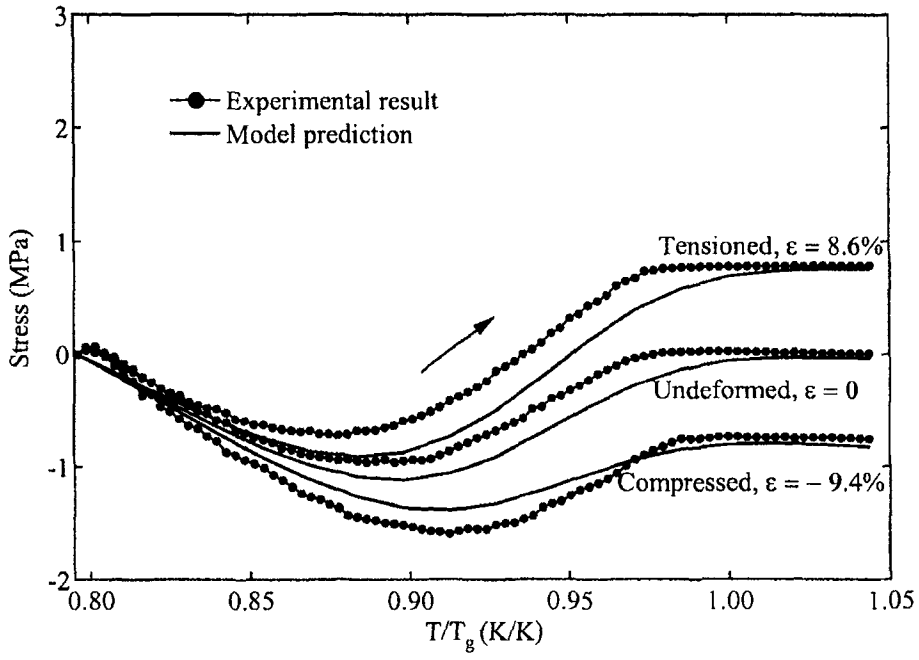

Figure 2.4 Prediction of the stress recovery responses during heating for polymers under different fixed-strain constraint conditions.

Source: Yiping Liu, Ken Gall, Martin L. Dunn, Alan R. Greenberg and Julie Diani "Thermomechanics of shape memory polymers: Uniaxial experiments and constitutive modeling" International Journal of Plasticity, Volume 2, Issue 2, February 2006, Pages 279-313.

CHAPTER 3

PRELIMINARIES

3.1 Introduction

Continuum mechanics is a branch of physics (specifically mechanics) that deals with continuous matter, including both solids and fluids (i.e., liquids and gases). The fact that matter is made of atoms and that it commonly has some sort of heterogeneous *microstructure* is ignored in the simplifying approximation that physical quantities, such as energy and momentum, can be handled in the infinitesimal limit. Differential equations are employed in solving problems in continuum mechanics. Some of these differential equations are specific to the materials being investigated and are called constitutive equations, while others capture fundamental physical laws, such as conservation of mass or conservation of momentum.

The field of continuum mechanics consists mainly of the following:

(1) The study of motion and deformation (Kinematics)

(2) The study of stress in continuum

(3) Fundamental laws of physics governing the motion of a continuum.

A brief introduction to the following terms and concepts is discussed.

(a) Configuration and Motion of Continuum Bodies

(b) Velocity and Acceleration Fields

(c) Deformation Gradient

(d) Stretch Tensor

(e) Stress Tensor

(f) Conservation laws: Mass, Linear Momentum and Angular Momentum.

3.2 Body, Motion and Deformation

A *body*, denoted by *B* may be viewed as having a continous distribution of matter in space. The regions which are occupied by the continuum body *B* at a given time are known as the *configurations* of *B* at that time. The region with a fixed reference time is referred to as the *reference* (or undeformed) *configuration* where as the region occupied by the continuum body *B* at time t > 0 is called its *current* (or deformed) configuration.

In the reference configuration the *velocity* of a particle is given by $\mathbf{V}(\mathbf{X},t)=\frac{\partial \chi\ (\mathbf{X},t)}{\partial t}$, while the *acceleration* is given by $\mathbf{A}(\mathbf{X},t)=\frac{\partial^2 \chi\ (\mathbf{X},t)}{\partial t^2}$. such a description in which quantities are expressed with regard to a particle in a reference configuration is called *material* or *lagrangian* description.

In the current configuration the velocity and acceleration are given by:

$$\mathbf{v}(\mathbf{x},t) = \mathbf{V}[\chi^{-1}(\mathbf{X},t),t] \tag{3.1}$$

$$\mathbf{a}(\mathbf{x},t) = \mathbf{A}[\chi^{-1}(\mathbf{X},t),t] \tag{3.2}$$

This type of description is called *spatial* or *eulerian* description.

The *deformation gradient* **F**(**X**, t) is a second order tensor which acts on a vector d**X** to generate a vector d**x**. Thus **F**(**X**, t) with respect to reference configuration is defined as follows:

$$\mathbf{F}(\mathbf{X},t)=\frac{\partial \chi(\mathbf{X},t)}{\partial \mathbf{X}} \tag{3.3}$$

The deformation gradient **F** can be decomposed in to a pure stretch and pure rotation via the polar decomposition. At each point $\mathbf{X} \in \Omega_O$ and each time t there is a unique polar decomposition of the deformation gradient

$$\mathbf{F} = \mathbf{RU} = \mathbf{VR} \tag{3.4}$$

$$\text{where } \mathbf{R}^T\mathbf{R} = \mathbf{I};\ \mathbf{U} = \mathbf{U}^T;\ \mathbf{V} = \mathbf{V}^T \tag{3.5}$$

U and V are unique, positive definite, symmetric tensors; R is a proper orthogonal tensor.

3.3 Stress Tensor

Stress Tensor: Motion and deformation give rise to interactions between the material and neighboring material in the interior part of the body. One consequence of these interactions is stress, which has physical dimension force per unit of area. To discuss the concept of various types of stress a deformable body during finite motion is considered. It is assumed that arbitrary forces act on parts or the whole of the boundary surface (called *external forces or traction forces*) and within the interior of the body (called *internal forces or body forces*) in some distributed manner.

The *Cauchy's stress theorem* combines the surface traction with the stress tensor and is one of the most important axioms in continuum mechanics. It is given by the following equation

$$\mathbf{t}(\mathbf{x}, t, \mathbf{n}) = \sigma(\mathbf{x}, t)\mathbf{n} \tag{3.6}$$

3.4 Conservation Principles and Thermodynamics

The *conservation of mass* states that the mass of a closed system of substances will remain constant, regardless of the processes acting inside the system. The spatial form of the conservation of mass is:

$$\frac{\partial \mathbf{v}}{\partial t} + div(\rho \mathbf{v}) = 0 \tag{3.7}$$

And the referential form is:

$$\rho_o = \rho \det \mathbf{F} \tag{3.8}$$

The principle of *conservation of momentum* states that the total momentum of a closed system of objects (which has no interactions with external agents) is constant. The conservation of linear momentum in eularian form is given by the following equation

$$\rho\left[\frac{\partial \mathbf{v}}{\partial t} + [\nabla \mathbf{v}]\mathbf{v}\right] = div\mathbf{T}^{T} + \mathbf{b} \tag{3.9}$$

And in referential form is given as:

$$\rho_o\left[\frac{d\mathbf{v}}{dt}\right] = Div\mathbf{P} + \mathbf{B} \tag{3.10}$$

where the *Div* is the divergence taken in the reference configuration, P is first Piola-kirchoff stress tensor and **B** is the body force in reference configuration.

The *balance of angular momentum* for a body in the absence of internal couples requires that the stress tensor be symmetric.

$$\mathbf{T} = \mathbf{T}^{T} \tag{3.11}$$

Conservation of energy states that the total amount of energy in an isolated system remains constant, although it may change forms.

The balance of mechanical energy known as power theorem can be written as:

$$\frac{D}{Dt}\kappa(t) + P_{\text{int}}(\text{t}) = P_{\text{ext}}(\text{t}) \tag{3.12}$$

where, $\mathcal{K}$ is kinetic energy, $\mathcal{P}_{\text{int}}$ is rate of internal mechanical work or stress power and $\mathcal{P}_{ext}$ represents rate of external mechanical work.

Equation (3.14) can be written in more general form that is suitable for continuum occupying some arbitrary region Ω as

$$\frac{d}{dt}\int_{\Omega}\frac{1}{2}\rho\mathbf{v}\bullet\mathbf{v}dv + \int_{\Omega}\mathbf{T}\bullet\mathbf{L}dv = \int_{\partial\Omega}\mathbf{T}^{T}\mathbf{n}\bullet\mathbf{v}da + \int_{\Omega}\rho\mathbf{b}\bullet\mathbf{v}dv \tag{3.13}$$

The first law of Thermodynamics can be thought of as implicit definition of energy. This law of Thermodynamics correlates between mechanical energy and the other form of energy known as 'heat'. There exists a physical quantity known as 'internal energy', ε, that closes the energy balance equation. A statement for the first law can be then stated as "The sum of the variations of kinetic energy, $\mathcal{K}$, and of internal energy ε (the sum of two can be depicted as $(\dot{\mathcal{E}})$) is equal to sum of the rate at which work is done by the external forces, $\mathcal{W}$, and of the energy per unit time that enter the system as heat transfer, $\mathcal{Q}$". Mathematical representation of the statement is as follows:

$$\dot{\mathcal{E}} = \dot{\mathcal{Q}} + \dot{\mathcal{W}} \tag{3.14}$$

where,

$$\begin{aligned}
\dot{\mathcal{E}} &= \frac{d}{dt}\int_{\Omega}\frac{1}{2}\rho\mathbf{v}\bullet\mathbf{v}dv + \frac{d}{dt}\int_{\Omega}\rho\varepsilon dv, \\
\dot{\mathcal{Q}} &= \frac{d}{dt}\int_{\Omega}\rho r dv + \frac{d}{dt}\int_{\partial\Omega}\mathbf{q}\bullet\mathbf{n}da, \\
\dot{\mathcal{W}} &= \int_{\partial\Omega}\mathbf{T}^{T}\mathbf{n}\bullet\mathbf{v}da + \int_{\Omega}\rho\mathbf{b}\bullet\mathbf{v}dv,
\end{aligned} \tag{3.15}$$

and r is the radiant heating, q is the heat flux through the surface Ω. As Ω is arbitrary surface, combining the power theorem and the first law of thermodynamics the local form of the balance of energy for a continuum can be written as follows

$$\rho \dot{\varepsilon} + div\mathbf{q} = \mathbf{T}\bullet\mathbf{L} + \rho r. \tag{3.16}$$

The second law of Thermodynamics identifies the fundamental difference between the two forms of energy namely mechanical energy in form of work and thermal energy in form of heat. The second law of Thermodynamics can be stated, according to Kelvin, as follows: "*It is impossible to devise an engine which, working in a cycle, shall produce no effect other than extraction of hear from a reservoir and the performance of an equivalent amount of mechanical work.*" This observation cannot be deduced from the first law. Only second law can indicates the direction of an energy transfer process.

The useful form for the second law is known as entropy inequality principle. It is important to introduce the concept of entropy before writing the statement. Entropy, $\mathcal{S}$, is defined as fundamental state variable. Assuming the entropy is possessed by continuum body Ω occupying some region is defined to be

$$\mathcal{S} = \int_{\Omega} \rho \eta dv, \tag{3.17}$$

where η is entropy per unit mass. The production of entropy is the difference between the rate of change on entropy and the rate of entropy input in to body at an absolute temperature θ. According to the second law of thermodynamics, this rate of entropy production for all the thermodynamics process is never negative. The mathematical expression for the statement is

$$d\mathcal{S} - \frac{dQ}{\theta} = d\xi \geq 0. \tag{3.18}$$

where $d\xi$ is entropy produced. For reversible process $d\xi$ is equal to zero and for irreversible process $d\xi$ is positive. Hence, for any realistic process Equation (3.20) can also be written as

$$\frac{d\mathcal{S}}{dt} - \frac{1}{\theta}\frac{dQ}{dt} = \frac{d\xi}{dt}. \tag{3.19}$$

It can be showed that using Equation, second term in Equation (3.20) and Equation (3.21) the balance law for entropy can have following form

$$\rho\dot{\eta} + div\left(\frac{q}{\theta}\right) = \rho\frac{r}{\theta} + \rho\xi \tag{3.20}$$

Combining the balance of energy, Equation (3.18), and the balance of entropy, Equation (3.22) results in the reduced energy-dissipation equation. The reduced energy-dissipation equation is

$$\mathbf{T}\bullet\mathbf{L} - \rho\dot{\varepsilon} + \rho\theta\dot{\eta} - \frac{\mathbf{q}\bullet grad\theta}{\theta} = \rho\theta\xi := \zeta \geq 0, \tag{3.21}$$

Where ζ is defined as the rate of dissipation. Both ξ and ζ are constrained to be non-negative for an acceptable process. Here it should be noted that the rate of dissipation is positive if and only if the rate of entropy production is positive. As the entropy production can take place because of the variety reasons, for e.g., due to phase change, chemical reactions, heat conductions etc., the rate of dissipation as defined through Equation (3.23) is non-zero whenever entropy production is zero. Equation (3.23) can also be written as

$$\mathbf{T}\bullet\mathbf{L} - \rho\dot{\Psi} + \rho\eta\dot{\theta} - \frac{\mathbf{q}\bullet grad\theta}{\theta} = \rho\theta\xi := \zeta \geq 0, \tag{3.22}$$

where ψ is the Helmholtz potential and is given by $\Psi = \varepsilon - \theta\eta$. This form of reduced energy dissipation equation is useful to place restriction for the constitutive equations. As mentioned above, for any realistic process the rate of entropy production is zero and so consequently the rate of dissipation will also be zero. Most thermo-mechanical processes are irreversible process and for that entropy production is greater than zero. It can also be assumed that the rate of dissipation can be split in to a part that is due to heat conduction and another part that is a consequence of other irreversible affects, i.e.,

$$\mathbf{T}\bullet\mathbf{L} - \rho\dot{\Psi} + \rho\eta\dot{\theta} - \frac{\mathbf{q}\bullet grad\theta}{\theta} = \rho\theta\xi := \zeta = \zeta_c + \zeta_d \geq 0. \tag{3.23}$$

where ζ_c is the rate of dissipation due to heat conduction and ζ_d is the rate of dissipation due to other processes. The rate of dissipation due to conduction is assumed to be given by

$$\zeta_c = -\frac{\mathbf{q}\bullet grad\theta}{\theta} \geq 0. \tag{3.24}$$

Substituting Equation (3.26) in to Equation ; following can be obtained

$$\mathbf{T}\bullet\mathbf{L} - \rho\dot{\Psi} + \rho\eta\dot{\theta} = \zeta_d \geq 0. \tag{3.25}$$

3.5 Theory of Natural Configurations

The response functions of many materials depend upon the currently active microstructure and its deformation. While the notion of a deformation gradient from any configuration to any other configuration is well established, it is not immediately apparent as to how to represent the different microstructures that come into play [22], [23], [24]. Typically, this aspect of the problem is dealt with by referring to "internal variables" whose definitions and properties are not explicitly clear. Since evolution

equations and corresponding initial conditions need to be specified for these quantities, it is necessary to be able to measure their values or at least infer their values from some suitable measurement [25], [26], [27].

The problem of the evolution of the microstructure is addressed by noting that in spite of the disparate ways in which these structural changes occur, a striking macroscopic manifestation of these changes is that the body does not retrace its path in configuration space unlike the case of an elastic body. Rather, when the forces that are acting on the body are removed, the body goes to different configurations at different instants depending upon its structure and chemical composition at the start of the removal of the load and the speed with which the load is removed. The configurations that the body attains when all the external stimuli (such as stress, heat flux etc.) are removed are called the "relaxed" or natural configurations of the material. These relaxed or natural configurations represent the different microstructures, and a change in the microstructure being represented by a change in the natural configuration [25], [26], [27], [28].

To elaborate, consider a body in some configuration $k_t(B)$ at the current time t. In general, it is subject to various stimuli from its environment. These include the working due to the applied traction, the supply of energy in its thermal form (heat) due to conduction, irradiation by electromagnetic waves, etc.

The body responds to these external stimuli. However, how it responds depends upon other conditions that the environment imposes on the body as well as internal constraints. For instance, the body may be so constrained as to be incompressible, there by being capable of only isochoric processes, or the body may be thermally isolated thereby allowing no heat flow into or out of the body so that the body is only capable of

adiabatic processes. Thus, it is possible for a body to proceed from a stressed state to an unstressed state in a variety of ways, and depending on the allowed class of processes, the unstressed states that are achieved may be different. Appropriate choices have to be made for these stress free configurations to describe the response of specific materials in a specific class of processes and this is itself a constitutive specification.

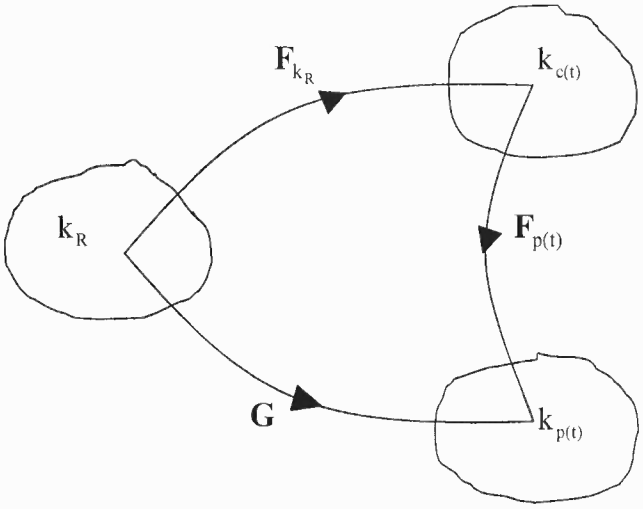

Figure 3.1 Natural configurations associated with a viscoelastic melt.

Source: I.J Rao, K.R Rajagopal "A thermodynamic framework for the study of crystallization in polymers" Zeitschrift für Angewandte Mathematik und Physik (ZAMP) Volume 53, Number 3, May, 2002 Pages 365-406.

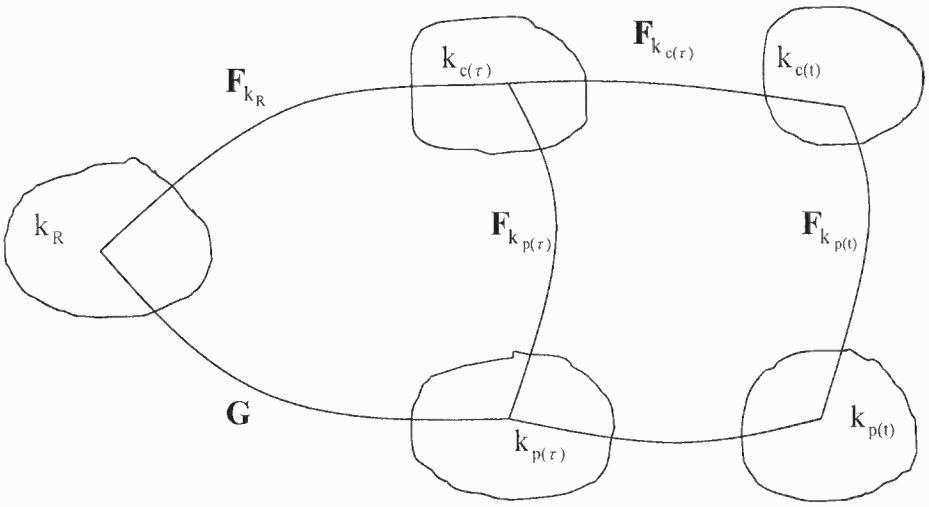

Figure 3.2 Natural configurations associated with the fluid-solid mixture undergoing glass transition.

Source: I.J Rao, K.R Rajagopal "A thermodynamic framework for the study of crystallization in polymers" Zeitschrift für Angewandte Mathematik und Physik (ZAMP) Volume 53, Number 3 / May, 2002 Pages 365-406.

Figures 3.1 and 3.2 are an illustration of use of natural configurations in modeling the crystallization of polymers [29]. The derivation of the constitutive equations for the stress is based on this theory. In modeling the melt, the Helmholtz potential (stored energy function) and the stress in the fluid are determined from the mapping between the tangent spaces of the natural configuration of the fluid at a material point to the current configuration occupied by it. In Figure 3.1, k_R is a reference configuration, $k_{c(t)}$ is the configuration currently occupied by the material and $k_{p(t)}$ is the natural configuration associated with the material that is currently in the configuration $k_{c(t)}$, that is if the tractions on $k_{c(t)}$ are removed, the body will take the configuration $k_{p(t)}$. In modeling the fluid-solid mixture, in the elastic solid that is formed, the stress depends on the deformation gradient from a configuration of known stress (usually a stress free configuration) and the current configuration. The thermodynamic quantities, the internal

energy and entropy (at time t) in the body due to solid fraction born at time τ is determined by the deformation gradient from the configuration of the body at time τ to the current configuration at time t, i.e., $F_{k_{c(\tau)}}$ while the internal energy and entropy of the amorphous phase is determined by $F_{k_{p(t)}}$.

CHAPTER 4

CONSTITUTIVE MODELING OF CSMP

4.1 Introductions and Phases Associated with CSMP

The constitutive modeling of shape memory polymers (Barot et al 2006) is presented as a prelude for modeling glassy SMP. A constitutive equation in general is a relation between two physical quantities is specific to a material or substance, and does not follow directly from physical law. It is combined with other equations that do represent physical laws to solve physical problems, like the flow of a fluid in a pipe, or the response of a crystal to an electric field. In structural analysis, constitutive relations connect applied stresses or forces to strains or deformations.

In modeling polymers constitutive equations relate quantities like the stress tensor and the Helmholtz potential with the history of the deformation that the body has undergone.

CSMP modeling involves four stages

(1) Loading(Rubbery Phase)

(2) Cooling (Crystallization)(Phase Transition)

(3) Unloading (Semi crystalline Phase)

(4) Heating (Melting)(Phase Transition)

4.2 Isotropic Rubbery Phase

The amorphous region contains randomly oriented networks of the polymer chain segments along with the randomly oriented hard blocks that act as connecting points. The presence of these hard blocks or connecting points is due to one of the co-polymers used to form crystallizable shape memory polymers. The co-polymer used can have a higher glass transition temperature or a higher crystallization temperature than the transition temperature of the crystallizable shape memory polymers. These hard blocks are actually are responsible for remembering the 'original shape' above the transition temperature of the crystallizable shape memory polymers.

A crystallizable shape memory polymer above the recovery temperature is modeled as a hyper-elastic incompressible isotropic solid that is capable of strain hardening for large deformations. The deformation gradient $\mathbf{F}_{\kappa_R}$ denotes the mapping between the tangent space associated with κ_R, at a point in the reference configuration and the tangent space associated with $\kappa_{c(t)}$. The natural configuration is fixed and does not change as in the case of a viscous fluid, and hence there will be no dissipation of energy.

A so called 'hyperelastic material' postulates the existence of a Helmholtz free-energy function Ψ, which is defined per unit reference volume. The Helmholtz potential is also referred to as the strain-energy function or stored-energy function. For this type of material, the strain-energy function depends only upon the deformation gradient $\mathbf{F}$.

In general, for a hyperelastic incompressible material the Cauchy stress σ is given by:

$$\mathbf{T} = -p\mathbf{I} + 2\rho\mathbf{F}_{\kappa_a}\frac{\partial\Psi_a}{\partial\mathbf{C}_{\kappa_a}}\mathbf{F}_{\kappa_a}^T, \tag{4.1}$$

where, p is the Lagrange multiplier due to the constraints of incompressibility, $\mathbf{F}_{\kappa_a}$ is the deformation gradient measured from reference configuration $\kappa_R = \kappa_a$ associated with the amorphous rubbery phase, ρ is the density, Ψ_a is the Helmholtz potential.

For an isotropic incompressible phase, the form for the internal energy and the entropy depend on $\mathbf{F}_{\kappa_a}$ through the first two invariants of $\mathbf{B}_{\kappa_a}$. i.e.

$$I_{\mathbf{B}_a} = I_{\mathbf{C}_a} = tr\left(\mathbf{B}_{\kappa_a}\right) = tr\left(\mathbf{C}_{\kappa a}\right), II_{\mathbf{B}_a} = II_{\mathbf{C}_a} = tr\left(\mathbf{B}_{\kappa_a}^2\right) = tr\left(\mathbf{C}_{\kappa_a}^2\right)$$

therefore the internal energy, the entropy and, consequently, the Helmholtz potential can have the forms:

$$\begin{aligned}
\varepsilon_a &= \varepsilon_a\left(\theta, I_{\mathbf{C}_a}, II_{\mathbf{C}_a}\right), \\
\eta_a &= \eta_a\left(\theta, I_{\mathbf{C}_a}, II_{\mathbf{C}_a}\right), \\
\Psi_a &= \Psi_a\left(\theta, I_{\mathbf{C}_a}, II_{\mathbf{C}_a}\right)
\end{aligned} \tag{4.2}$$

The form chosen for the internal energy, entropy, Helmholtz potential and viscous dissipation

$$\varepsilon_a = C_a\theta + A_a, \tag{4.3}$$

$$\eta_a = C_a\ln(\theta) + B_a - \bar{\mu}_a\left(I_{\mathbf{C}_a} - 3\right) \tag{4.4}$$

$$\Psi_a = \Psi_a\left(\theta, I_{\mathbf{C}_a}\right) \tag{4.5}$$

$$\zeta_d = \zeta_a\left(\theta, \mathbf{B}_{\kappa_a}\right) \tag{4.6}$$

Substituting these forms in the reduced energy dissipation equation we get

$$\left(\mathbf{T}-2\rho\left[\frac{\partial\Psi_a}{\partial I_{C_a}}\mathbf{B}_{\kappa_a}\right]\right)\bullet\mathbf{D}_{\kappa_a}-\left(\frac{\partial\Psi_a}{\partial\theta}+\eta_a\right)\dot{\theta}=\zeta_a=0. \tag{4.7}$$

$$\mathbf{T}=-p\mathbf{I}+2\rho\left[\frac{\partial\Psi_a}{\partial I_{C_a}}\right]\mathbf{B}_{\kappa_a} \tag{4.8}$$

4.3 Phase Transition: Amorphous Phase to Semi-crystalline Phase

During the phase transition, one can find both, the amorphous phase and the crystalline phase, at the same time. The newly formed crystalline material is also an elastic solid. The stress in the current configuration can be calculated by finding the deformation gradient from a configuration of known stress to the current configuration the internal energy, entropy and the Helmholtz potential of the newly formed crystalline phase are given by

$$\begin{aligned}\varepsilon_c &= \varepsilon_c(\theta,\mathbf{C}_{\kappa_{c(\tau)}}),\\ \eta_c &= \eta_c(\theta,\mathbf{C}_{\kappa_{c(\tau)}}),\\ \Psi_c &= \Psi_c(\theta,\mathbf{C}_{\kappa_{c(\tau)}})\end{aligned} \tag{4.9}$$

The internal energy and the entropy of the mixture are assumed to be additive and can be given by (4.10) and (4.11), the Helmholtz potential follows the same form and is given by (4.12):

$$\varepsilon = i_\varepsilon + (1-\alpha)\varepsilon_a + \int_{t_s}^{\tau}\varepsilon_c\frac{d\alpha}{d\tau}d\tau, \tag{4.10}$$

$$\eta = i_\eta + (1-\alpha)\eta_a + \int_{t_s}^{\tau}\eta_c\frac{d\alpha}{d\tau}d\tau, \tag{4.11}$$

$$\Psi = i_{\Psi} + (1-\alpha)\Psi_a + \int_{t_s}^{\tau} \Psi_c \frac{d\alpha}{d\tau} d\tau. \tag{4.12}$$

Where i_{ε}, i_{η} and i_{ψ} are the interfacial internal energy, entropy and Helmholtz potential.

For an incompressible orthotropic elastic solid, the Helmholtz potential depends on the first two invariants of the right Cauchy-Green tensor, $\mathbf{C}_{\kappa_{c(\tau)}}$, which is denoted by $I_{\mathbf{C}_c}, II_{\mathbf{C}_c}$ and the following scalars

$$\begin{aligned} J_1 &= \mathbf{n}_{\kappa_{c(\tau)}} . \mathbf{C}_{\kappa_{c(\tau)}} \mathbf{n}_{\kappa_{c(\tau)}}, \\ K_1 &= \mathbf{m}_{\kappa_{c(\tau)}} . \mathbf{C}_{\kappa_{c(\tau)}} \mathbf{m}_{\kappa_{c(\tau)}}, \end{aligned} \tag{4.13}$$

The Helmholtz potential for an incompressible orthotropic elastic solid then can be written as:

$$\Psi_c = \Psi_c \left(\theta, I_{\mathbf{C}_c}, II_{\mathbf{C}_c}, J_1, K_1 \right), \tag{4.14}$$

the rate of dissipation can be split into two parts, the first related to the dissipation associated with the amorphous phase and the second related to the phase change.

$$\zeta_d = \zeta_a + \zeta_p \geq 0, \tag{4.15}$$

Substituting the Helmholtz potential and ζ_p to the reduced energy dissipation Equation, we obtain

$$\begin{aligned} &\left(\mathbf{T} - (1-\alpha) 2\rho \left[\frac{\partial \Psi_a}{\partial I_{\mathbf{C}_a}} \mathbf{B}_{\kappa_a} \right] - 2\rho \left[\int_{t_s}^{\tau} \mathbf{F}_{\kappa_{c(t)}} \frac{\partial \Psi_c}{\partial I_{\mathbf{C}_c}} \mathbf{F}^T_{\kappa_{c(t)}} \right] \right) \bullet \mathbf{D} + \\ &- \left(\frac{\partial \Psi}{\partial \theta} + \eta \right) \dot{\theta} + \rho \left(\Psi_a - \Psi_c \big|_{\mathbf{C}_{\kappa_{c(t)}} = \mathbf{I}} - \frac{\partial i_{\Psi}}{\partial \alpha} \right) \dot{\alpha} = \zeta_p \geq 0. \end{aligned} \tag{4.16}$$

It is assumed that the following form for the stress that satisfies the above equation:

$$\mathbf{T} = -p\mathbf{I} + 2(1-\alpha)\rho \left[\frac{\partial \Psi_a}{\partial I_{\mathbf{C}_a}} \mathbf{B}_{\kappa_a} \right] + 2\rho \left[\int_{t_s}^{\tau} \mathbf{F}_{\kappa_{c(t)}} \frac{\partial \Psi_c}{\partial I_{\mathbf{C}_c}} \mathbf{F}^T_{\kappa_{c(t)}} \frac{d\alpha}{d\tau} d\tau \right]. \tag{4.17}$$

For crystalline materials, there is not significant change in the configurational entropy with the deformation, while the internal energy does depend on the deformation, because of which, the following forms for the internal energy and the entropy of the crystalline phase are assumed,

$$\varepsilon_c = C_c\theta + A_c + \frac{1}{2\rho}\left(\mu_c\left(I_{C_c} - 3\right) + \mu_{c1}\left(J_1 - 1\right)^2 + \mu_{c2}\left(K_1 - 1\right)^2\right) \tag{4.18}$$

$$\eta_c = C_c \ln(\theta) + B_c, \tag{4.19}$$

where C_c is the specific heat associated with the crystalline phase, A_c and B_c are constants and μ_c, μ_{c1} and μ_{c2} are material moduli associated with the crystalline phase.

4.4 Semi-crystalline Phase

After the cessation of the crystallization, the temporary shape is the mixture of the amorphous solid and the crystalline solid. The stress in the material can be found out by the mapping between the current configuration and the original configuration, along with the summation of all the mappings between configurations of the body at every instant that a new crystal was born to the current configuration. The Helmholtz potential for such a hyperelastic solid can be then given by

$$\Psi = i_\Psi + (1-\alpha)\Psi_a + \int_{t_s}^{t_f} \Psi_c \frac{d\alpha}{d\tau} d\tau. \tag{4.20}$$

The Cauchy stress in the solid at this point can be prescribe by

$$\mathbf{T} = -p\mathbf{I} + (1-\alpha)\mu_a \mathbf{B}_{\kappa_a} + \int_{t_s}^{t_f} \mu_c \mathbf{B}_{\kappa_{c(\tau)}} \frac{d\alpha}{d\tau} d\tau + \int_{t_s}^{t_f} \left(\mathbf{F}_{\kappa_{c(\tau)}} \left(\mu_{c1} (J_1 - 1) \mathbf{n}_{\kappa_{c(\tau)}} \otimes \mathbf{n}_{\kappa_{c(\tau)}} + \mu_{c2} (K_1 - 1) \mathbf{m}_{\kappa_{c(\tau)}} \otimes \mathbf{m}_{\kappa_{c(\tau)}} \right) \mathbf{F}^T_{\kappa_{c(\tau)}} \right) \frac{d\alpha}{d\tau} d\tau. \quad (4.21)$$

4.5 Phase Transition: Semi-Crystalline Phase to Amorphous Phase

The return to the original shape is accomplished by heating the material above the recovery temperature. At the beginning of heating, the two phases will have different stress-free states because of which shape fixity is possible. Due to the melting of the crystals, the material will pass through all the different stress free configurations, ending up in the stress free configuration of the permanent shape.

The Helmholtz potential of the mixture during the melting at any given point of time can be then calculated using following equation:

$$\Psi = i_\Psi + (1-\alpha)\Psi_a + \int_{t_s}^{\overset{*}{\tau}} \Psi_c \frac{d\alpha}{d\tau} d\tau, \quad \text{with } \overset{*}{\tau} \in \left[t_s, t_f \right] \quad \text{and} \quad \alpha(\overset{*}{\tau}) = \alpha(t). \quad (4.22)$$

The rate of dissipation associated with the phase change during melting can be give by:

$$\zeta_m = \zeta_m (\alpha, \dot{\alpha}, \theta, ...) \geq 0.$$

The reduced energy dissipation equation for the melting process is given as

$$\left(\mathbf{T}-(1-\alpha)2\rho\left[\frac{\partial\Psi_a}{\partial I_{\mathbf{C}_a}}\mathbf{B}_{\kappa_a}\right]-2\rho\left[\int_{t_s}^{\overset{*}{\tau}}\mathbf{F}_{\kappa_c(t)}\frac{\partial\Psi_c}{\partial\mathbf{C}_{\kappa_{c(t)}}}\mathbf{F}^T_{\kappa_c(t)}\right]\right)\bullet\mathbf{D}+$$

$$-\left(\frac{\partial\Psi}{\partial\theta}+\eta\right)\dot{\theta}+\rho\left(\Psi_c\big|_{\mathbf{C}_{\kappa_{c(t)}^{*}}}-\Psi_a\big|_{\mathbf{C}_{\kappa_a}}-\frac{\partial i_\Psi}{\partial\alpha}\right)\dot{\alpha}=\zeta_m\geq 0, \qquad (4.23)$$

with $\overset{*}{\tau}\in\left[t_s,t_f\right]$ and $\alpha(\overset{*}{\tau})=\alpha(t)$.

the Cauchy stress

$$\mathbf{T}=0=-p\mathbf{I}+(1-\alpha)\mu_a\mathbf{B}_{\kappa_a}+\int_{t_s}^{\overset{*}{\tau}}\mu_c\mathbf{B}_{\kappa_{c(t)}}\frac{d\alpha}{d\tau}d\tau+$$

$$\int_{t_s}^{\overset{*}{\tau}}\left(\mathbf{F}_{\kappa_{c(t)}}\left(\mu_{c1}(J_1-1)\mathbf{n}_{\kappa_{c(t)}}\otimes\mathbf{n}_{\kappa_{c(t)}}+\mu_{c2}(K_1-1)\mathbf{m}_{\kappa_{c(t)}}\otimes\mathbf{m}_{\kappa_{c(t)}}\right)\mathbf{F}^T_{\kappa_{c(t)}}\right)\frac{d\alpha}{d\tau}d\tau, \qquad (4.24)$$

with $\overset{*}{\tau}\in\left[t_s,t_f\right]$ and $\alpha(\overset{*}{\tau})=\alpha(t)$.

CHAPTER 5

CONSTITUTIVE MODELING OF GLASSY SHAPE MEMORY POLYMERS

5.1 Introduction

Constitutive modeling is the mathematical description of how materials respond to various loadings. In structural analysis, constitutive relations connect applied stresses or forces to strains or deformations. The constitutive relation for linear materials is linear, and is commonly known as Hooke's law.

More generally, in physics, a constitutive equation is a relation between two physical quantities (often described by tensors) that is specific to a material or substance, and does not follow directly from physical law. It is combined with other equations that do represent physical laws to solve physical problems, like the flow of a fluid in a pipe, or the response of a crystal to an electric field.

The Constitutive Modeling of Glassy Shape Memory Polymer discussed here is based on uniaxial experiments in tension (Yiping Liu et al. 2005) so as to take in to account the thermal expansion of polymers and its associated effect on stress-strain response.

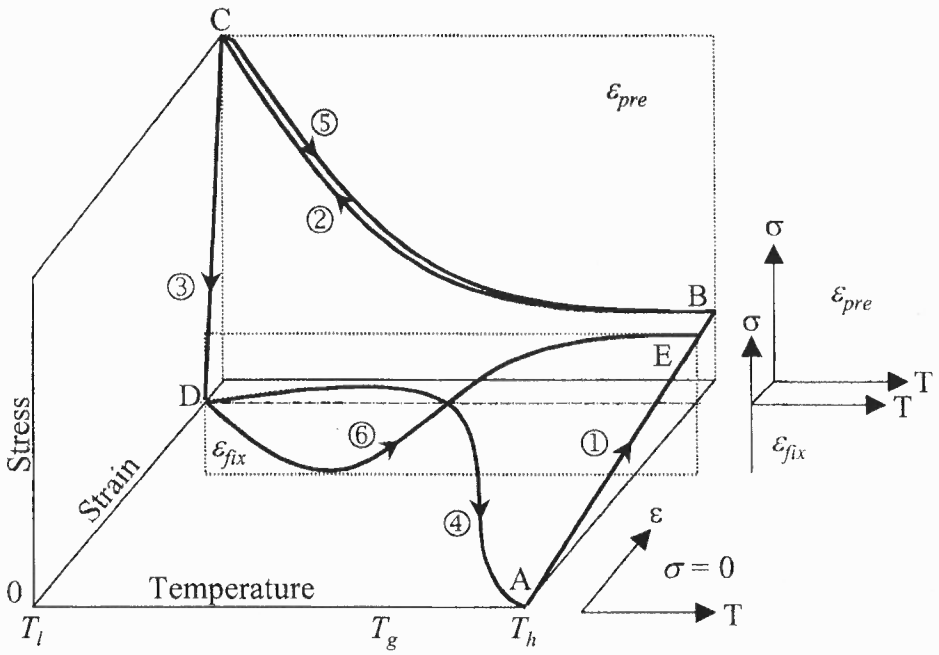

Figure 5.1 Stress–strain–temperature diagram illustrating the thermomechanical behavior of a pre-tensioned shape memory polymer under different strain/stress constraint conditions.

Source: Yiping Liu, Ken Gall, Martin L. Dunn, Alan R. Greenberg and Julie Diani "Thermomechanics of shape memory polymers: Uniaxial experiments and constitutive modeling" International Journal of Plasticity, Volume 2, Issue 2, February 2006, Pages 279-313.

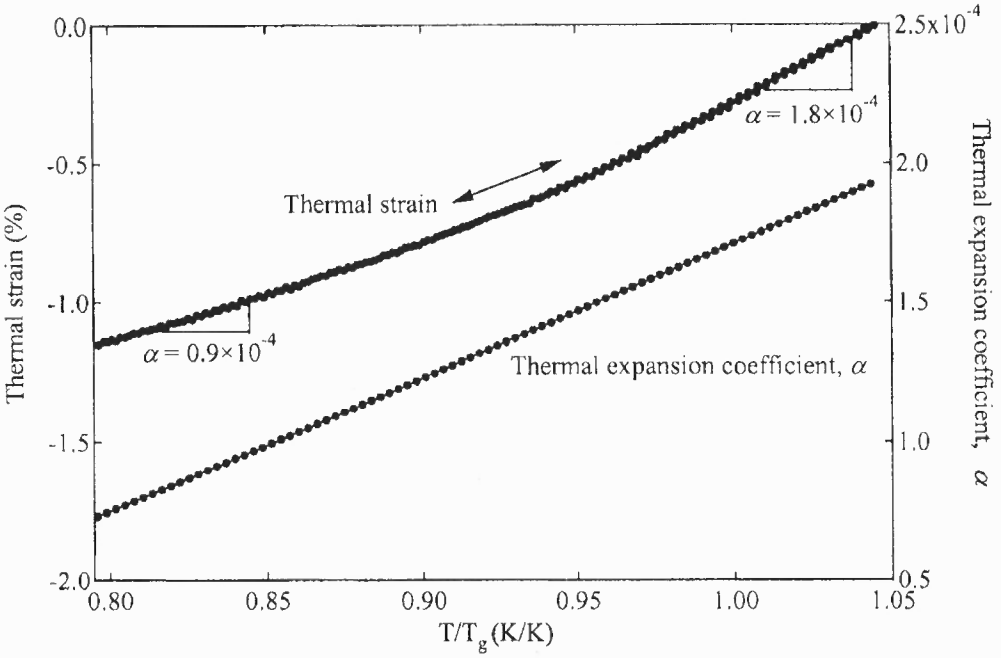

Figure 5.2 Thermal expansion strain as a function of temperature in the temperature range from T_l to T_h.

Source: Yiping Liu, Ken Gall, Martin L. Dunn, Alan R. Greenberg and Julie Diani "Thermomechanics of shape memory polymers: Uniaxial experiments and constitutive modeling" International Journal of Plasticity, Volume 2, Issue 2, February 2006, Pages 279-313.

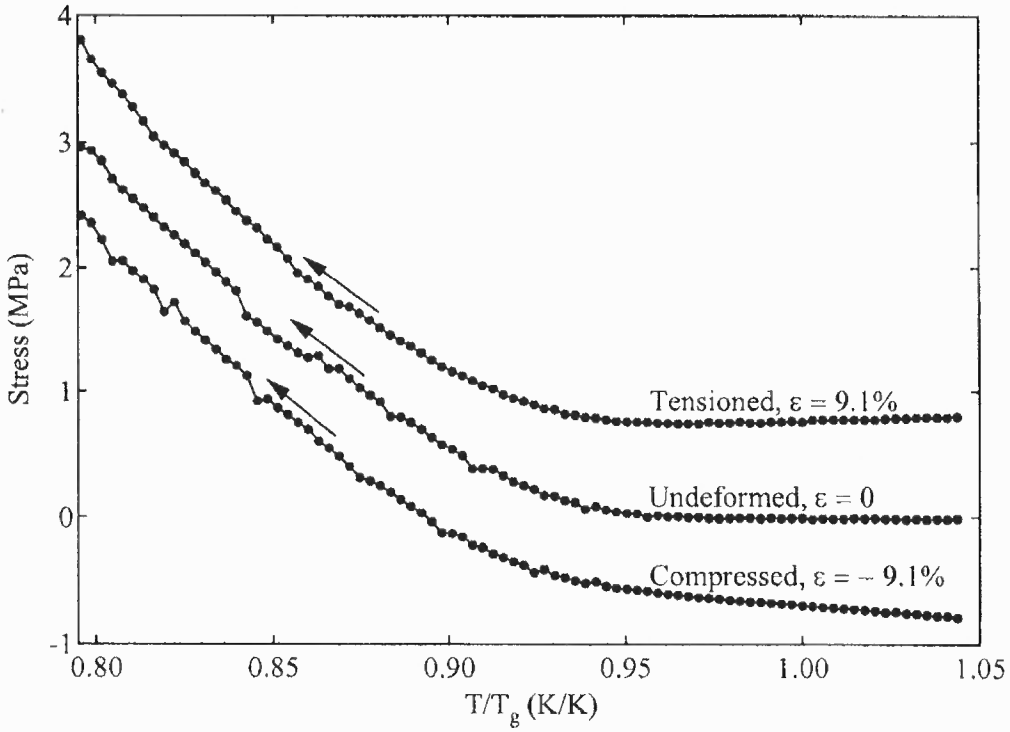

Figure 5.3 Stress Responses of the polymer during cooling under different strain constraints.

Source: Yiping Liu, Ken Gall, Martin L. Dunn, Alan R. Greenberg and Julie Diani "Thermomechanics of shape memory polymers: Uniaxial experiments and constitutive modeling" International Journal of Plasticity, Volume 2, Issue 2, February 2006, Pages 279-313.

A typical tensile deformation and strain recovery cycle for a polymer can be described in four steps. To start the thermomechanical cycle, the polymer is brought to state A at an elevated temperature, T_h, at zero strain and zero stress. The first step of the cycle involves a high-strain deformation in the rubbery state. The second step is a "strain storage" process whereby the polymer is cooled. The tensile stress needed to maintain the pre-deformed shape increases as the temperature decreases due to thermal contraction (which is quantified by the coefficient of thermal expansion of the polymer). In the glassy state, the polymer molecular chain segments are gradually frozen by thermally reversible molecular chain interactions. The third step involves low temperature unloading. The low

temperature unloading process is sometimes referred to as spontaneous "springback". Due to the higher elastic modulus at low temperature the springback strain is very low compared to the original deformation strain which is mostly stored in the glassy state. Here the temporary shape of the polymer is fixed. The retained strain corresponding to the fixed shape is called fixed strain. The fourth step involves heating the polymer above the glass transition temperature and hence recovery of the induced strain. During the heating process the strain is recovered near T_g.

Figure 5.3 the thermal strain was measured during both the cooling and heating and the curves overlap. The thermal expansion coefficient α is defined as the slope of the thermal strain curve. The average thermal expansion coefficient in the rubbery state (α = 1.8 × 10e-4 1/K) is about two times of that in the glassy state (α = 0.9 × 10e-4 1/K) and is attributed to change in free volume fraction during the glass transition.

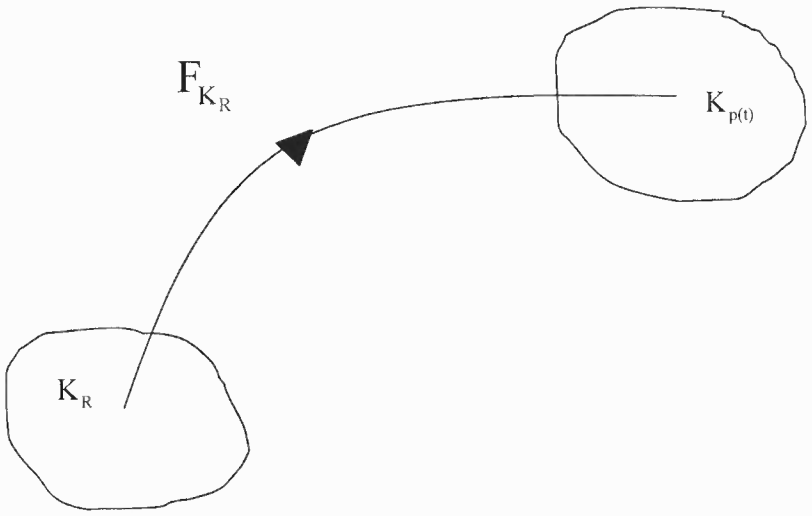

Figure 5.4 Natural Configurations associated with the amorphous or rubbery phase.

Source: Gautam Barot, I J Rao "Constitutive Modeling and Simulation of the Thermo-Mechanics Associated with Crystallizable Shape Memory Polymers"Zeitschrift für Angewandte Mathematik und Physik (ZAMP) Volume 57, Number 4 / July, 2006.

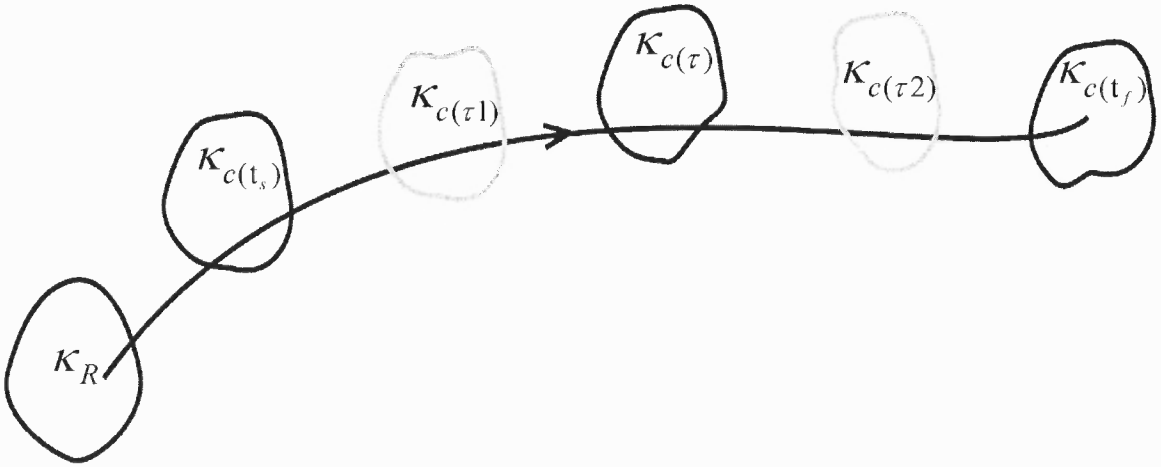

Figure 5.5 At time t_s crystallization begins and stops at time t_f. Between these times newly formed crystals are formed with different natural configurations.

Source: Gautam Barot, I J Rao "Constitutive Modeling and Simulation of the Thermo-Mechanics Associated with Crystallizable Shape Memory Polymers"Zeitschrift für Angewandte Mathematik und Physik (ZAMP) Volume 57, Number 4 / July, 2006.

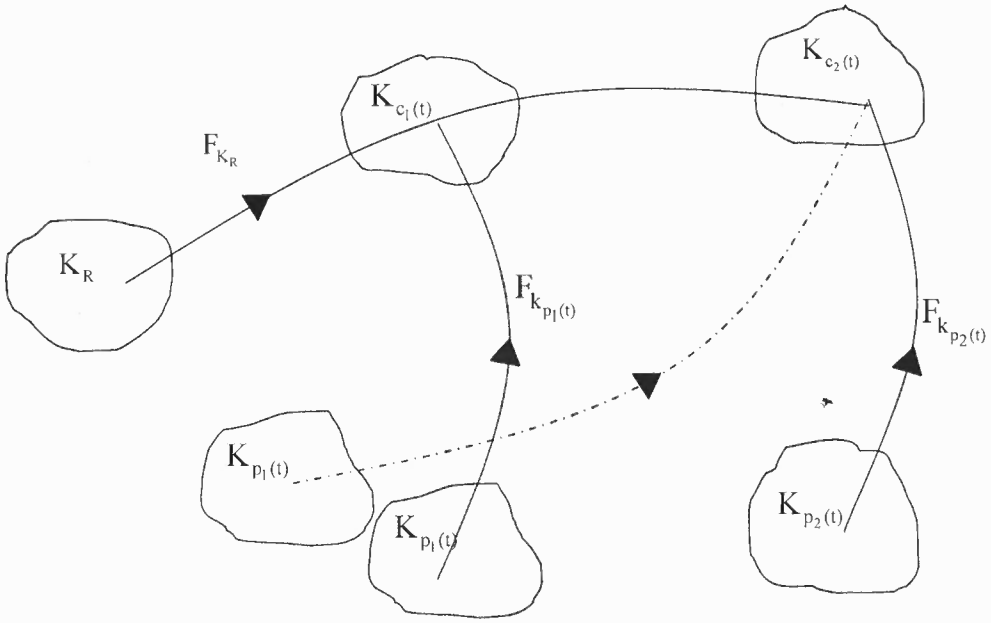

Figure 5.6 Natural Configurations associated with the rubbery phase – glassy solid phase mixture undergoing glass transition.

Figure 5.6 shows Natural Configuration associated with the amorphous or rubbery phase. It is important to note that since material above the glass transition temperature is in its rubbery form it has only one natural configuration which is its reference configuration. The stress in the material is determined by the deformation gradient F_{K_R} between the current configuration and the reference configuration. Figure 5.6 shows the natural configurations associated with the rubbery phase – glassy solid phase mixture. When the shape memory polymer is cooled below the glass transition temperature the glassy material is formed in different configurations. Each configuration in which the glassy material is formed has its own natural configuration. Thus the natural configurations evolve. The evolution of natural configurations is underscored by the fact that when a new material is formed the natural configuration associated with the previous

material moves to a new position on account of constrained cooling i.e the material is trying to shrink due to thermal effects but it cannot as it is constrained. This concept of shifting of the natural configuration to a new configuration is used for the constitutive modeling of the glassy shape memory polymer. For example the stress in the current material comes from the deformation gradient from the natural configuration associated with the current configuration and all the previous natural configurations which have been shifted to new positions on account of constrained thermal shrinkage.

5.2 Isotropic Rubbery Phase

Shape memory polymers above the glass transition temperature show the characteristics of an elastomer. The retractive force is governed by changes in entropy while the internal energy changes are trivial.

$$T_{11} = \mu_a \left(\Lambda_a^2 - \frac{1}{\Lambda_a} \right) \tag{5.1}$$

where T is the stress in the rubbery part of the polymer and μ_a is the modulus of the rubbery phase. The above equation is derived as follows.

The stress in the amorphous(rubbery) part of the polymer is given by:

$$\mathbf{T} = -p\mathbf{I} + \mu_a \mathbf{B}_{K_a} \tag{5.2}$$

where p is the lagrange multiplier due to constraints of incompressibility and B_{K_a} is the left Cauchy stretch tensor. The deformation gradient F_{k_a} and the left Cauchy stress tensor B_{k_a} is given as follows

$$\boldsymbol{F}_{k_a} = \begin{pmatrix} \Lambda(t) & 0 & 0 \\ 0 & \dfrac{1}{\sqrt{\Lambda(t)}} & 0 \\ 0 & 0 & \dfrac{1}{\sqrt{\Lambda}(t)} \end{pmatrix} \tag{5.3}$$

$$\boldsymbol{B}_{k_a} = \boldsymbol{F}_{k_a}\boldsymbol{F}_{k_a}^{T} = \begin{pmatrix} \Lambda^2(\mathrm{t}) & 0 & 0 \\ 0 & \dfrac{1}{\Lambda(\mathrm{t})} & 0 \\ 0 & 0 & \dfrac{1}{\Lambda(\mathrm{t})} \end{pmatrix} \tag{5.4}$$

Thus, the equation for stress takes the following form in a matrix

$$\cdot\begin{pmatrix} T_{11} & T_{12} & T_{13} \\ T_{21} & T_{22} & T_{23} \\ T_{31} & T_{32} & T_{33} \end{pmatrix} = \begin{pmatrix} -P & 0 & 0 \\ 0 & -P & 0 \\ 0 & 0 & -P \end{pmatrix} + \begin{pmatrix} \mu\Lambda^2(\mathrm{t}) & 0 & 0 \\ 0 & \dfrac{\mu}{\Lambda(\mathrm{t})} & 0 \\ 0 & 0 & \dfrac{\mu}{\Lambda(\mathrm{t})} \end{pmatrix} \tag{5.5}$$

$$\begin{aligned} T_{11} &= -p + \mu\Lambda^2 \\ T_{22} &= -p + \frac{\mu}{\Lambda} \\ T_{33} &= -p + \frac{\mu}{\Lambda} \end{aligned} \tag{5.6}$$

For uniaxial extension $\quad T_{22} = T_{33} = 0 \Rightarrow p = \dfrac{\mu}{\Lambda}$

Substituting for p in T_{11} we get

$$T_{11} = \mu\left(\Lambda^2 - \frac{1}{\Lambda}\right) \tag{5.7}$$

5.3 Phase Transition: Amorphous Phase to Glassy Phase

During cooling the glassy phase is born in a stressed state and the stress is assumed to be equal to the stress in rubbery phase at glass transition. The polymer is cooled below its glass transition temperature and thus the stress comes from two parts (a) Stress in the Amorphous (Rubbery) part and (b) Stress in the Amorphous (Glassy) part which is given as follows.

$$\begin{aligned} \mathbf{T} &= -p\mathbf{I} + \mu_a(1-\alpha)\mathbf{B}_{k_a} + \mu_g\alpha\mathbf{B}_{k_g} \\ \mathrm{T} &= -p\mathrm{I} + (1-\alpha)\mathrm{T}_a + \int_0^t \mathrm{B}_{m(\tau)}(t)\frac{d\alpha}{d\tau}d\tau \\ \mathrm{T} &= -p\mathrm{I} + (1-\alpha)\mathrm{T}_a + \int_0^t f(\mathrm{F}_{m(\tau)}(t))\frac{d\alpha}{d\tau}d\tau \end{aligned} \tag{5.7}$$

The deformation gradient is given as $\boldsymbol{F}_{m(\tau)}(t) = \boldsymbol{F}_{m(\tau)}(\tau)\boldsymbol{F}^{-1}_{\theta(\tau)}(t)$ where $\boldsymbol{F}_{m(\tau)}$ represents the mechanical part of the deformation gradient and $\boldsymbol{F}^{-1}_{\theta(\tau)}(t)$ represents the thermal part of the deformation gradient. τ is the time at which the amorphous(glassy) material is born and t is the current time. The evolution of the stress is governed by the fact that $\boldsymbol{F}_{m(\tau)}(t)$ increases while $\boldsymbol{F}^{-1}_{\theta(\tau)}(t)$ decreases so that the total deformation gradient $\boldsymbol{F}_{m(\tau)}(\tau)$ remains constant. Thus the deformation gradients and hence the left Cauchy stretch tensors take the following form.

$$\boldsymbol{F}_{m(\tau)}(t) = \begin{pmatrix} \Lambda_m(\mathrm{t}) & 0 & 0 \\ 0 & \dfrac{1}{\sqrt{\Lambda_m(\mathrm{t})}} & 0 \\ 0 & 0 & \dfrac{1}{\sqrt{\Lambda_m(\mathrm{t})}} \end{pmatrix} \tag{5.8}$$

$$\boldsymbol{F}_{\theta(\tau)}(t) = B\underset{\sim}{\mathbf{I}} \tag{5.9}$$

Where $B = 1 + \int \alpha(\theta(t) - \theta(\tau))$

$$\boldsymbol{F}_{\mathrm{m}(\tau)}(\tau) = \begin{pmatrix} \Lambda_g(\tau) & 0 & 0 \\ 0 & \dfrac{1}{\sqrt{\Lambda_g(\tau)}} & 0 \\ 0 & 0 & \dfrac{1}{\sqrt{\Lambda_g(\tau)}} \end{pmatrix} \tag{5.10}$$

$$\boldsymbol{F}_{\mathrm{m}(\tau)}(t) = \begin{pmatrix} \dfrac{\Lambda_g(\mathrm{t})}{B} & 0 & 0 \\ 0 & \dfrac{1}{B\sqrt{\Lambda_g(\mathrm{t})}} & 0 \\ 0 & 0 & \dfrac{1}{B\sqrt{\Lambda_g(\mathrm{t})}} \end{pmatrix} \tag{5.11}$$

Thus $\boldsymbol{B}_{\mathrm{m}(\tau)}(t)$ is written as follows

$$\therefore \boldsymbol{B}_{\mathrm{m}(\tau)}(t) = \boldsymbol{F}_{\mathrm{m}(\tau)}(t)\boldsymbol{F}^{T}{}_{\mathrm{m}(\tau)}(t) = \begin{pmatrix} \dfrac{\Lambda_g{}^2(\tau)}{B^2(\mathrm{t})} & 0 & 0 \\ 0 & \dfrac{1}{B^2(\mathrm{t})\Lambda_g(\tau)} & 0 \\ 0 & 0 & \dfrac{1}{B^2(\mathrm{t})\Lambda_g(\tau)} \end{pmatrix} \tag{5.12}$$

$$\mathrm{T} = (1-\alpha)\left(\Lambda_a^2(\mathrm{t}) - \frac{1}{\Lambda_a(\mathrm{t})}\right) + \frac{\mu_g}{\mu_a}\int_0^t \left(\frac{\Lambda_g^2(\tau)}{B^2(\mathrm{t})} - \frac{1}{B^2(\mathrm{t})\Lambda_g(\tau)}\right)\frac{d\alpha}{d\tau}d\tau \tag{5.13}$$

Where Λ_a is the stretch in the amorphous (rubbery) phase and Λ_m is the stretch in the glassy phase.

α is the amount of glassy material formed and $\frac{d\alpha}{d\tau}$ is the rate at which amount of amorphous(rubbery) material gets converted in to glassy material.

5.4 Glassy Phase

During unloading, the polymer which is cooled below its glass transition temperature is unloaded so that it retains it shape. The stress in the mixture is given by the following equation.

$$\begin{aligned} \mathbf{T} &= -p\mathbf{I} + \mu_a(1-\alpha)\boldsymbol{B}_{k_a} + \mu_g\alpha\boldsymbol{B}_{k_g} \\ T &= (1-\alpha)\left(\Lambda_a^2 - \frac{1}{\Lambda_a}\right) + \frac{\mu_g}{\mu_a}\int_0^t B_{n(\tau)}(t)dt \\ T &= (1-\alpha)\left(\Lambda_a^2 - \frac{1}{\Lambda_a}\right) + \frac{\mu_g}{\mu_a}\int_0^t f(F_{n(\tau)}(t))dt \end{aligned} \tag{5.14}$$

Thus the deformation gradient takes the following form, $\boldsymbol{F}_{n(\tau)}(t) = \boldsymbol{F}_{unload}(t)\boldsymbol{F}_{m(\tau)}(t)$

$$\boldsymbol{F}_{n(\tau)}(t) = \begin{pmatrix} \Lambda(t) & 0 & 0 \\ 0 & \frac{1}{\sqrt{\Lambda(t)}} & 0 \\ 0 & 0 & \frac{1}{\sqrt{\Lambda(t)}} \end{pmatrix} \begin{pmatrix} \frac{\Lambda_g(\tau)}{B} & 0 & 0 \\ 0 & \frac{1}{B\sqrt{\Lambda_g(\tau)}} & 0 \\ 0 & 0 & \frac{1}{B\sqrt{\Lambda_g(\tau)}} \end{pmatrix} \tag{5.15}$$

The equation of stress takes the following form

$$\boldsymbol{T} = (1-\alpha)\left(\Lambda_a^2 - \frac{1}{\Lambda_a}\right) + \frac{1}{B^2}\frac{\mu_g}{\mu_a}\int_0^t \left(\Lambda(t)\Lambda_g{}^2(\tau) - \frac{1}{\Lambda(t)\Lambda_g(\tau)}\right)\frac{d\alpha}{d\tau}d\tau \tag{5.16}$$

5.5 Phase Transition: Glassy Phase to Amorphous Phase

During melting the stress in the material is zero and the equation simplifies as follows

$$(1-\alpha)\left(\Lambda_a^2-\frac{1}{\Lambda_a}\right)+\frac{\mu_g}{\mu_a}\int_0^t\left(\frac{\Lambda_g^2}{B^2}-\frac{1}{B^2\Lambda_g}\right)\frac{d\alpha}{d\tau}d\tau=0 \tag{5.17}$$

The above equation is solved for Λ_a which eventually simplifies to

$$(1-\alpha)\Lambda_a^3+x\Lambda_a-(1+\alpha)=0 \tag{5.18}$$

where $x=-\frac{\mu_g}{\mu_a}\int_0^t\left(\frac{\Lambda_m^2}{B^2}-\frac{1}{B^2\Lambda_m}\right)\frac{d\alpha}{d\tau}d\tau$

5.6 Results

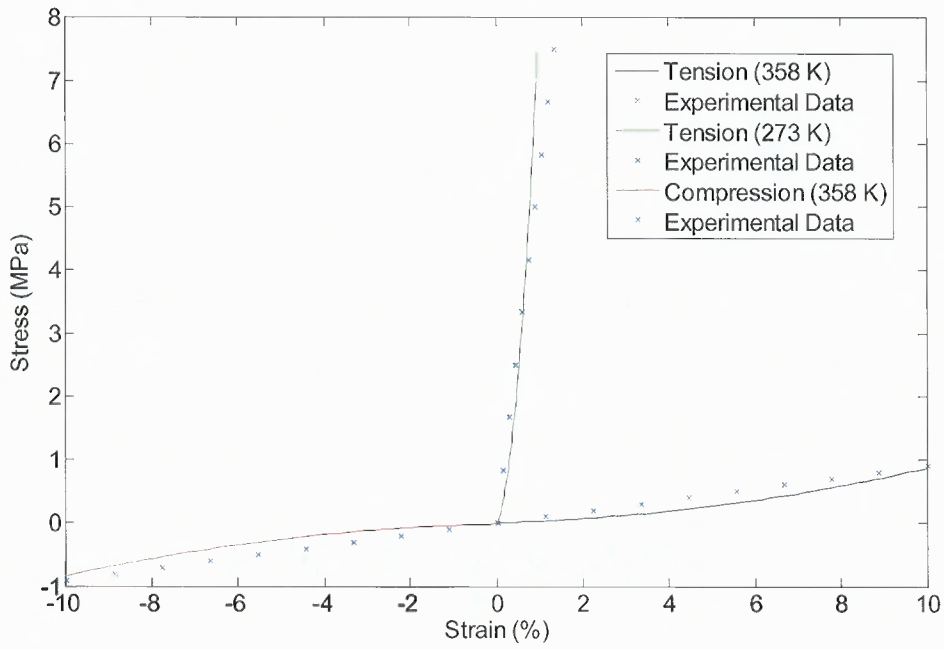

Figure 5.7 Stress vs strain plot (Yiping Liu et al. 2005).

Figure 5.7 shows the comparison between the experimental data and developed model for small strain (9.1%). Isothermal stress-strain tests were used for both tension and compression, both above and below the glass transition temperature. The experimental data validates the model so that the stress-strain relations are linear within the strain ranges considered.

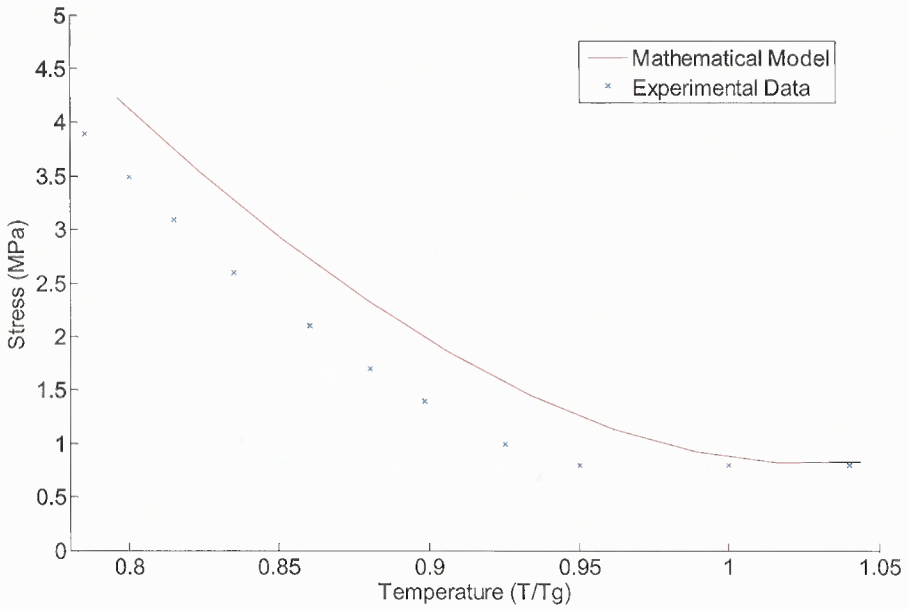

Figure 5.8 Stress vs temperature (Yiping Liu et al. 2005).

Figure 5.8 is a plot of stress and temperature and it captures glass transition of the shape memory polymer in detail. The evolution of stress on cooling is characterized by two stages. In the first stage which is within the vicinity of Tg the thermal stress is very small. In the second stage which corresponds to the glassy state the thermal stress rises rapidly. The transition between these two stages is gradual and smooth. The thermal stress during cooling provides a positive contribution to the total since the sample is attempting to contract under a fixed constraint.

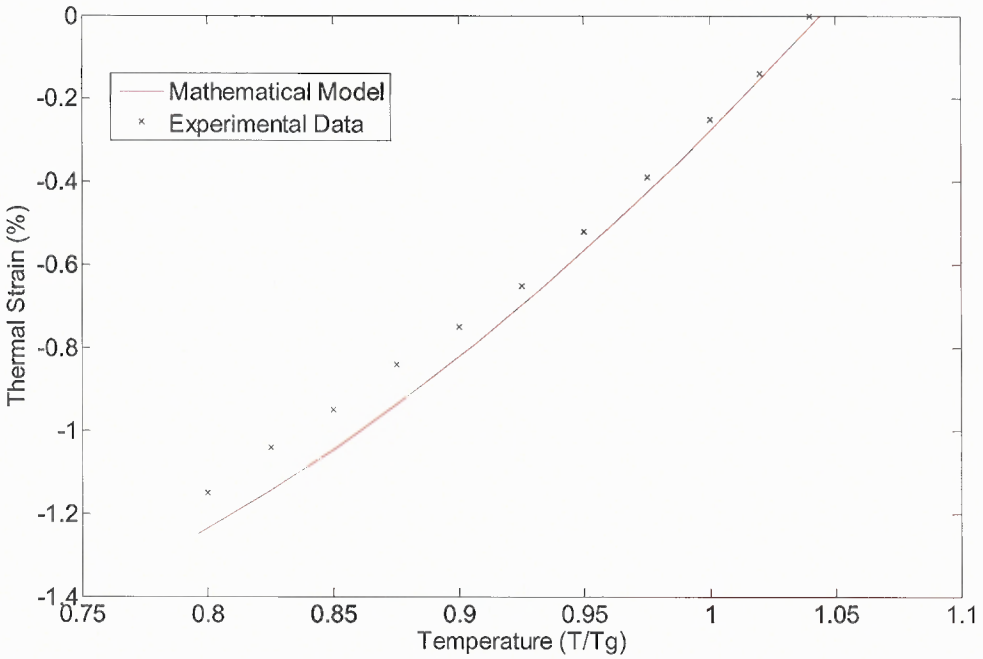

Figure 5.9 Thermal strain vs temperature (Yiping Liu et al. 2005).

Figure 5.9 shows that the thermal strain decreases on cooling. The co-efficient of the thermal expansion which is defined as the slope of thermal strain curve is more above the glass transition temperature and less below the glass transition temperature.

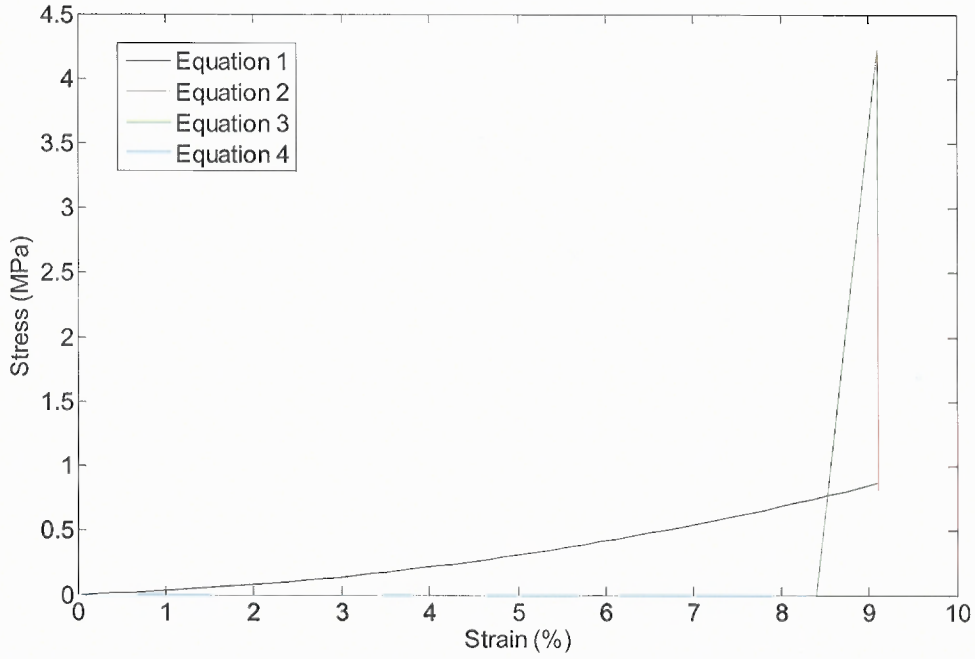

Figure 5.10 Stress vs strain for the complete SMP cycle (Yiping Liu et al. 2005).

Figure 5.10 shows the entire SMP cycle which is validated against the experimental data from Figure 5.1. On loading the stress and strain go up. Cooling below the glass transition the stress goes up as the glassy material in born in a stressed state. On unloading the stress goes to zero while only a small amount of strain is recovered thus helping in retaining the temporary shape. And on melting the SMP goes to its original shape

CHAPTER 6

NANOPARTICLE REINFORCED GLASSY SMP

6.1 Introduction

Although SMP materials have found a niche application as an actuation material in MEMS, they have not fully reached their technological potential. A significant drawback of unreinforced SMP materials is their low stiffness compared to metals and ceramics. The low stiffness of SMP resins results in a relatively small recovery force under constraint (actuation force) compared to alternative active actuation materials or schemes. On the other hand, adding reinforcements to the SMP matrix allows tailoring of the material stiffness and attainable clamping force for MEMS applications. A few researchers have studied macroscale composite materials based on a shape memory polymer matrix. Preliminary work in the late 90s demonstrated that fiberglass and Kevlar reinforcements increased the stiffness of the SMP resins and reduced recoverable strain levels. Moreover, discontinuous fiber reinforced composites showed shape recovery in all directions, while continuous fiber reinforced composites only showed recoverability under transverse tension or bending.

Recent work Gall et al. 2000 on continuous carbon fiber reinforced shape memory polymer composites has focused on materials for the deployable space structure industry. All previous work on SMP based composites has considered macro-scale composite materials. Gall et al 2002 have studied SMP-based composite materials fabricated at μm to mm size scales with nanoparticulate reinforcements. These materials are particularly attractive for MEMS applications where structure size scales are on the order of microns.

In order to tailor material properties for micron-sized structures, the heterogeneity of the reinforcement structure must be on the order of nanometers.

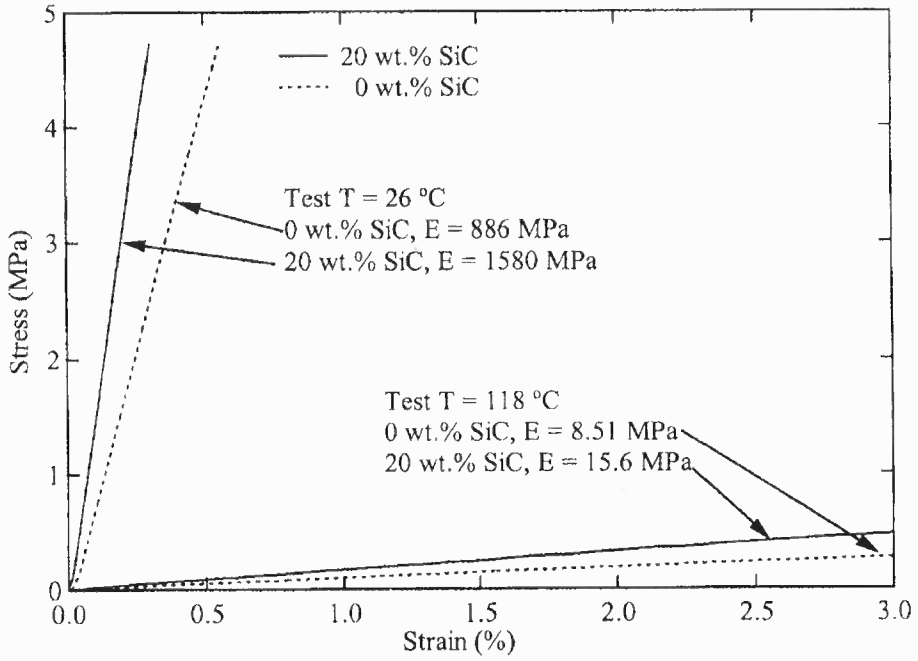

Figure 6.1 Elastic moduli of the SMP and SMP composite at 26 and 118 °C.

Figure 6.1 (Yiping Liu et al. 2003) shows the stress-strain response of a SMP above and below glass transition temperature. It is evident from the figure that at both 26 and 118 °C, the modulus of SMP nanocomposite with 20 wt.% of SiC is about two times that of the pure SMP.

Against the backdrop of the above discussion, a model for nanoparticles reinforced glassy shape memory polymer is being developed. The concentration factor of the nanoparticles is incorporated with the shear modulus of the amorphous phase which results in an improved stress strain response.

6.2 Rubbery Phase

The equation for stress in the rubbery phase is formulated by using the equation(5.1) of rubbery phase from the glassy SMP model developed.

$$T_{11} = \mu_a \left(\Lambda_a^2 - \frac{1}{\Lambda_a} \right) \tag{6.1}$$

Where **T** is the stress in the rubbery part of the polymer and μ_a is the modulus of the rubbery phase. k is the concentration of nanoparticles.

6.3 Glassy Phase

The equation for stress in the glassy phase is formulated by using equation 5.2 from the from the glassy SMP model developed.

$$T_{11} = (1-\alpha)\frac{\mu_a + \alpha_1 k}{\mu_a}\left(\Lambda_a^2(\mathrm{t}) - \frac{1}{\Lambda_a(\mathrm{t})} \right) + \frac{\mu_g + \alpha_2 k}{\mu_a} \int_0^t \left(\Lambda_m^2(\mathrm{t}) - \frac{1}{\Lambda_m^2(\mathrm{t})} \right) \frac{d\alpha}{d\tau} d\tau \tag{6.2}$$

$$\text{Where } \Lambda_m^2(\mathrm{t}) = \frac{\Lambda_g^2(\tau)}{B^2(\mathrm{t})}$$

6.4 Results

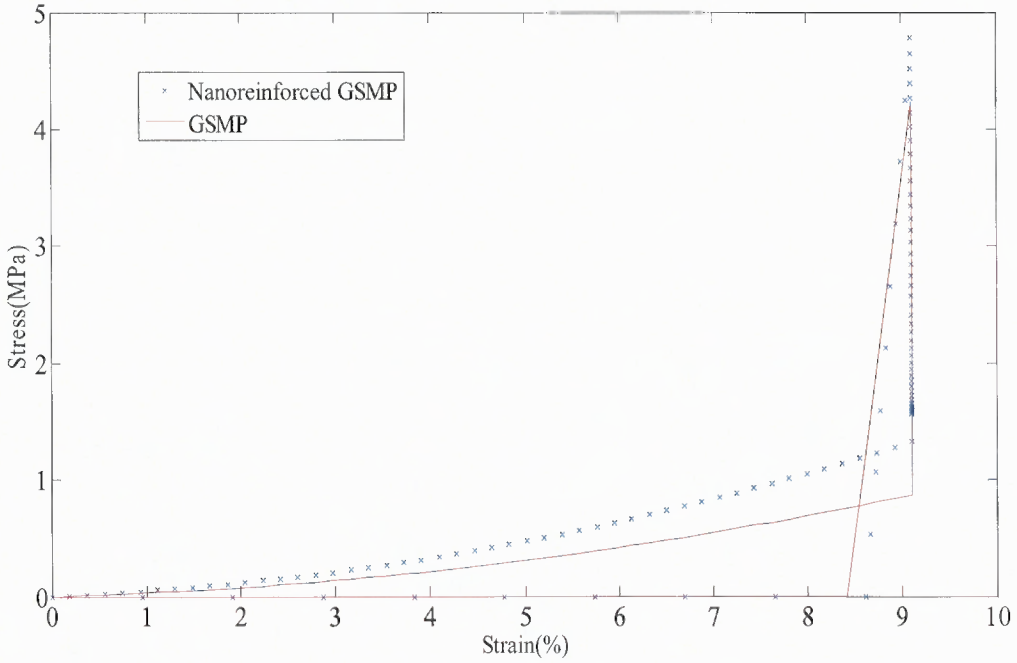

Figure 6.2 Stress vs strain (Yiping Liu et al. 2005).

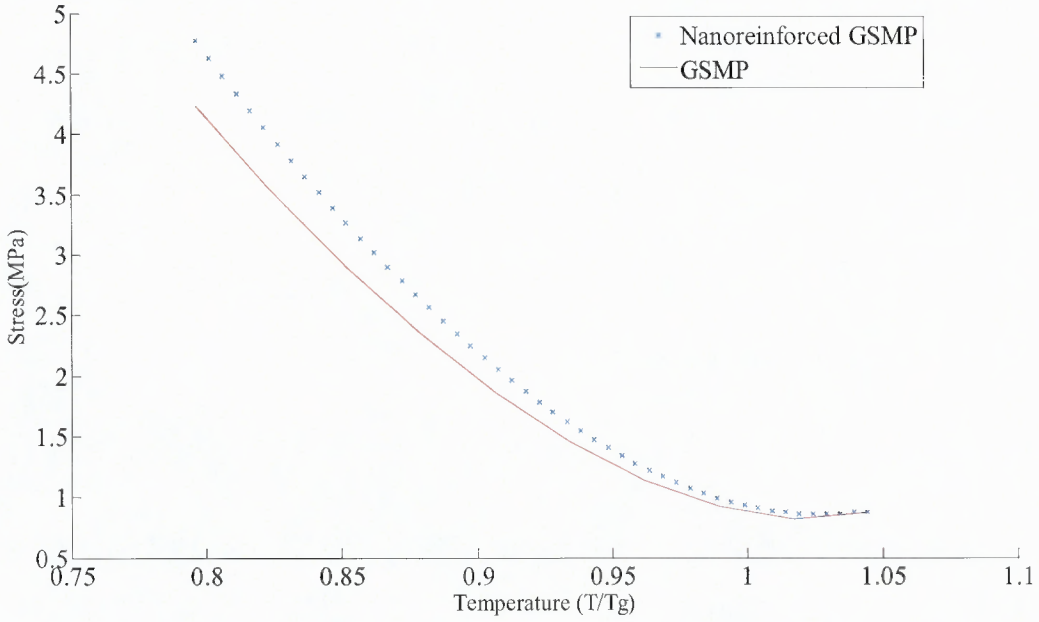

Figure 6.3 Stress vs temperature (Yiping Liu et al. 2005).

CHAPTER 7

APPLICATION OF THE CSMP MODEL TO ONE DIMENSIONAL PROBLEM - TORSION OF A CYLINDER

7.1 Introduction

In this section, the cycle of torsion of a shape memory polymer is presented as a representative for non-homogenous deformation. The geometry of the problem is illustrated in figure shown Figure 7.1. It is a long, circular cylinder which is fixed at one end. A moment per unit length is applied to the other end causing it to shear. The cylinder is then cooled below its crystallizing temperature keeping the shape fixed. Following this it is unloaded and then melting of the crystalline phase returns the cylinder to its original shape. The deformation of the cylinder in cylindrical co-ordinates is given by:

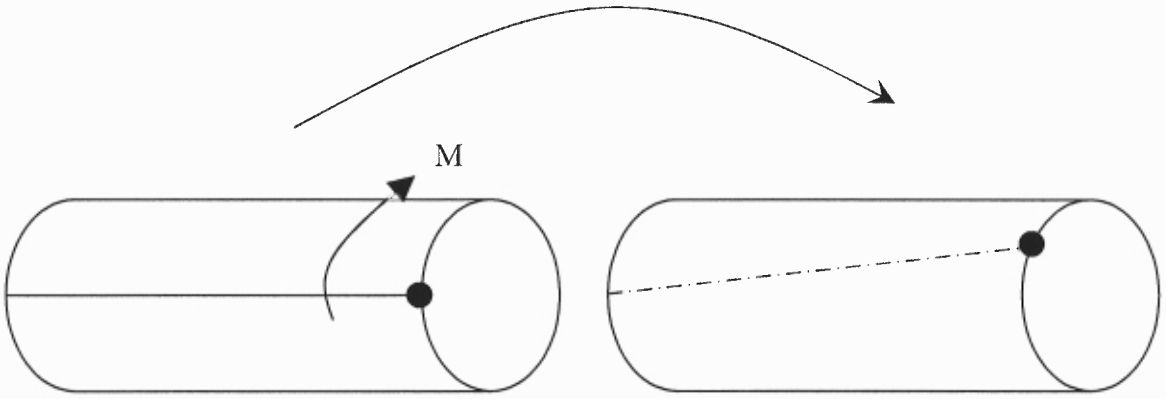

Figure 7.1 Torsion of a cylinder.

7.2 Kinematics

The motion is given as follows

$$\begin{aligned} r &= r(R), \\ \theta &= \Theta + kZ, \\ z &= Z. \end{aligned} \tag{7.1}$$

Where K is the shear,

The deformation gradient is given as

$$\mathbf{F} = \begin{pmatrix} \frac{dr}{dR} & 0 & 0 \\ 0 & \frac{r}{R} & rk \\ 0 & 0 & 1 \end{pmatrix} \tag{7.2}$$

Since material is incompressible det F = 1

$\frac{dr}{dR} \cdot \frac{r}{R} = 1$

Integrating above equation $\Rightarrow r = R$

The deformation gradient and the right Cauchy stretch tensor take the following form:

$$\mathbf{F}_{k_a} = \begin{pmatrix} 1 & 0 & 0 \\ 0 & 1 & rk \\ 0 & 0 & 1 \end{pmatrix}, \qquad \mathbf{B}_{k_a} = \mathbf{F}\mathbf{F}^{T} = \mathbf{F} = \begin{pmatrix} 1 & 0 & 0 \\ 0 & 1+r^2k^2 & rk \\ 0 & rk & 1 \end{pmatrix}, \tag{7.3}$$

$$\mathbf{F}_{k_{c(r)}} = \begin{pmatrix} 1 & 0 & 0 \\ 0 & 1 & r\Delta k \\ 0 & 0 & 1 \end{pmatrix}, \qquad \mathbf{B}_{k_{c(r)}} = \begin{pmatrix} 1 & 0 & 0 \\ 0 & 1+r^2\Delta k^2 & r\Delta k \\ 0 & r\Delta k & 1 \end{pmatrix}, \tag{7.4}$$

The stress in the cylinder is given by the following equation:

$$\mathbf{T} = -\mathrm{pI} + 2\mathrm{W}_1\mathbf{B} - 2\mathrm{W}_2\mathbf{B} \tag{7.5}$$

Whose cylindrical co-ordinates are given as follows:

$$\begin{aligned} T_{rr} &= -p + 2W_1 - 2W_2 \\ T_{\theta\theta} &= -p + 2W_1(1 + r^2k^2) - 2W_2 \\ T_{zz} &= -p + 2W_1 - 2W_2(1 + r^2k^2) \\ T_{\theta z} &= 2W_1 rk + 2W_2 rk \end{aligned} \tag{7.6}$$

Moment required for Torsion is given by:

$$M = \int_0^R T_{\theta z} \cdot r \cdot 2\pi r \, dr \tag{7.7}$$

For neo - hookean material, $T_{\theta z} = \mu rk$

$$\therefore M = \frac{\pi \mu k R^4}{2} \tag{7.8}$$

Using the above motion and kinematics the equations for the SMP cycle are written as follows.

Loading: When the moment is applied to the cylinder the relationship between moment and shear is given by the following relation.

$$T_{\theta z} = \frac{M(t)}{\frac{\pi \mu r^4}{2}} = k(t) \tag{7.9}$$

Cooling: The sheared cylinder is cooled below the crystallization under two different conditions resulting in different set of conditions.

(a) Crystallization Under Constant Shear:

$$T_{\theta z} = \frac{M(t)}{\frac{\pi \mu r^4}{2}} = (1 - \alpha(t))k(t) \tag{7.10}$$

(b) Crystallization Under Constant Moment:

$$T_{\theta z} = \frac{M(t)}{\frac{\pi \mu r^4}{2}} = k(t)(1 - \alpha(t) + I_1) + I_2 \tag{7.11}$$

$$\text{where } I_1 = \int_{t_1}^{t_2} \mu_1 \frac{d\alpha}{d\tau} d\tau$$

$$I_2 = \int_{t_1}^{t_2} -\mu_1 k(\tau) \frac{d\alpha}{d\tau} d\tau$$

Unloading: On unloading the temporary shape of the cylinder is fixed and following equation for shear is obtained.

$$T_{\theta z} = \frac{M(t)}{\frac{\pi \mu r^4}{2}} = k(t)(1 - \alpha(t) + I_1) + I_2 \tag{7.12}$$

Melting: Melting above the crystallization temperature takes the cylinder back to its original shape and the following relationship holds true.

$$T_{\theta z} = \frac{M(t)}{\frac{\pi \mu r^4}{2}} = k(t)(1 - \alpha(t) + I_1) + I_2 \tag{7.13}$$

7.3 Solution Method

Loading Process:

The cylinder is loaded by gradually increasing the applied moment at the outer radius, which produces shearing. Since during the loading process the polymer is amorphous, from the above equations, the shear inside the cylinder is given by:

$$T_{\theta z} = \frac{M(t)}{\frac{\pi \mu r^4}{2}} = k(t) \tag{7.14}$$

Cooling Process:

Once cooling is initiated, the rate at which crystallization takes place is given by a crystallization rate equation. The rate of crystallization is given through a differential equation for the mass fraction of the crystalline phase and is defined as follows:

$$\begin{aligned} &\alpha = 0, && \textit{for} \quad 0 < \mathrm{t} < \mathrm{t}_s, \\ &\frac{d\alpha}{d\mathrm{t}} = G(\mathrm{t} - \mathrm{t}_s)(\alpha_0 - \alpha), && \textit{for} \quad \mathrm{t}_s < \mathrm{t} < \mathrm{t}_f, \end{aligned} \tag{7.15}$$

where, G is a constant, α_0 is the maximum crystallinity possible in the material and t_s is the time at which crystallization is initiated. The above equation is solved numerically using a standard numerical scheme for ordinary differential equations. Once crystallization ceases, i.e., when, $\alpha = \alpha_0$ at a later time denoted by t_f, the material is unloaded. Crystallization is done under two different conditions. The first case is crystallization under constant shear and the second is crystallization under constant moment.

Crystallization under constant local shear: Once the maximum moment is applied, crystallization begins keeping the local shear constant. As the new crystals form in a stress free state during the crystallization process, the moment required to maintain a state of constant shear decreases. During the crystallization process the local shear remains constant, i.e.

$$\kappa(\tau) = \kappa(\mathrm{t}_1) \quad \textit{for} \quad \tau \in \left[\mathrm{t}_s, \mathrm{t}_f\right] \tag{7.16}$$

The equation for shear stress can be written as

$$\mathrm{T}_{\theta z} = \frac{\mathrm{M(t)}}{\frac{\pi \mu \mathrm{r}^4}{2}} = (1 - \alpha(\mathrm{t}))k(t) \tag{7.17}$$

Crystallization with constant applied moment: In the second case, after loading, the moment is kept constant, and crystallization is initiated. Because the newly crystallized material is formed in a stress free state, while the applied moment is kept constant, the polymer will continue to shear as crystallization proceeds. The reason is attributed to the fact that the ability of the amorphous polymer to carry the moment diminishes, as there is less amorphous polymer available. However, the newly formed crystalline polymer is formed in a stress free state and is unable to carry the load either. The only way the polymer can sustain this moment is to shear as the already present crystalline phase and the remaining amorphous phase take on the additional moment. The crystalline phase is a lot stiffer than the original amorphous phase and hence the magnitude of this incremental shear is much smaller than the original shear.

The equation for shear stress can be written as

$$T_{\theta z} = \frac{M(t)}{\frac{\pi \mu r^4}{2}} = k(t)(1-\alpha(t)+I_1)+I_2 \tag{7.18}$$

$$\text{where } I_1 = \int_{t_1}^{t_2} \mu_1 \frac{d\alpha}{d\tau} d\tau$$

$$I_2 = \int_{t_1}^{t_2} -\mu_1 k(\tau) \frac{d\alpha}{d\tau} d\tau$$

Unloading Process: To determine the shape recovery on unloading it is noted that the relationship between the shear and the applied moment is given by Equations (7.10) and (7.11) with the exception that the limits of the integrals are now fixed from time t_s (the time crystallization began) to time t_f (when crystallization ended). Substituting these integrals into Equation (7.10) the variation of shear at with time is determined by solving

the cubic equation for different decreasing values of moment, till the applied moment is zero.

Melting Process: After unloading, the polymer is in its temporary shape. Return to the original shape is accomplished by melting the crystalline phase. This is done by heating the polymer above the melting temperature of the crystalline phase. As described earlier, the temporary shape of the polymer is retained because the two phases have different stress-free states. As the crystalline phase melts, the shape of the polymer slowly returns to its original shape as the crystalline phase is no longer present to keep it in its temporary shape.

To track the evolution of the shape as it evolves from the temporary to permanent shape it is necessary to track which fraction of the crystalline phase is melting at any given time. This is particularly true for the case where crystallization takes place under constant stress as different crystals form at different stretches, and for this reason, the crystalline phase has different stress-free states. So, when a crystallite that is more stressed melts, the polymer as a whole will retract towards its original shape more than if a less stressed crystallite melted. For the constant stretch case all the crystals form in the same configuration, and therefore, the order in which the crystals melt does not impact the intermediate shapes occupied by the polymer. However, for crystallization under constant stress, or for a more general case wherein crystallization takes place under conditions of varying stress, the order in which the crystallites melt is important. The assumption made with regards to the melting process is that the crystallites formed last melt first, this assumption is supported from experiments as crystallites formed farthest from the equilibrium melting temperature (i.e. crystallites that were formed last) are

thinner and melt at lower temperatures (i.e. melt first). During the melting process, the crystalline phase begins to melt at some time denoted in this study

7.4 Results

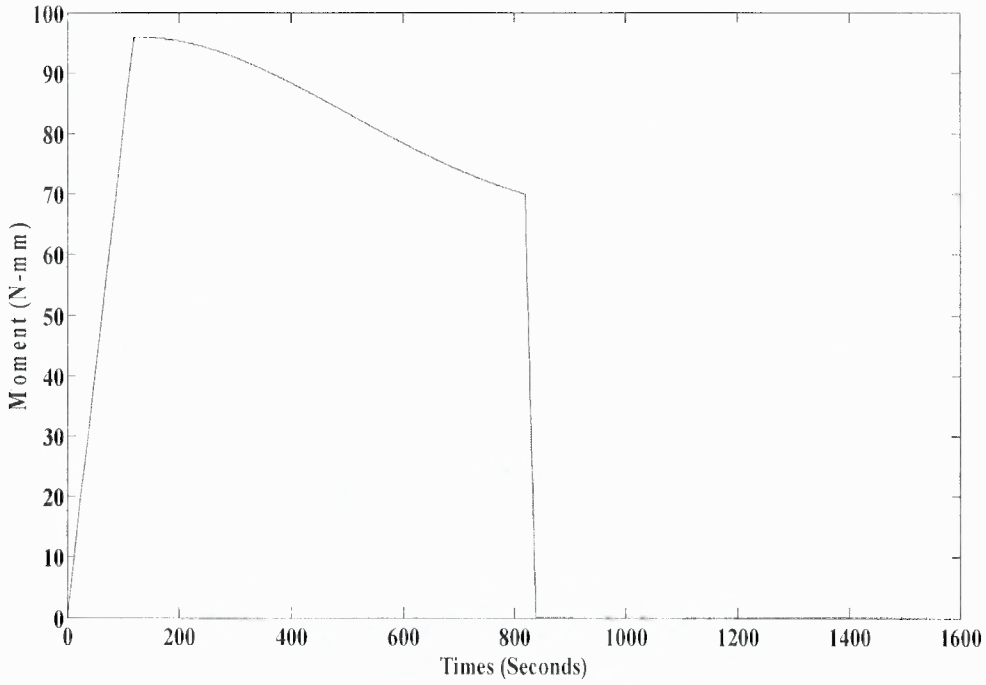

Figure 7.2 Moment vs Time (Torsion of a cylinder – Constant Shear). The constants used are mentioned in Table 7.1.

Table 7.1 Following Data were used to Simulate Torsion of a Cylinder (Constant Shear Process)

α_0	t_s	t_{ms}	G (in sec^{-2})	μ_a (in Mpa)	μ_c
0.53	120	800	0.00007	0.256	50

Figure 7.2 is a plot of Moment vs Time when the cylinder is cooled under constant shear. The moment increases on deforming the cylinder. When cooling under

constant shear the moment decreases and the decrease is governed by the rate of crystallization equation. On unloading the moment goes to zero and the cylinder retains its temporary shape. Heating above the melting temperature takes the cylinder to its original shape.

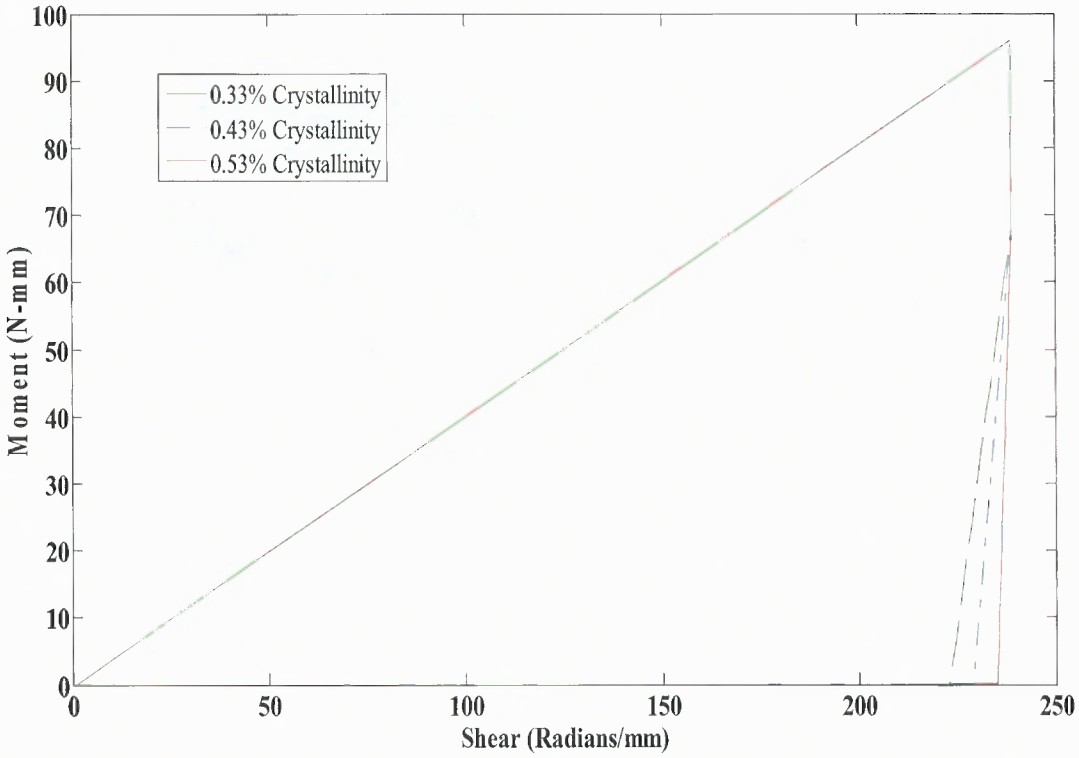

Figure 7.3 Moment vs Shear (Torsion of a cylinder – Constant Shear).

Figure 7.3 is a plot of Moment vs Shear. The moment and shear increase when the cylinder is deformed above the crystallization temperature. When cooling under constant shear the moment decreases, this is identical to cooling under constant strain for a uniaxial cycle. On unloading the moment goes to zero while there is a small recovery of shear which represents the shape fixity. Heating above the melting temperature, the moment and shear go to zero.

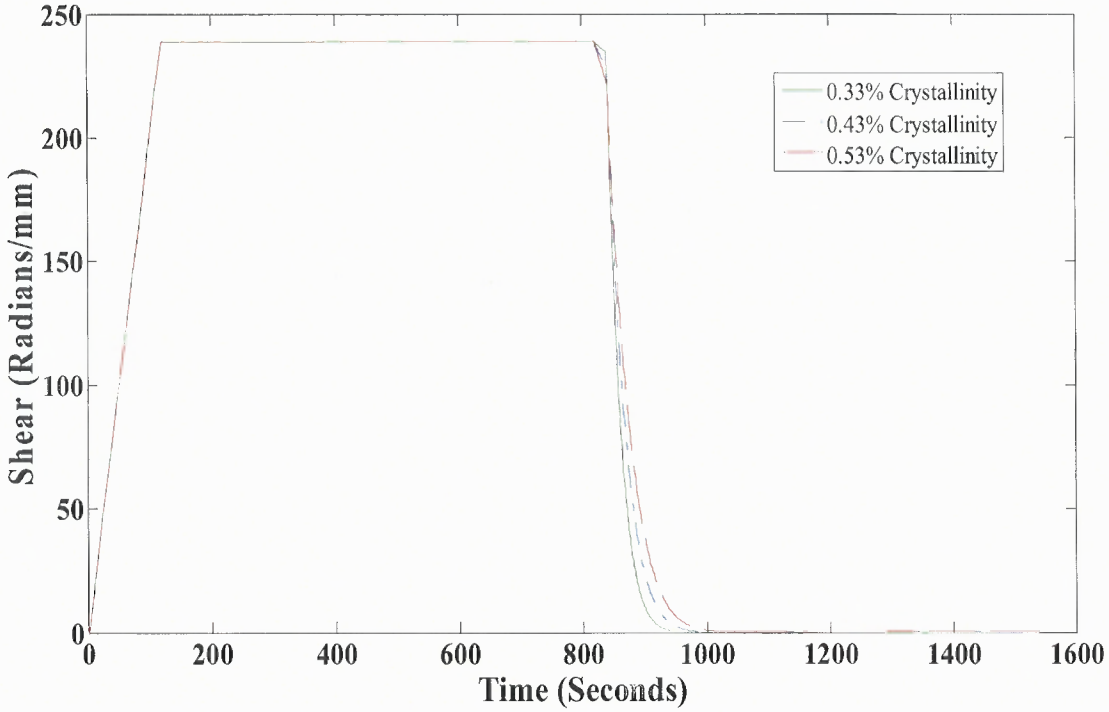

Figure 7.4 Shear vs Time (Torsion of a cylinder – Constant Shear).

Figure 7.4 is a plot of Shear vs time for constant shear. The shear goes up on applying the moment, remains constant on cooling below the crystallization temperature. On unloading there is a drop in shear when the temporary shape is fixed and finally goes the shear goes to zero on heating above the melting temperature.

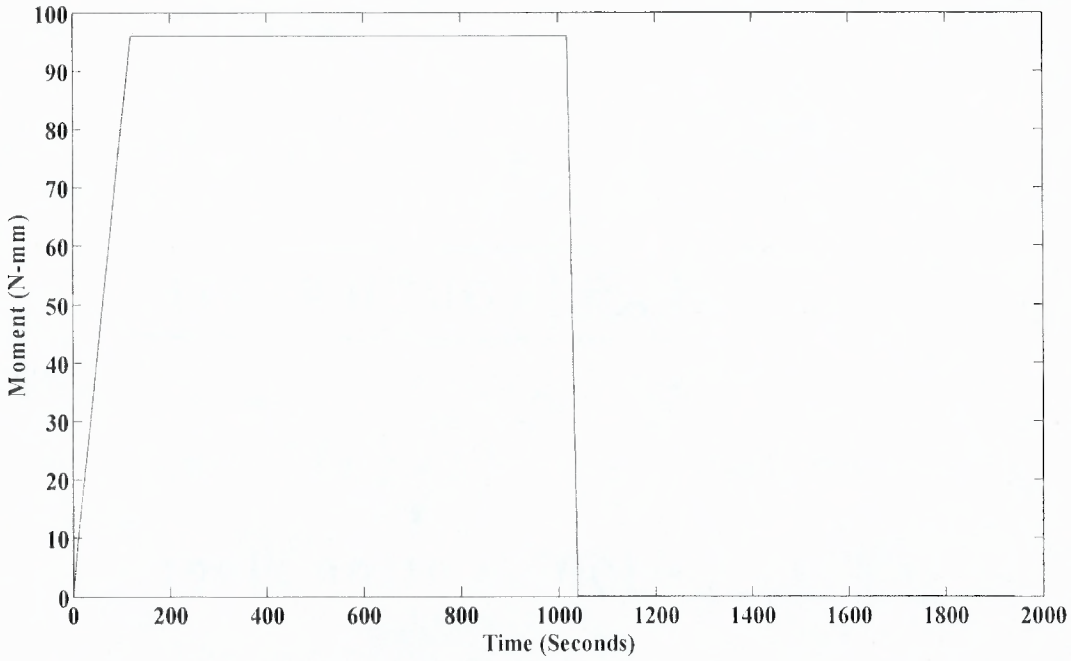

Figure 7.5 Moment vs Time (Torsion of a cylinder – Constant Moment). The constants used are mentioned in Table 7.2.

Table 7.2 Following Data used for Simulating of Torsion of Cylinder (Constant Moment Process)

α_0	t_s	t_{ms}	G (in sec^{-2})	μ_a (in Mpa)	μ_c
0.33	120	1200	0.00007	0.256	50

Figure 7.5 is a plot of Shear vs time for crystallization under constant moment. The shear goes up on applying the moment and increases when cooling below the crystallization temperature. On unloading there is a drop in shear when the temporary shape is fixed and finally goes the shear goes to zero on heating above the melting temperature.

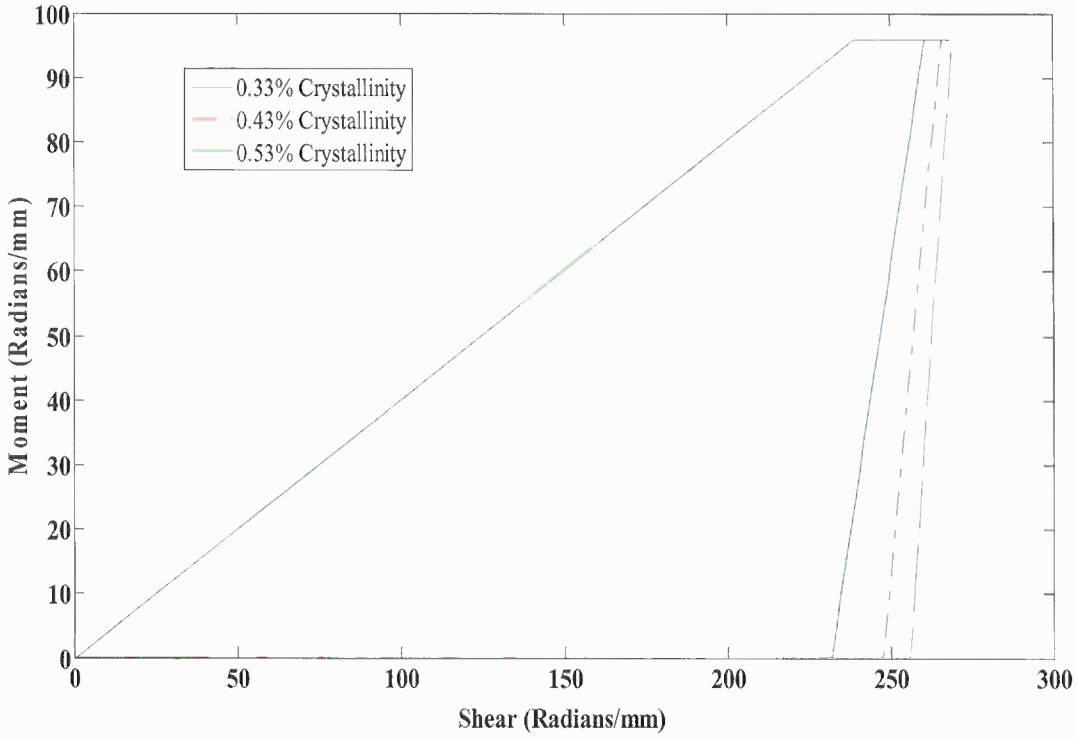

Figure 7.6 Moment vs Shear (Torsion of a cylinder).

Figure 7.6 is a plot of Moment vs Shear for crystallization under constant moment. The moment and shear increase when the cylinder is deformed above the crystallization temperature. When cooling under constant moment the shear increases. On unloading the moment goes to zero while majority of the shear is retained, which represents the shape fixity. Heating above the melting temperature, the moment and shear go to zero.

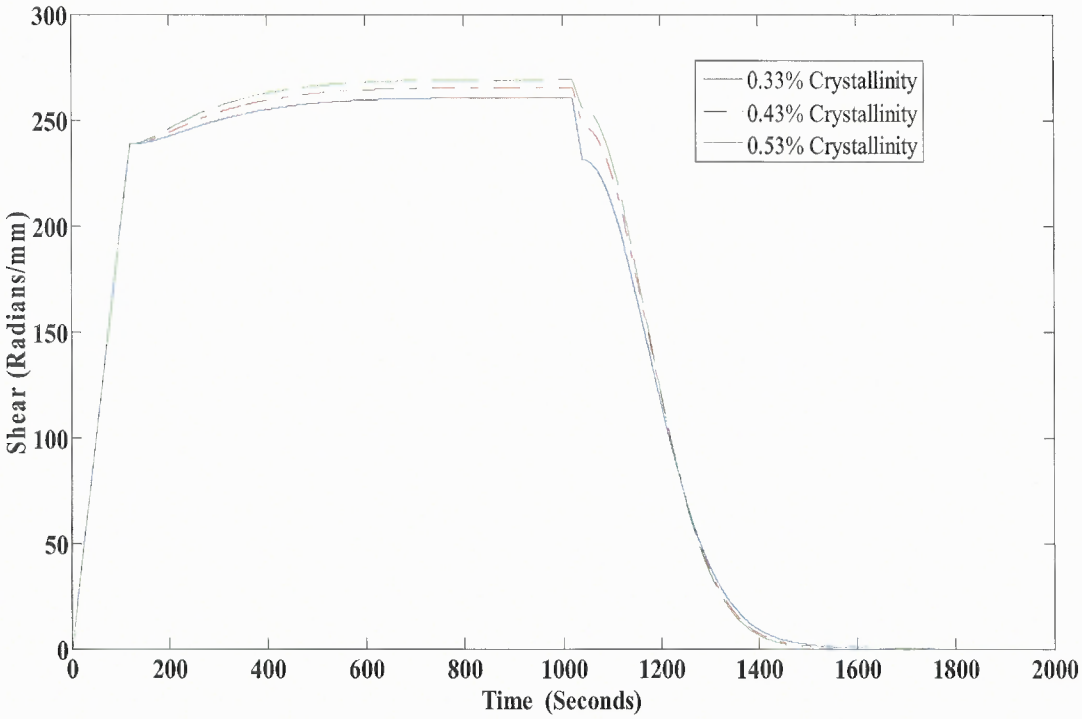

Figure 7.7 Shear vs Time (Torsion of a cylinder – Constant Moment).

Figure 7.7 is a plot of Shear vs time for crystallization under constant moment. The shear goes up on applying the moment and increases when cooling below the crystallization temperature. On unloading there is a drop in shear when the temporary shape is fixed and finally goes the shear goes to zero on heating above the melting temperature.

7.4.1 Torsion of a Cylinder for GSMP (Glassy Shape Memory Polymer)

The representative cycle is further solved for a shape memory polymer undergoing glass transition and where there is complete conversion of the amorphous rubbery phase in to a glassy solid. A moment per unit length is applied at one end of the cylinder causing it to shear. The cylinder is then cooled below its glass transition temperature keeping the shape fixed. Following this it is unloaded and then melting of the glassy phase returns the

cylinder to its original shape. The deformation of the cylinder in cylindrical co-ordinates and the kinematics is given in Sections 7.1 and 7.2. The solution methodology is analogous to that of crystallizable shape memory polymer cycle and is given by Section 7.3.

7.4.2 Results

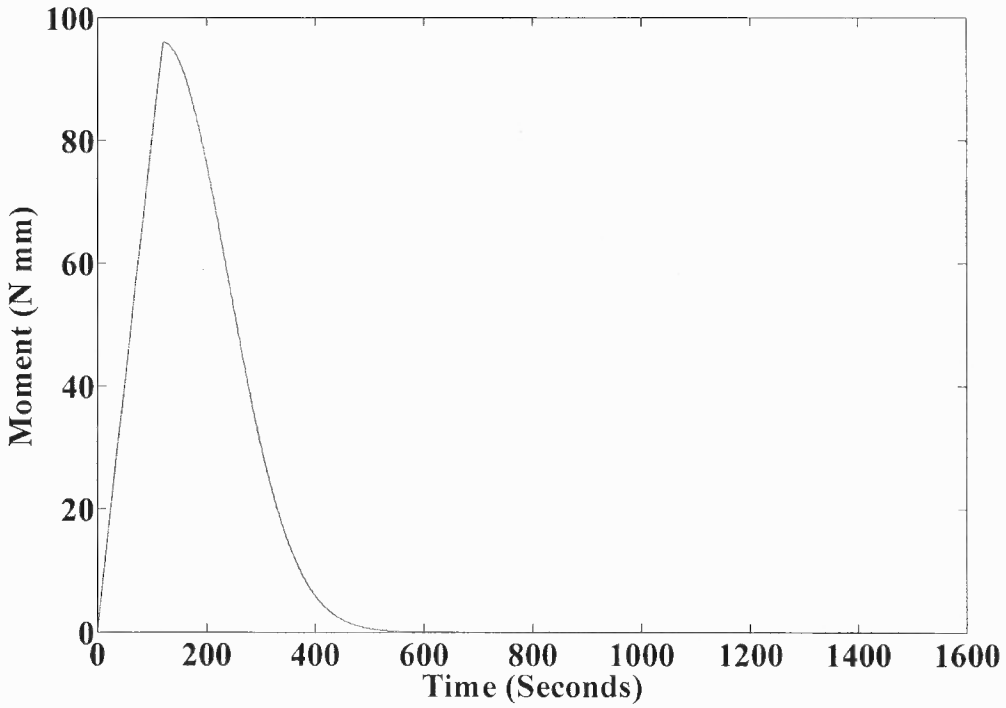

Figure 7.8 Moment vs Time (Torsion of a cylinder for GSMP).

Figure 7.8 is a plot of Moment vs Time when the cylinder is cooled under constant shear. The moment increases on deforming the cylinder. When cooling under constant shear, the moment decreases and the decrease is governed by the rate of crystallization equation. The moment eventually goes to zero as there is complete conversion of the material in to glassy phase. On unloading the moment remains zero and

the cylinder retains its temporary shape. Heating above the melting temperature takes the cylinder to its original shape.

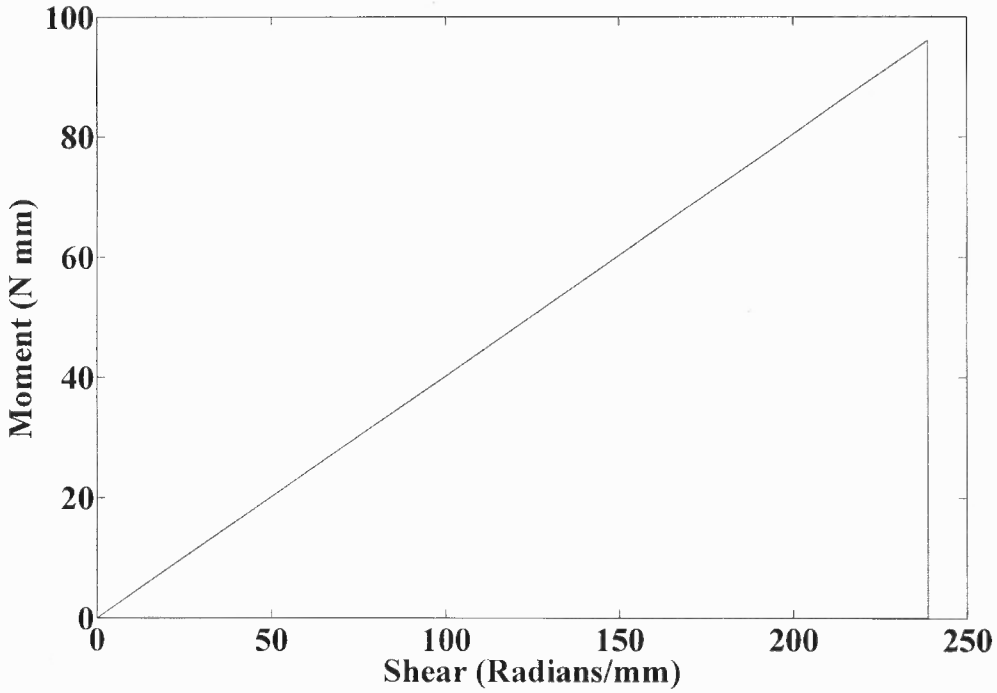

Figure 7.9 Moment vs Shear (Torsion of a cylinder for GSMP).

Figure 7.9 is a plot of Moment vs Shear. The moment and shear increase when the cylinder is deformed above the glass transition temperature. When cooling under constant shear, the moment decreases (this is identical to cooling under constant strain for a uniaxial cycle) and goes to zero. On unloading the moment remains zero and there is shape fixity. Heating above the melting temperature, the moment and shear go to zero.

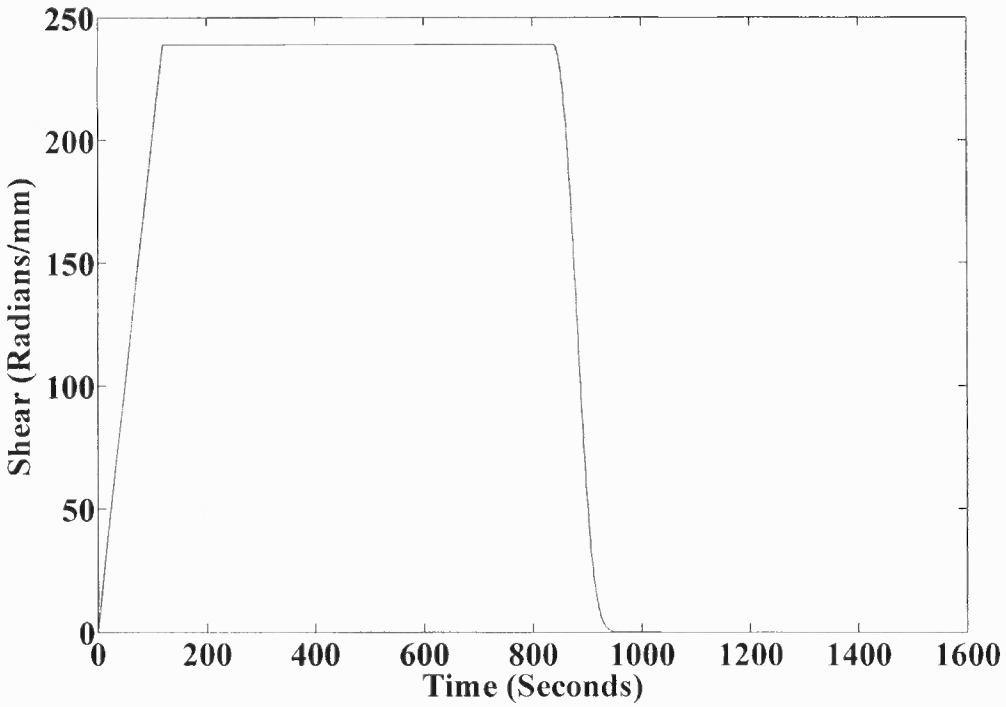

Figure 7.10 Shear vs Time (Torsion of a cylinder for GSMP).

Figure 7.10 is a plot of Shear vs Time for constant shear. The shear goes up on applying the moment and remains constant on cooling below the glass transition temperature. On unloading the shear remains constant and temporary shape is fixed. Heating above the melting temperature the shear goes to zero.

CHAPTER 8

FINITE ELEMENT MODULE FOR CRYSTALLIZABLE /GLASSY SHAPE MEMORY POLYMERS

8.1 Introduction

Finite element analysis (FEA) is a numerical method for analyzing complex structural and thermal problems. It is a powerful computer-based tool widely used by engineers and scientists for understanding the mechanics of physical systems. FEA uses a complex system of points called nodes which make a grid called a mesh. This mesh is programmed to contain the material and structural properties which define how the structure will react to certain loading conditions. Nodes are assigned at a certain density throughout the material depending on the anticipated stress levels of a particular area. Regions which will receive large amounts of stress usually have a higher node density than those which experience little or no stress. Points of interest may consist of: fracture point of previously tested material, fillets, corners, complex detail, and high stress areas. The mesh acts like a spider web in that from each node, there extends a mesh element to each of the adjacent nodes.

There are generally two types of analysis that are widely used: 2-D modeling, and 3-D modeling. While 2-D modeling conserves simplicity and allows the analysis to be run on a relatively normal computer, it tends to yield less accurate results. 3-D modeling, however, produces more accurate results while sacrificing the ability to run on all but the fastest computers effectively. Within each of these modeling schemes, the programmer can insert numerous algorithms (functions) which may make the system behave linearly

or non-linearly. Linear systems are far less complex and generally do not take into account plastic deformation. Non-linear systems do account for plastic deformation, and many also are capable of testing a material all the way to fracture.

There are multiple loading conditions which may be applied to a system.

- Point, pressure, thermal, gravity, and centrifugal static loads
- Thermal loads from solution of heat transfer analysis
- Enforced displacements
- Heat flux and convection
- Point, pressure and gravity dynamic loads

Each FEA program may come with an element library, or one is constructed over time. Some sample elements are:

- Rod elements
- Beam elements
- Plate/Shell/Composite elements
- Shear panel
- Solid elements
- Spring elements
- Mass elements
- Rigid elements
- Viscous damping elements

Many FEA programs also are equipped with the capability to use multiple materials within the structure such as:

- Isotropic, identical throughout
- Orthotropic
- General anisotropic.

It is imperative that finite element software have good nonlinear capabilities, while dealing with polymers. Generally, nonlinear analysis is an add-on, not provided in the base package. Currently, there is no mathematical model available for GSMPs (glassy shape memory polymers) hence; there is no add-on available to add in of the commercial software package available. It is now possible to create the finite element module with help of the mathematical model described in the Chapter 4.

In this chapter, the basic theory used and step by step procedure required to develop finite element module is described. ABAQUS is one of the few commercial finite element software which allows user to include user define finite element module for newer material. Creating user subroutine (UMAT) in FORTRAN for GSMPs, finite element analysis can be carried out in ABAQUS/CAE. Required test to validate developed user subroutine (UMAT) based on the current model is also performed. ABAQUS is a highly sophisticated, general purpose finite element program, designed primarily to model the behavior of solids and structures under externally applied loading. ABAQUS includes the following features:

1. Capabilities for both static and dynamic problems.

2. The ability to model very large shape changes in solids, in both two and three dimensions.

3. A very extensive element library, including a full set of continuum elements, beam elements, shell and plate elements, among others.

4. A sophisticated capability to model contact between solids.

5. An advanced material library, including the usual elastic and elastic – plastic solids; models for foams, concrete, soils, piezoelectric materials, and many others.

6. Capabilities to model a number of phenomena of interest, including vibrations, coupled fluid/structure interactions, acoustics, buckling problems, and so on.

8.2 Weak Formulation, Linearization and Stiffness Matrix

The finite element method requires the formulation of the balance laws in the form of variational principles. From the developed model in Chapter 4, it can be said that any finite element analysis for GSMPs would be a non-linear problem and so, linearization of a weak form is essential. Balance of linear momentum is most important equation needed to be converted in to weak form to perform finite element analysis of structural problems

8.2.1 Weak Formulation and Linearization

The derivation of weak form of balance of linear momentum that can be used in finite element analysis is described as follows.

Assuming displacement, $\mathbf{u}$ is given by

$$\mathbf{u} = \mathbf{x} - \mathbf{X}, \tag{8.1}$$

The balance of linear momentum (Equation (1.11) can be rewritten in following format for body Ω

$$f(\mathbf{u}) = \int_{\Omega} (\rho \ddot{\mathbf{u}} - div\sigma - \mathbf{b}) dv = 0. \tag{8.2}$$

The weak form for the balance of linear momentum can be achieved by multiplying test function, $\eta = \eta(\mathbf{x}) = \eta(\mathbf{x}, t)$ to Equation (8.2).

$$f(\mathbf{u}) = \int_{\Omega} (\rho \mathbf{u} - div\sigma - \mathbf{b}) dv = 0 \tag{8.3}$$

Using the Equation (3.8), assuming that body Ω is in equilibrium and using standard identities of tensor algebra, following standard format of the weak can be derived

$$f(\mathbf{u}, \eta) = \int_{\Omega} \sigma \bullet gra\delta\eta dv - \int_{\Omega} \mathbf{b} \bullet \eta dv - \int_{\Omega} \mathbf{t} \bullet \eta da \tag{8.4}$$

If we look upon η as the virtual displacement field $\delta\mathbf{u}$, defined on the current configuration then Equation (8.4) becomes

$$f(\mathbf{u}, \eta) = \int_{\Omega} \sigma \bullet gra\delta\mathbf{u} dv - \int_{\Omega} \mathbf{b} \bullet \eta dv - \int_{\Omega} \mathbf{t} \bullet \eta da \tag{8.5}$$

The internal (mechanical) virtual work, δW_{int} and external (mechanical) virtual work, δW_{ext} can be defined as

$$\delta W_{\text{int}} = \int_{\Omega} \sigma \bullet gra\delta\mathbf{u} dv \tag{8.6}$$

Using Equation (8.5) and Equation (8.6) principal of virtual work can be written as follows:

$$\delta W_{\text{int}} = \delta W_{\text{ext}}. \tag{8.7}$$

The weak form of the balance of linear momentum in reference configuration as also be described below

$$f(\mathbf{u},\eta_0) = \int_{\Omega_0} \mathbf{P}\bullet Grad\eta_0\, dV - \int_{\Omega_0} \mathbf{B}\bullet\eta_0\, dV - \int_{\partial\Omega_0} \mathbf{t}_0\bullet\eta_0\, dA = 0. \tag{8.8}$$

Since the constitution equation developed is non-linear, the weak form will also be non-linear and the Newton-Raphson method, an iterative method is used to solve the problem. It is necessary to solve linearized form of the weak form for each iteration. Given a non-linear function $f(\bar{\mathbf{x}},\Delta\mathbf{u})$ one can linearize the function with respect to some direction $\hat{\mathbf{u}}$ about some known configuration $\mathbf{x}$ as

$$f(\bar{\mathbf{x}},\Delta\mathbf{u}) = f(\mathbf{x},\Delta\mathbf{u}) + Df(\mathbf{x},\Delta\mathbf{u})[\hat{\mathbf{u}}] + \mathbf{o}(\hat{\mathbf{u}}), \tag{8.9}$$

where

$$Df(\mathbf{x},\Delta\mathbf{u})[\hat{\mathbf{u}}] = \lim_{\varepsilon\to 0}\frac{f(\mathbf{x}+\varepsilon\hat{\mathbf{u}}) - f(\mathbf{x})}{\varepsilon}. \tag{8.10}$$

For Newton's method setting $f(\bar{\mathbf{x}},\Delta\mathbf{u}) = 0$ and neglecting higher order terms, we get

$$Df(\mathbf{x},\Delta\mathbf{u})[\hat{\mathbf{u}}] = -f(\mathbf{x},\Delta\mathbf{u}). \tag{8.11}$$

It is important to find the useful form of the linearized weak form of the momentum equation. It is assumed that body force $\mathbf{b}$ and surface traction $\mathbf{t}$ are independent of the deformation of the body in consideration thus the corresponding linearization of the external virtual work vanishes and the linearization will only affect the internal virtual work. For this work, the linearization of the weak form is prescribed in reference configuration. The internal virtual work in material description can be given by:

$$\delta W_{\text{int}} = \int_{\Omega_0} \mathbf{P}\bullet Grad\delta\mathbf{u}\, dV = \int_{\Omega_0} \mathbf{S}\bullet\mathbf{F}^T Grad\delta\mathbf{u}\, dV, \tag{8.12}$$

where $\mathbf{S}$ is the second Piola- Kirchoff stress. linearizing (8.12) the following is obtained

$$D_{\Delta \mathbf{u}}\delta W_{\text{int}} = \int_{\Omega_0} \left(D_{\Delta \mathbf{u}}\mathbf{S} \bullet \mathbf{F}^T Grad\delta\mathbf{u} + \mathbf{S} \bullet D_{\Delta \mathbf{u}}\mathbf{F}^T Grad\delta\mathbf{u} \right) dV. \tag{8.13}$$

(8.13) is the equation needed to be solved.

8.2.2 Stiffness Matrix

Applying linearization defined in Equation (8.10), solution of Equation (8.13) can be achieved. Solving for hyperelastic materials the following form is obtained

$$D_{\Delta \mathbf{u}}\delta W_{\text{int}} = 2\int_{\Omega_0} \left(\mathbb{C}\mathbf{F}^T Grad\Delta\mathbf{u} \bullet \mathbf{F}^T Grad\delta\mathbf{u} \right) dV + \int_{\Omega_0} \left(Grad\Delta\mathbf{u}\mathbf{S} \bullet Grad\delta\mathbf{u} \right) dV, \tag{8.14}$$

where $\mathbb{C}$ is 4th order tangent stiffness matrix and can be defined as

$$\mathbb{C} = \frac{\partial \mathbf{S}}{\partial \mathbf{C}} = 2\rho_0 \frac{\partial^2 \psi}{\partial \mathbf{C}^2}. \tag{8.15}$$

First term in above Equation (8.14) is the material contribution to the tangent stiffness matrix and the second term represents geometrical contribution to the tangent stiffness matrix. In this work, ABAQUS/standard solver is used for the calculations. It requires 4th order tangent stiffness matrix defined through the Kirchoff stress tensor instead of second Piola stress tensor. In such case, linearized form of the principal of virtual work will take following form

$$D_{\Delta \mathbf{u}}\delta W_{\text{int}} = \int_{\Omega} \left(\tau^J + \mathbf{W}\tau - \tau\mathbf{D} \right) \bullet grad\delta\mathbf{u} dV, \tag{8.16}$$

while, tangent stiffness matrix $\mathbb{C}$ is defined as

$$\mathbb{C} = \frac{1}{J}\frac{\partial \tau^J}{\partial \mathbf{D}}. \tag{8.17}$$

Here, τ^J is the Jawman rate of the Kirchoff stress. Thus the following procedure has been adopted to derive the components of the tangent stiffness matrix (See appendix A for complete derivation of tangent stiffness matrix for CSMP).

The Cauchy stress tensor(σ), in terms of the stored energy function(ψ), is given by the following equation

$$\sigma = \frac{2}{J}\mathbf{F}\frac{\partial \psi}{\partial \mathbf{C}}\mathbf{F}^T \tag{8.18}$$

- Find the Kirchoff stress(τ), by multiplying volume ratio to Equation (8.18)
- Take the material time derivative of the Kirchoff stress $(\dot{\tau})$.
- Bring it to Jawman rate (τ^J), using following equation

$$\tau^J = \dot{\tau} - \mathbf{W}\tau - \tau\mathbf{W}^T. \tag{8.19}$$

- Use Equation (8.17) to calculate tangent stiffness matrix.

The finite element module is developed with the calculated stiffness matrix.

8.3 Development of Finite Element Module

A finite element module that contains information regarding properties of a material is called material module. Using material module, it is possible apply material properties to a solid model. The combination of a solid model and a material module makes a material model of a part under consideration. The solid model follows instructions prescribed in a material module. A material module facilitates user to input different physical properties and related constants associated with material used to form the real object. Some finite element software provide various material modules for various commonly used materials such as metals, glass, polymers etc.. whereas some finite element software not only

provide material modules for more commonly used material but also allows user to create their own material module for the specific material for which use of standard material is not appropriate.

In this chapter, the process simulation in which GSMP is used is shown. GSMPs are recently developed polymer while comparing it to other commonly used polymer such as polyethylene, polypropylene, PET, Nylon etc. Use of a material module that is made for commonly used polymer is not appropriate for our purpose. Hence, a new material module based on the constitutive equation derived in Chapter 4 is developed. The material module will be used along with different solid models made for different solids used in different processes.

In this work, ABAQUS/CAE as finite element software is used. ABAQUS/CAE allows users to create their material module for the specific material. Creating material module requires a formulation of FORTRAN code known as UMAT (User Material). UMAT essentially contains all required information to carry out structural analysis that may require definition of stress, strain, tangent stiffness matrix etc.

8.3.1 UMAT

User-defined mechanical behavior in ABAQUS can be included by adding a user subroutine UMAT in to a library of the models. A constitutive model is programmed in a user subroutine. For finite-strain applications the interface for subroutine UMAT is implemented using Cauchy stress components ("true" stress) and integrated rate-of-deformation as the strain increment. While solving problem the user subroutine UMAT is called for each nodal points of mesh at every increment. User subroutine UMAT

includes the instructions for updating stresses and solution-dependent state variables to their values at the end of the increment. It is also necessary to include the material Jacobian matrix for the mechanical constitutive model. Jacobian matrix usually defined through the variation in Kirchoff stress. Jacobian matrix prescribed in rate form is integrated numerically in the subroutine.

There is a particular way user can define the stress and strain components in ABAQUS as shown in Table 8.1.

Table 8.1 Convention Followed in ABAQUS for Stress and Strain

σ_{11} : Direct stress in the 1-direction	ε_{11} : Direct strain in the 1-direction
σ_{22} : Direct stress in the 2-direction	ε_{22} : Direct strain in the 2-direction
σ_{33} : Direct stress in the 3-direction	ε_{33} : Direct strain in the 3-direction
σ_{12} : Shear stress in the 1-2 plane	ε_{12} : Shear strain in the 1-2 plane
σ_{13} : Shear stress in the 1-3 plane	ε_{13} : Shear strain in the 1-3 plane
σ_{23} : Shear stress in the 2-3 plane	ε_{23} : Shear strain in the 2-3 plane

Moreover, for linearized elasticity matrix following relationship holds

$$\sigma = \mathbb{C}\varepsilon \quad \Rightarrow \quad \sigma_{ij} = \mathbb{C}_{ijkl}\varepsilon_{kl}. \tag{8.20}$$

As one can see $\mathbb{C}$ is a 4^{th} order tensor and it contains 81 components. Due to energy consideration and geometric symmetry these 81 components reduce to 36 components. Using the Voight notations, above Equation (8.20) can be re written as:

$$
\begin{array}{l}
I/J \\
\\
\\
\end{array}
\begin{array}{cccccc}
1 & 2 & 3 & 4 & 5 & 6 \\
11 & 22 & 33 & 12 & 13 & 23 \\
ij & I & & & &
\end{array}
\begin{array}{c}
J \\
\\
kl \quad J
\end{array}
$$

$$
\begin{bmatrix} \sigma_{11} = \sigma_1 \\ \sigma_{22} = \sigma_2 \\ \sigma_{33} = \sigma_3 \\ \sigma_{12} = \sigma_4 \\ \sigma_{13} = \sigma_5 \\ \sigma_{23} = \sigma_6 \end{bmatrix} = \begin{bmatrix} C_{11} & C_{12} & C_{13} & C_{14} & C_{15} & C_{16} \\ C_{21} & C_{22} & C_{23} & C_{24} & C_{25} & C_{26} \\ C_{31} & C_{32} & C_{33} & C_{34} & C_{35} & C_{36} \\ C_{41} & C_{42} & C_{43} & C_{44} & C_{45} & C_{46} \\ C_{51} & C_{52} & C_{53} & C_{54} & C_{55} & C_{56} \\ C_{61} & C_{62} & C_{63} & C_{64} & C_{65} & C_{66} \end{bmatrix} \begin{bmatrix} \varepsilon_{11} = \varepsilon_1 \\ \varepsilon_{22} = \varepsilon_2 \\ \varepsilon_{33} = \varepsilon_3 \\ \varepsilon_{12} = \varepsilon_4 \\ \varepsilon_{13} = \varepsilon_5 \\ \varepsilon_{23} = \varepsilon_6 \end{bmatrix} \tag{8.21}
$$

where,

$$
C_{IJ} = \mathbb{C}_{ijkl} = \frac{1}{2}\left[\mathbb{C}_{ijkl} + \mathbb{C}_{ijlk}\right]. \tag{8.22}
$$

Table 8.2 The Standard Template for UMAT

(Source: ABAQUS/CAE manual)

```
      SUBROUTINE UMAT(STRESS,STATEV,DDSDDE,SSE,SPD,SCD,
     1 RPL,DDSDDT,DRPLDE,DRPLDT,
     2 STRAN,DSTRAN,TIME,DTIME,TEMP,DTEMP,PREDEF,DPRED,CMNAME,
     3 NDI,NSHR,NTENS,NSTATV,PROPS,NPROPS,COORDS,DROT,PNEWDT,
     4 CELENT,DFGRD0,DFGRD1,NOEL,NPT,LAYER,KSPT,KSTEP,KINC)
C
      INCLUDE 'ABA_PARAM.INC'
C
      CHARACTER*80 CMNAME
      DIMENSION STRESS(NTENS),STATEV(NSTATV),
     1 DDSDDE(NTENS,NTENS),DDSDDT(NTENS),DRPLDE(NTENS),
     2 STRAN(NTENS),DSTRAN(NTENS),TIME(2),PREDEF(1),DPRED(1),
     3 PROPS(NPROPS),COORDS(3),DROT(3,3),DFGRD0(3,3),DFGRD1(3,3)

      user coding to define DDSDDE, STRESS, STATEV, SSE, SPD, SCD
      and, if necessary, RPL, DDSDDT, DRPLDE, DRPLDT, PNEWDT

      RETURN
      END
```

DDSDDE(NTENS,NTENS)
Jacobian matrix of the constitutive model. DDSDDE(I,J) defines the change in the I^{th} stress component at the end of the time increment caused by an infinitesimal perturbation of the J^{th} component of the strain increment array.

STRESS(NTENS)
This array is passed in as the stress tensor at the beginning of the increment and must be updated in this routine to be the stress tensor at the end of the increment.

STATEV(NSTATV)
An array containing the solution-dependent state variables.

SSE, SPD, SCD
Specific elastic strain energy, plastic dissipation, and "creep" dissipation, respectively. Only in a fully coupled temperature-displacement analysis.

RPL
Volumetric heat generation per unit time at the end of the increment caused by mechanical working of the material.

DDSDDT(NTENS)
Variation of the stress increments with respect to the temperature.

DRPLDE(NTENS)
Variation of RPL with respect to the strain increments.

DRPLDT
Variation of RPL with respect to the temperature.

Stiffness matrix C is denoted as DDSDDE in a UMAT. It is very essential for user to prescribe it in above mentioned format while writing UMAT. Table 8.2 shows the standard template provided in ABAQUS user manual to create user subroutine UMAT. Using the template shown in Table 8.2 and constitutive equation derived in Chapter 4, our own UMATs (See appendix A and appendix B) are created for iso-thermal and non-isothermal processes those were simulated. Detail description of problems solved is given in following sections.

8.3.2 SDVINI

SDVINI is the user subroutine through which user can define solution dependent state variable such as crystallinity. User subroutine SDVINI can also be called to specify the initial conditions. The user can then define all solution-dependent state variables at each point as functions of coordinates, element number, etc. Solution dependent state variable initialized in SDVINI can be updated in UMAT and UMATHT. Using template shown in Table 8.3 user sub routine SDVINI was created.

Table 8.3 Standard Template for SDVINI

(Source: ABAQUS/CAE manual)

```
      SUBROUTINE SDVINI(STATEV,COORDS,NSTATV,NCRDS,NOEL,NPT,
     1 LAYER,KSPT)
C
      INCLUDE 'ABA_PARAM.INC'
C
      DIMENSION STATEV(NSTATV),COORDS(NCRDS)
      user coding to define STATEV(NSTATV)
      RETURN
      END
```

STATEV(NSTATV)
An array containing the solution-dependent state variables.

8.4 Testing of the Material Module

To check the validity of the material module which is created, it is mandatory to test it with different boundary conditions. There are different tests one can perform to test the material module such as single element test, single element test with oriented co-ordinate system, convergence test and multiple element test. Above mentioned test is performed on subroutine UMAT.

8.4.1 Tensile Test Using Multiple Elements

In this test, solid model is developed and then the material model (created by the user) is applied to it. Once the material model is created, boundary conditions are applied to the

model. An appropriate mesh is applied to perform the finite element analysis. Post processor is then used to see different results obtained from the finite element solver.

A multiple element test is used to validate user subroutine UMAT. A UMAT can be tested by performing static general structural analysis. In Chapter 5, a SMP cycle was simulated using MATLAB. Simulating the same cycle using ABAQUS/CAE with the aid of developed UMAT and comparing its results with one obtained in Chapter 5 will be able to test UMAT. Following is the step by step procedure for simulating uni-axial stretching cycle.

Step 1. Create a solid model: A solid model can be created using standard CAD software such as Pro/ENGINEER, Solid Works, ABAQUS, AutoCAD etc. In this simulation, the solid model using 'part module' of the ABAQUS/CAE was created. Figure 9.1 shows the extruded part is stored with name 'cube'.

Step 2. Create a material model: Using the UMAT developed and 'property module' of the ABAQUS/CAE material model of 'part' can be developed. Creating a section and applying material created to it makes the material model. Applying this material module by assigning section to solid model makes the material model of 'part' made with GSMP. (See appendix A for material module)

Step 3. Define processes: A process can be defined in 'step module' of the ABAQUS/CAE. The SMP cycle consists of four processes namely: Loading, Cooling, Unloading and Heating. Hence, four steps are required to solve the problem. However, the process here is simulated using four steps.

Step 4. Applying boundary conditions: Boundary conditions can be applied using the 'load module' of the ABAQUS/CAE. Here, object of the study is to see validity of the

user subroutine UMAT hence, instead of prescribing pressure condition or force condition at surfaces or edges or at nodes, displacement boundary conditions were applied to the edges. Figure 8.2 shows the applied boundary conditions.

Step 5. Mesh the model: Using the 'mesh module' of ABAQUS/CAE solid model can be meshed to carry out solution. In this test, it is required that 'cube' is meshed with only one element. The element chosen for this test is C3D8: A 8-node linear brick, hybrid element that allows linear pressure and reduced integration.

Step 6. Solve the finite element model: Using the 'job module' of ABAQUS/CAE user subroutine UMAT can be called for solving the problem. User subroutine UMAT (umat.f) is used for solving the problem.

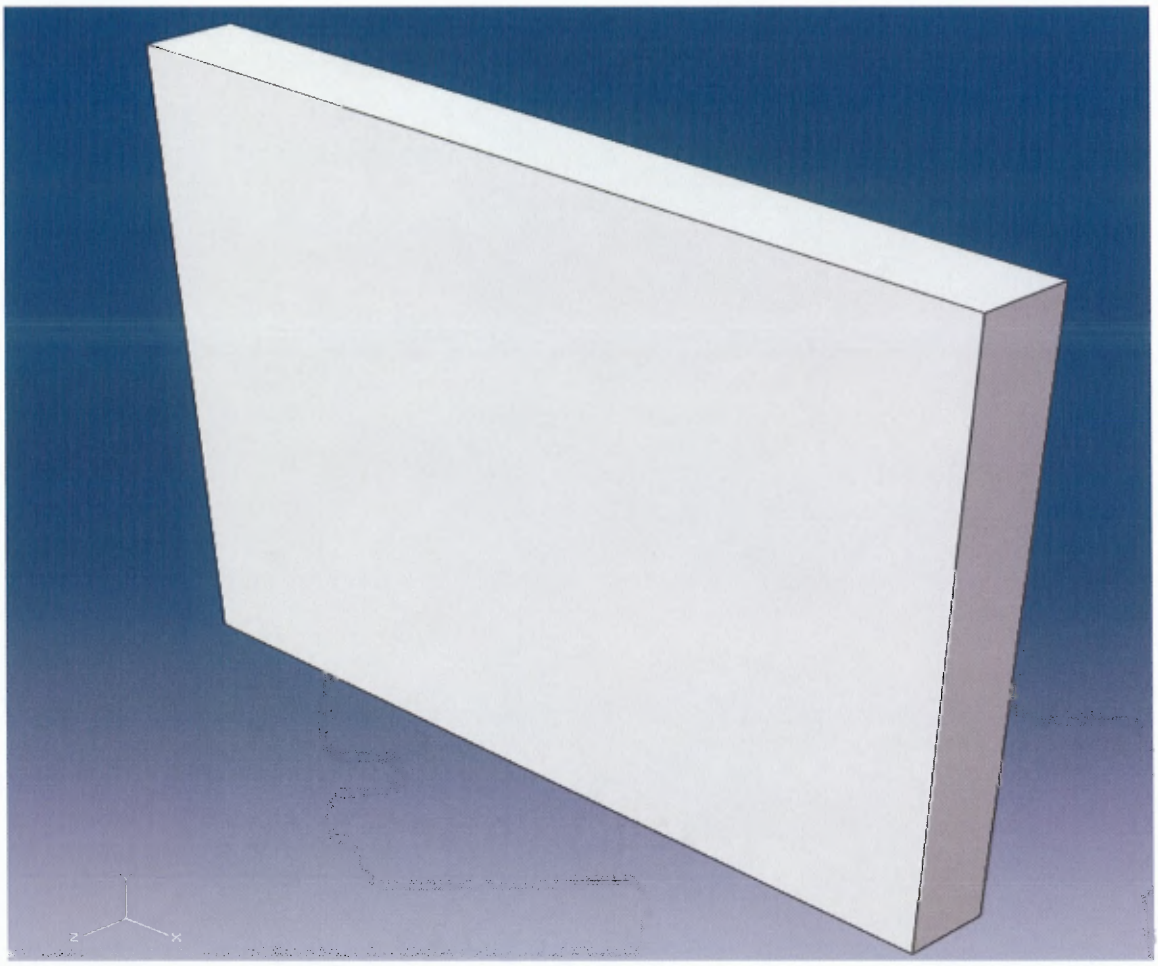

Figure 8.1 A snapshot of ABAQUS/CAE interface showing solid model of the part (Uni-axial tensile test).

Figure 8.1 shows the part for uniaxial tensile test created in part module. The material of the created part is defined by the user through the user subroutine.

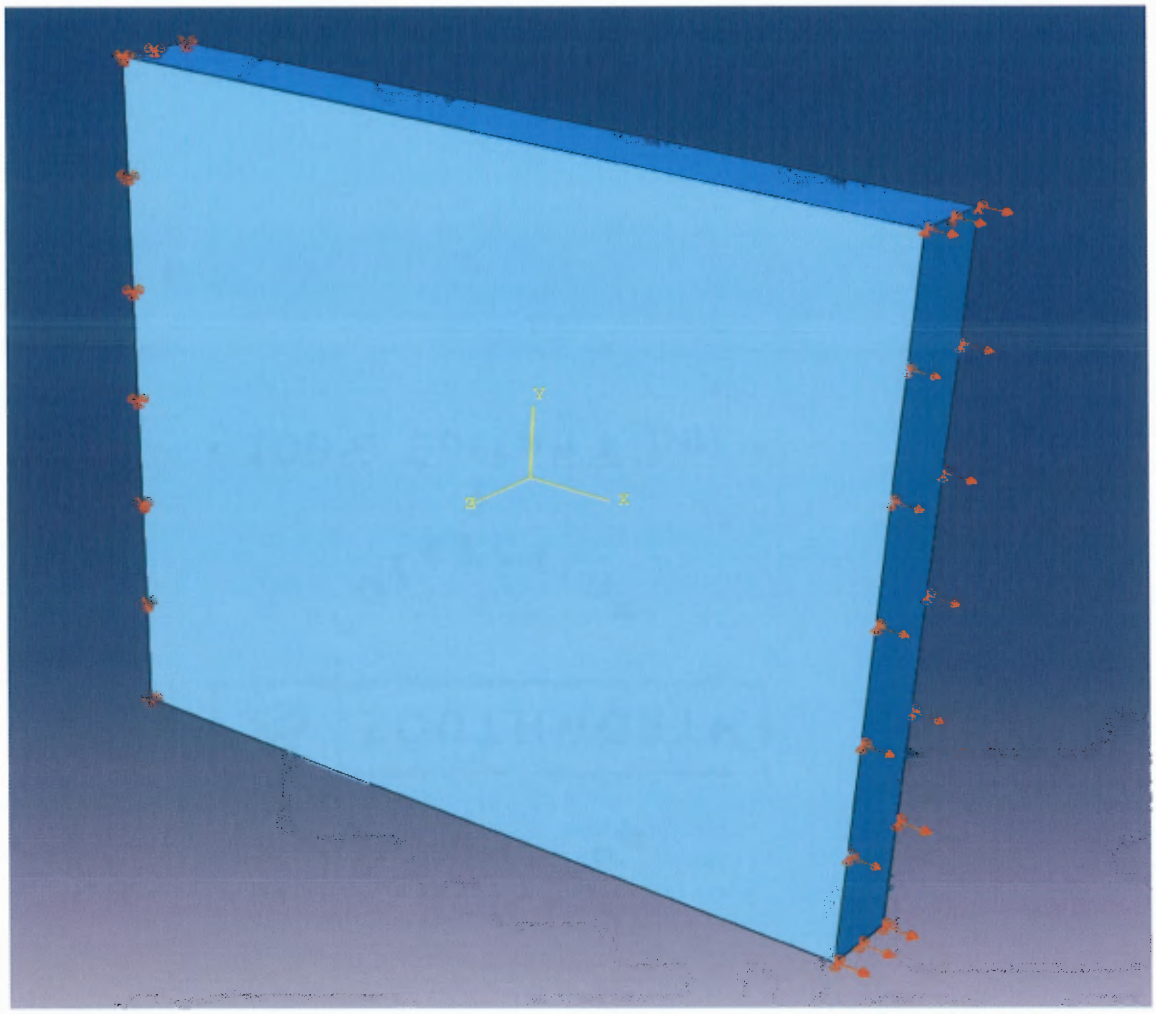

Figure 8.2 A snapshot of ABAQUS/CAE interface showing applied boundary conditions (Uni-axial tensile test).

Figure 8.2 shows the part is constrained at one end (fixed boundary condition) and a load is applied at the other end. The boundary conditions and the applied load are prescribed using the load module.

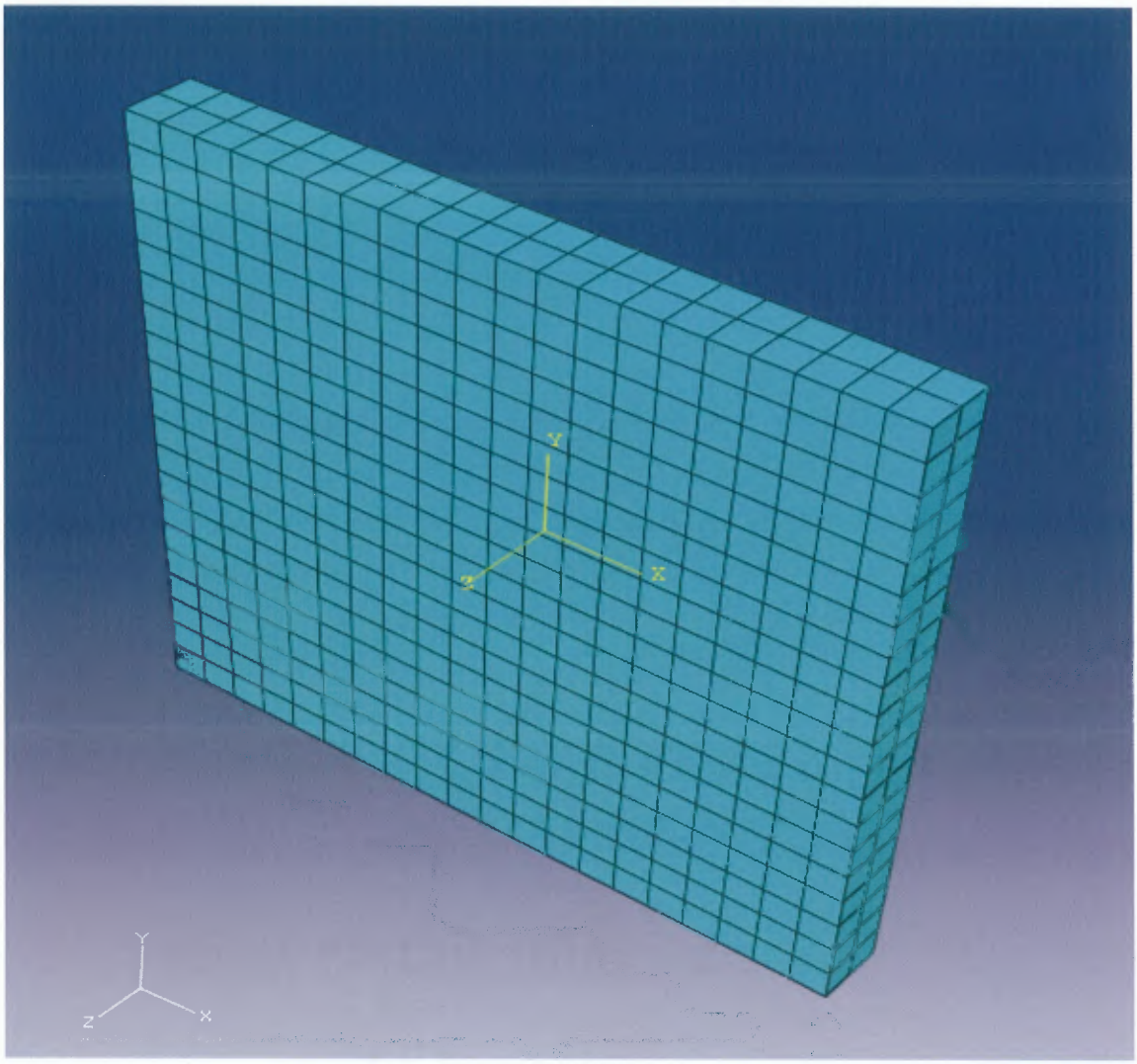

Figure 8.3 A snapshot of ABAQUS/CAE interface showing the part with the applied mesh.

Figure 8.3 shows mesh applied to the part. Standard, linear elements with reduced integration and hourglass control were used.

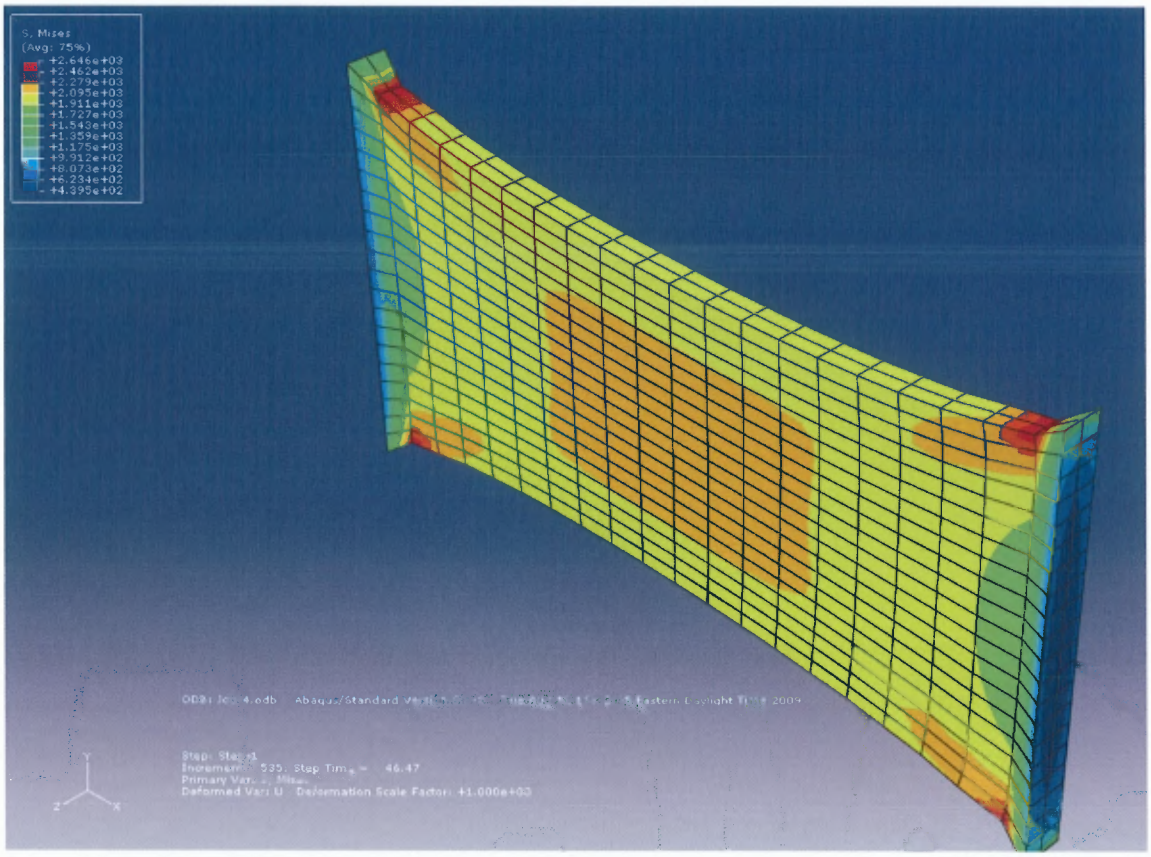

Figure 8.4 Step 1 Large Deformation on the part with multiple elements.

Figure 8.4 shows when the load is applied at one end keeping other end fixed, the stress in the material increases.

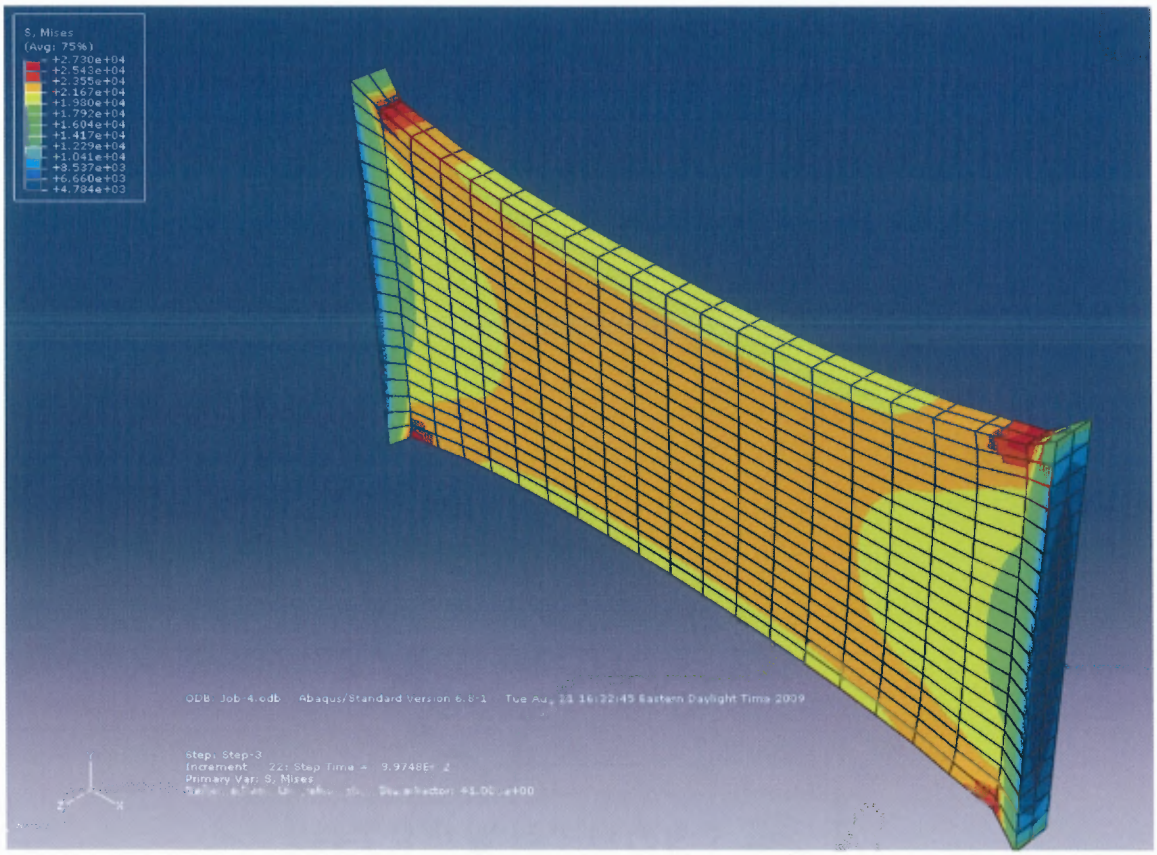

Figure 8.5 Step 2 Cooling – glass transition of the material.

Figure 8.5 shows on cooling below the glass transition material the stress in the material increases, as the material is born in a stressed state and it is further augmented by the increase in thermal stress.

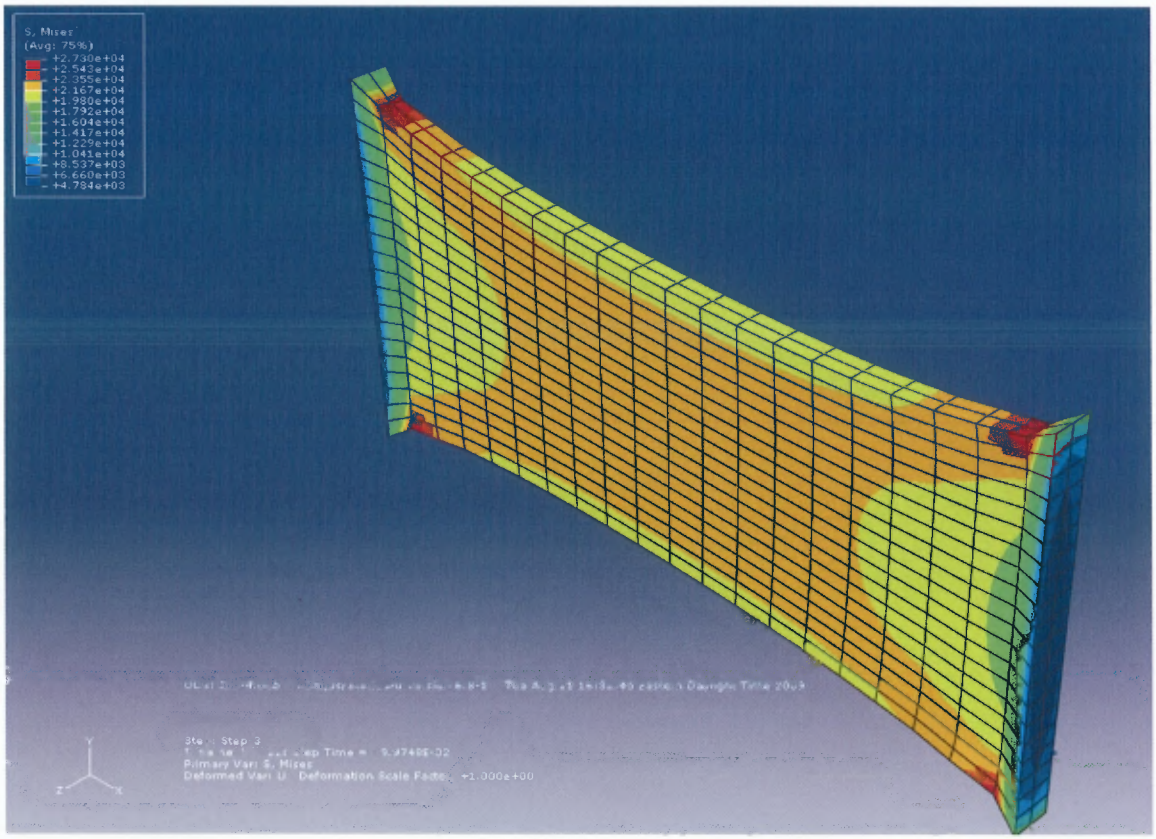

Figure 8.6 Step 3 Unloading of the glassy material – Small amount of strain recovery.

Figure 8.6 shows on unloading below the glass transition material, there is a small amount of strain recovery and the temporary shape of the material is fixed.

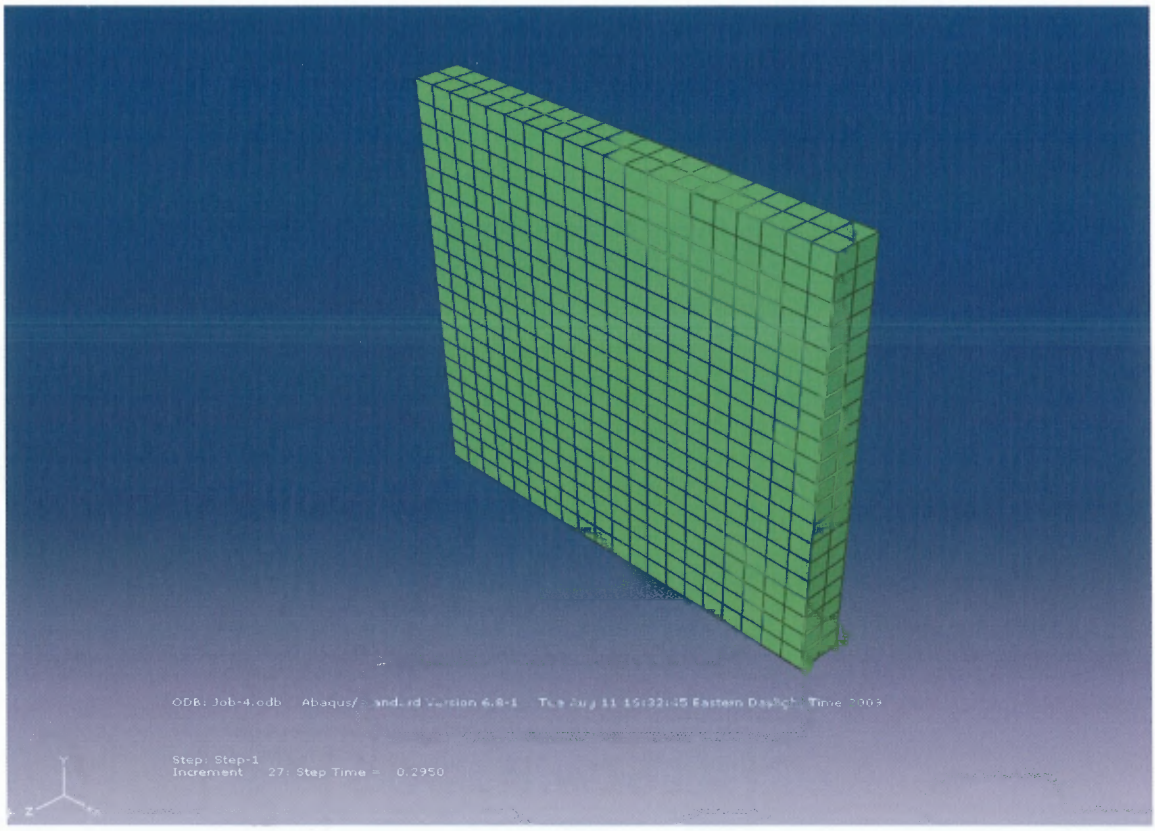

Figure 8.7 Step 4 Melting above the glass transition temperature to retain original shape.

Figure 8.7 shows on heating above the glass transition temperature, the material retains its original shape.

8.4.2 Tensile Test Using Single Element

Below are results of a simulation of a shape memory cycle on a single element using an UMAT (User Defined Material) for CSMP. A strain of 100% (large deformation) has been applied to the element and the resulting deformation is seen. The following figures show steps involved in the shape memory cycle.

Step 1 – Large Deformation on the single element

Step 2 – Constraining the element to retain its temporary shape

Step 3 – Removing load – Small amount of strain recovery

Step 4 – Back to Original Shape

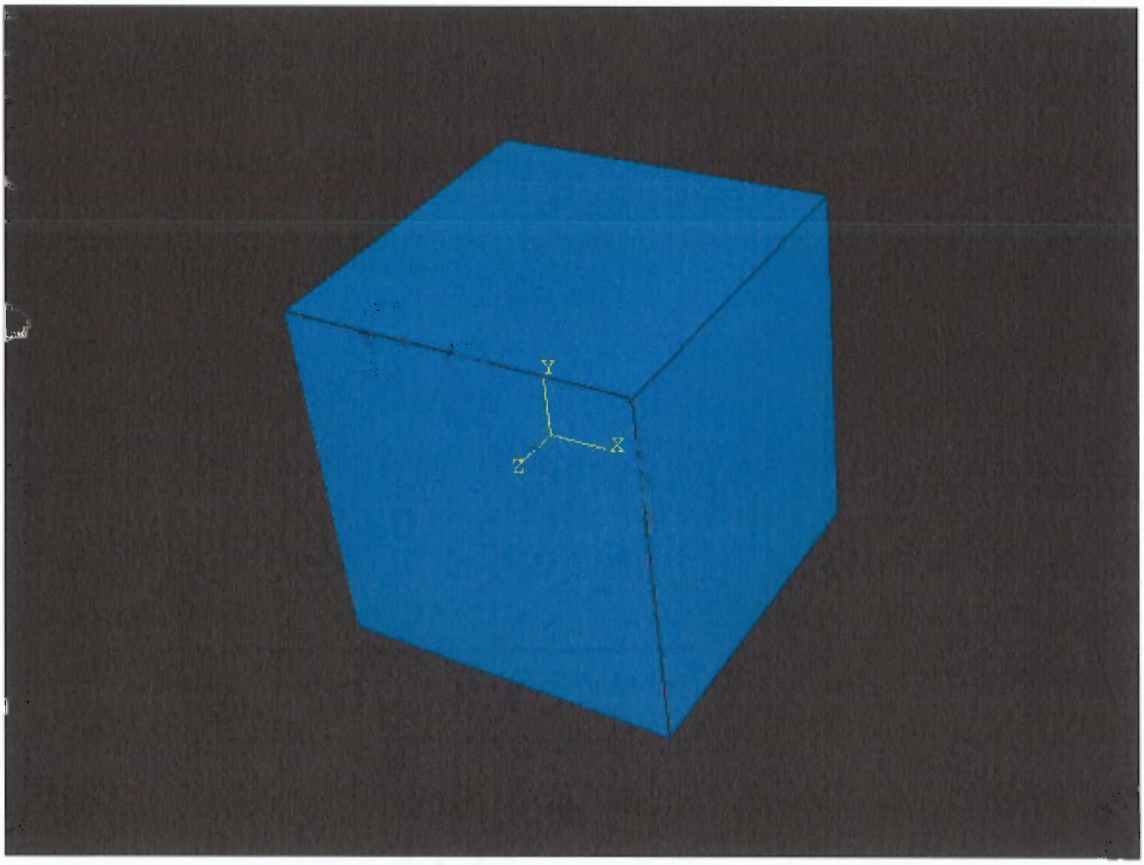

Figure 8.8 Original shape of a single element cube.

Figure 8.8 shows a single element cube of unit dimensions is created using the part module in ABAQUS CAE. The material of the created part is defined by the user. A UMAT written in Fortan was used to run the simulation.

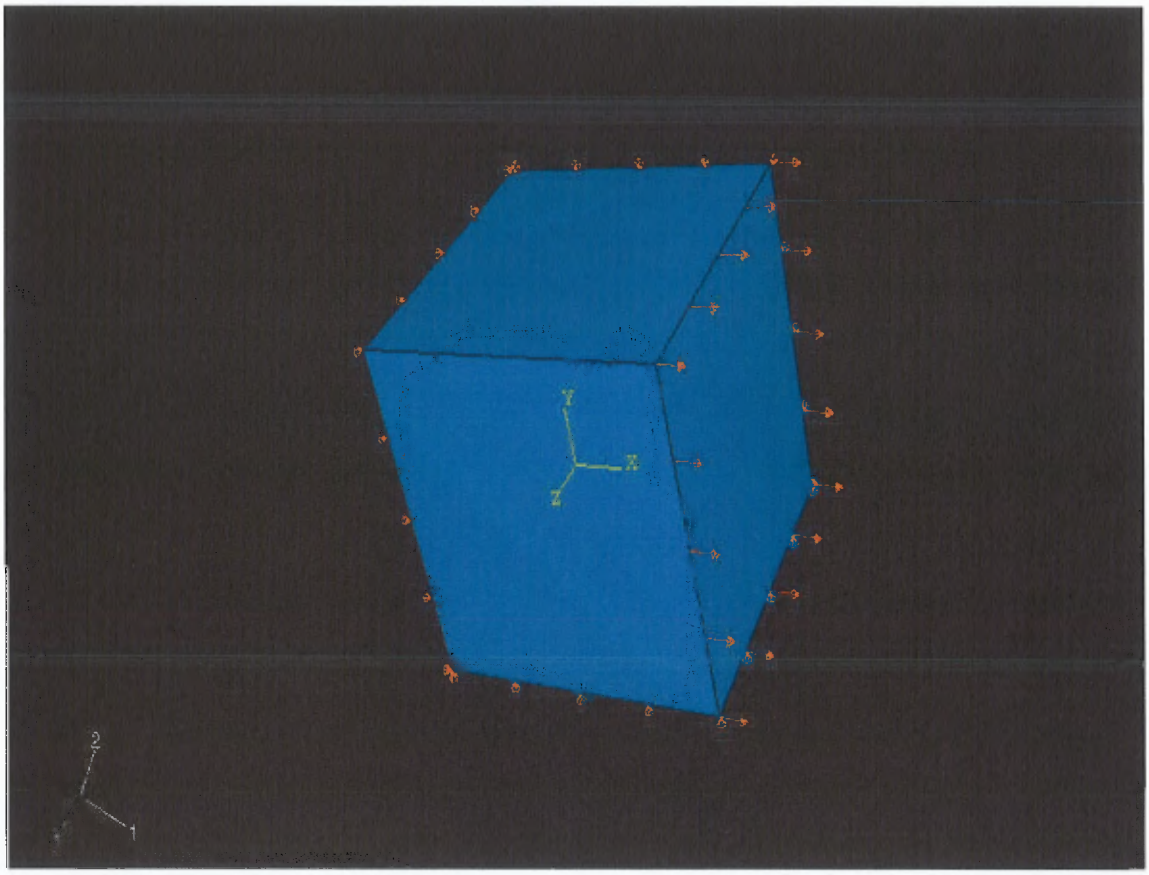

Figure 8.9 Applied load to the element.

Figure 8.9 shows that the cube is constrained and a strain (displacement) of 100% is applied to one its faces resulting in a large deformation. Following this the cube goes through the SMP cycle.

5. RESULTS

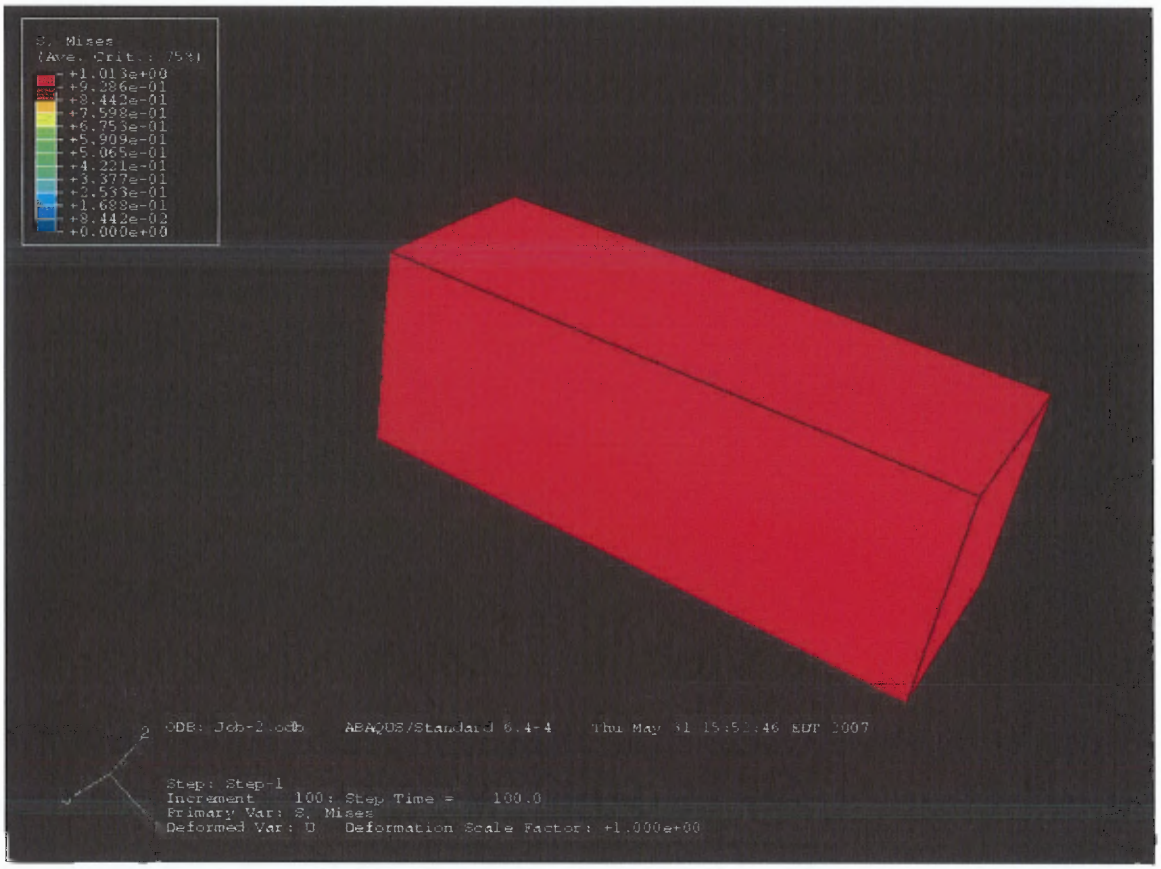

Figure 8.10 Step 1 Large deformation on the single element.

Figure 8.10 shows the single element cube after applying the 100% strain undergoes a large deformation. The cube in this constrained condition is cooled below its crystallization temperature.

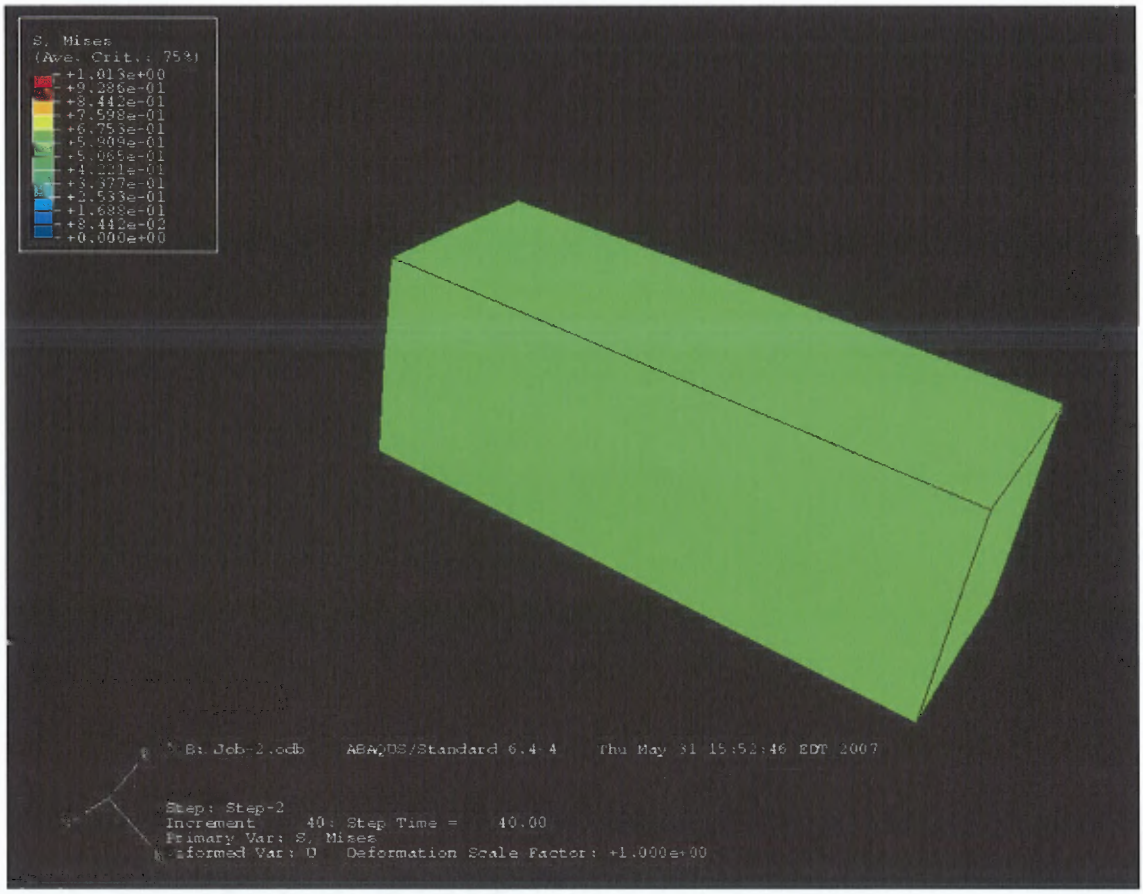

Figure 8.11 Step 2 Constraining the element to retain its temporary shape.

Figure 8.11 shows that the cube when cooled below its crystallization temperature shows a drop in stress, which will eventually unloaded to retain the temporary shape.

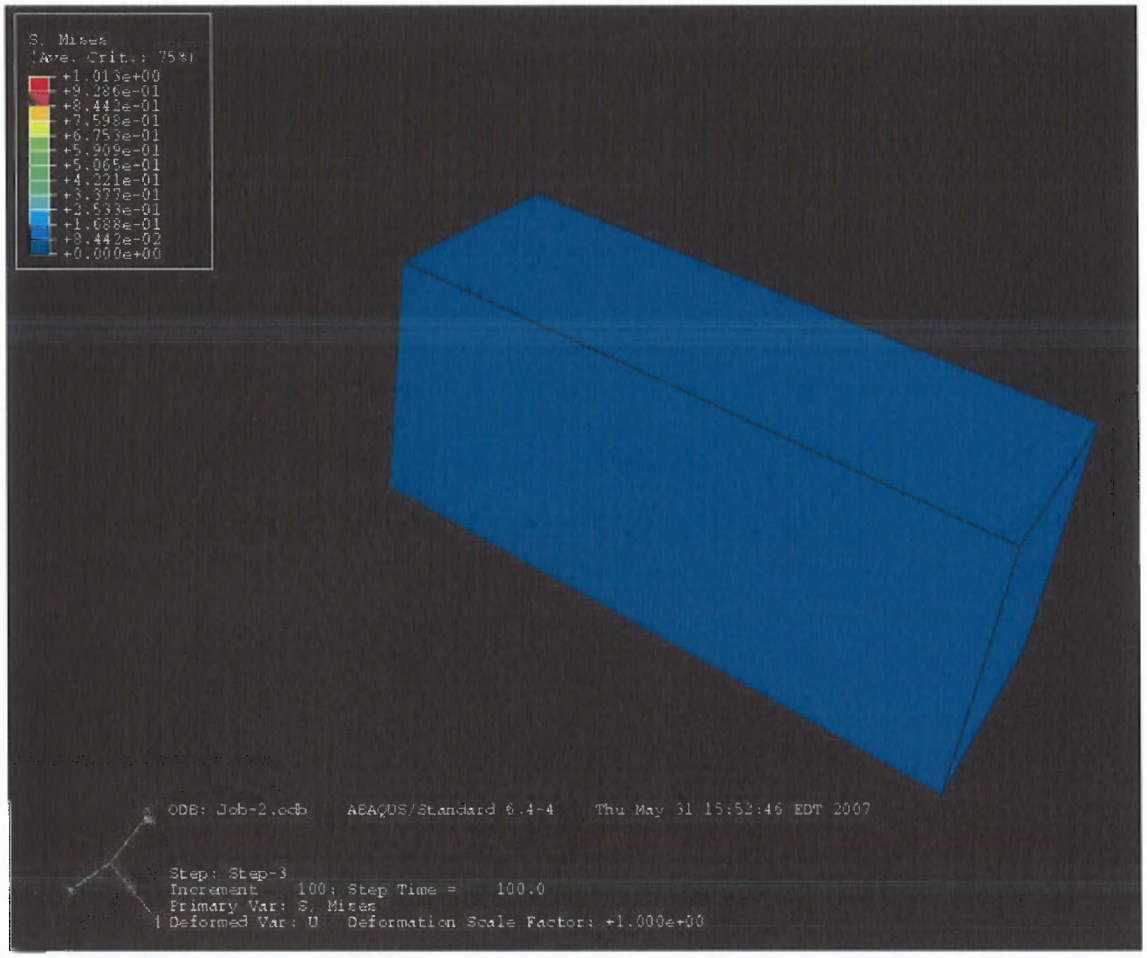

Figure 8.12 Step 3 Removing load – Small amount of strain recovery.

Figure 8.12 shows that after unloading there is a small amount of strain recovery and the deformed shape is retained.

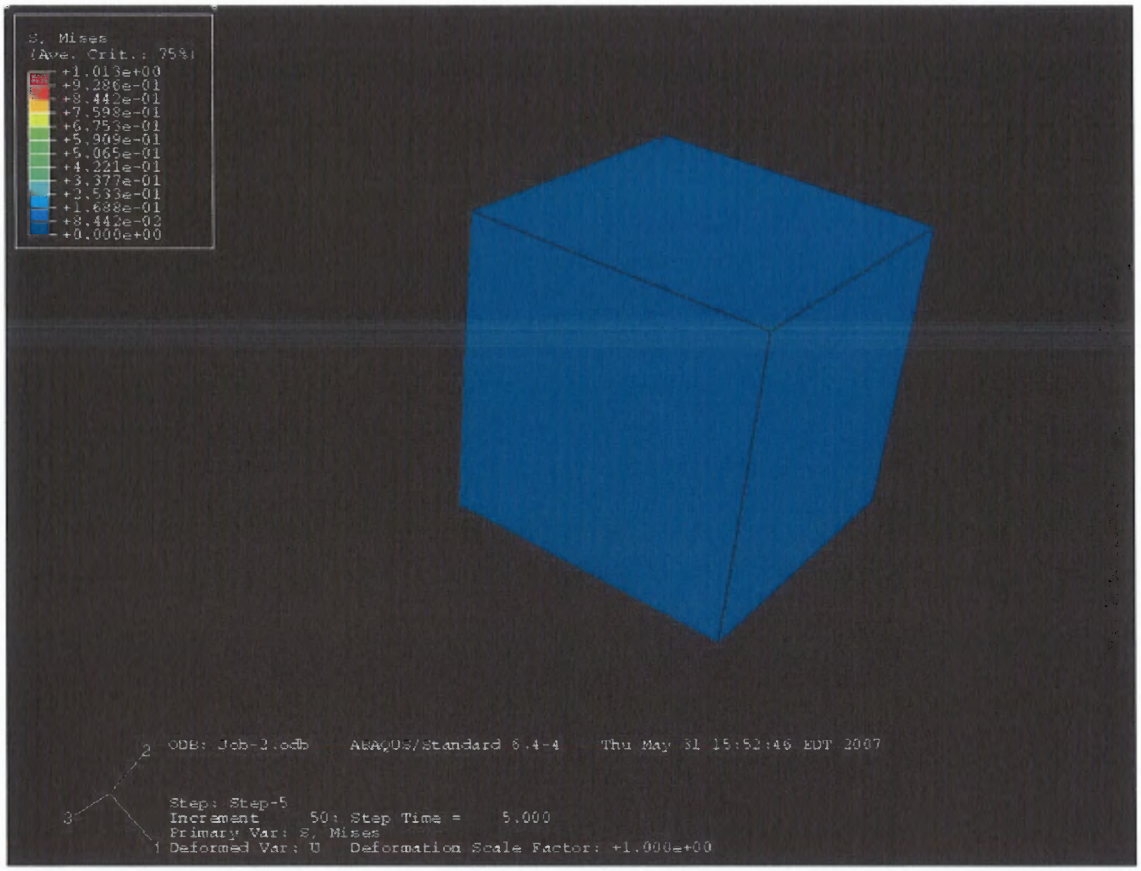

Figure 8.13 Step 4 Back to original shape.

Figure 8.13 shows after heating above melting temperature the material retains its original shape after undergoing the SMP cycle.

CHAPTER 9

CONCLUSION AND SCOPE OF RESEARCH

9.1 Summary

The goal of this research was to study the response (stress-strain) of shape memory polymers with emphasis on mechanics and thermodynamics associated with phase transition and mechanism for the return to the original shape. Thus the following things have been accomplished and presented in this dissertation:

A framework for glassy shape memory polymers using the notion of natural configurations of a material which takes in to account the thermal expansion of polymers.

A finite element module for GSMPs is formulated based on the mathematical model developed for the GSMPs. All required tests are performed to validate the finite element module.

The following sections present conclusions of the research and recommendations future work.

9.2 Conclusion

The theory of natural configurations developed to model variety of nonlinear materials and has been successfully applied to a diverse class of problems is the underlying theory to formulate constitutive model of shape memory materials. Thus the following key points serve as a conclusion for the research.

- Thorough understanding of modeling hyper elastic materials (shape memory polymers, elastomers).
- Constitutive model for crystallizable shape memory polymer (CSMP) served as the basis for current research.

- Developed a model for glassy shape memory polymers (GSMP) using the theory of natural configurations.
- The model takes in to account the effect of thermal expansion of polymers on the stress-strain response.
- Validated the developed GSMP model against experimental data.
- Used the CSMP model for solving a non-homogenous problem (torsion of a cylinder) as an illustration of shape memory polymer cycle.
- Simulated the CSMP cycle for a single element cube using ABAQUS.
- Developed UMAT for GSMP and performed required tests to validate the finite element module.

9.3 Recommendations for Future Work

In the current research the GSMP model is developed by assuming the process to be isothermal. The effects of temperature variation and phase transition changes associated with it can be studied in greater detail.

Since the experimental data available in literature is for 1-D processes, the model is validated against it. For further validation more physical testing should be carried out and used as a basis for justifying the theory.

The user material subroutine has been developed in a mechanical setting. To fully capture the GSMP model a comprehensive thermodynamic framework will be a challenging and worthwhile research study.

APPENDIX A

USER SUBROUTINE (UMAT)

This user subroutine is for glassy shape memory polymer and it can be used for when it is assumed that crystallization occurs at constant temperature and constant strain.

```
      SUBROUTINE UMAT(STRESS,STATEV,DDSDDE,SSE,SPD,SCD,
     1 RPL,DDSDDT,DRPLDE,DRPLDT,STRAN,DSTRAN,
     2 TIME,DTIME,TEMP,DTEMP,PREDEF,DPRED,MATERL,NDI,NSHR,NTENS,
     3 NSTATV,PROPS,NPROPS,COORDS,DROT,PNEWDT,CELENT,
     4 DFGRD0,DFGRD1,NOEL,NPT,KSLAY,KSPT,KSTEP,KINC)
C
      INCLUDE 'ABA_PARAM.INC'
C
      CHARACTER*8 MATERL
      DIMENSION STRESS(NTENS),STATEV(NSTATV),
     1 DDSDDE(NTENS,NTENS),DDSDDT(NTENS),DRPLDE(NTENS),
     2 STRAN(NTENS),DSTRAN(NTENS),DFGRD0(3,3),DFGRD1(3,3),
     3 TIME(2),PREDEF(1),DPRED(1),PROPS(NPROPS),COORDS(3),DROT(3,3)
C
C ----------------------------------------------------------------
C
          DIMENSION FBAR1(3,3),DFGRD2(3,3),FBAR2(3,3),
     1DFG(3,3),FIN(3,3),BAMOR(3,3),BCRY(3,3),BBARN(3,3),BBARP(3,3),
     2CBAR2(3,3),C1(6,6),C2(6,6)

      REAL KRON, TRBAR1, TRBAR2
C
      PARAMETER(ZE=0.D0, ON=1.D0, TW=2.D0, TH=3.D0, FO=4.D0, EI=8.D0,
     1  NI= 9.D0 )
C----------------------------------------------------------------
C
C Initialize
      L1 = 0
      L2 = 0
      I = 0
      J = 0
      L = 0
      K = 0
C
      C10=PROPS(1)
      D1 =PROPS(2)
```

```
      C20=PROPS(3)
      D2 =PROPS(4)
      C201 = PROPS(5)
      C202 = PROPS(6)
C
C
C     Incremental crystallinity dalph
      Dalph = 0.01
      Dalph1 = 0.001

C
C        CHECKING IF INTERMIEDIATE CONFIG NEEDS
C        TO BE INITIALIZED
C
C-new-start

      STATEV(1) = 1.0d0
      STATEV(2) = 0.0d0
      STATEV(3) = 0.0d0
      STATEV(4) = 0.0d0
      STATEV(5) = 1.0d0
      STATEV(6) = 0.0d0
      STATEV(7) = 0.0d0
      STATEV(8) = 0.0d0
      STATEV(9)=  1.0d0

C-new-END
      IF (KSTEP.EQ.2) THEN
       IF (KINC.EQ.1) THEN
         STATEV(1) = DFGRD1(1,1)
         STATEV(2) = DFGRD1(1,2)
         STATEV(3) = DFGRD1(1,3)
         STATEV(4) = DFGRD1(2,1)
         STATEV(5) = DFGRD1(2,2)
         STATEV(6) = DFGRD1(2,3)
         STATEV(7) = DFGRD1(3,1)
         STATEV(8) = DFGRD1(3,2)
         STATEV(9)=  DFGRD1(3,3)
       ENDIF
       STATEV(10) = STATEV(10) + Dalph
       IF (STATEV(10).GT.1) THEN
         STATEV(10) = 1
       END IF
      ENDIF
      IF (KSTEP.EQ.4) THEN
```

```
      STATEV(10) = STATEV(10) - Dalph
      IF (STATEV(10).LT.0)THEN
       STATEV(10)=0
      END IF
     END IF

     IF (KSTEP.EQ.5) THEN
      STATEV(10) = STATEV(10) - Dalph1
      IF (STATEV(10).LT.0)THEN
       STATEV(10)=0
      END IF
     END IF


C
C       INITIALISING VALUES
C
      DFG(1,1) = STATEV(1)
      DFG(1,2) = STATEV(2)
      DFG(1,3) = STATEV(3)
      DFG(2,1) = STATEV(4)
      DFG(2,2) = STATEV(5)
      DFG(2,3) = STATEV(6)
      DFG(3,1) = STATEV(7)
      DFG(3,2) = STATEV(8)
      DFG(3,3) = STATEV(9)
      ALP = STATEV(10)

C     INVERTING DFG MATRIX
      DETF = DFG(1,1)*(DFG(2,2)*DFG(3,3) - DFG(2,3)*DFG(3,2))
     1      - DFG(1,2)*(DFG(2,1)*DFG(3,3) - DFG(2,3)*DFG(3,1))
     2      + DFG(1,3)*(DFG(2,1)*DFG(3,2) - DFG(2,2)*DFG(3,1))
      FIN(1,1) = (DFG(2,2)*DFG(3,3) - DFG(2,3)*DFG(3,2))/DETF
      FIN(2,1) = -(DFG(2,1)*DFG(3,3) - DFG(2,3)*DFG(3,1))/DETF
      FIN(3,1) = (DFG(2,1)*DFG(3,2) - DFG(2,2)*DFG(3,1))/DETF
      FIN(1,2) = -(DFG(1,2)*DFG(3,3) - DFG(1,3)*DFG(3,2))/DETF
      FIN(2,2) = (DFG(1,1)*DFG(3,3) - DFG(1,3)*DFG(3,1))/DETF
      FIN(3,2) = -(DFG(1,1)*DFG(3,2) - DFG(1,2)*DFG(3,1))/DETF
      FIN(1,3) = (DFG(1,2)*DFG(2,3) - DFG(1,3)*DFG(2,2))/DETF
      FIN(2,3) = -(DFG(1,1)*DFG(2,3) - DFG(1,3)*DFG(2,1))/DETF
      FIN(3,3) = (DFG(1,1)*DFG(2,2) - DFG(1,2)*DFG(2,1))/DETF
C
C       PRESCRIBING DEF GRAD FOR CRYSTALLINE PHASE
C
     DO  K1 = 1, 3, 1
```

```
      DO K2 = 1, 3, 1
        TEMP = ZE
        DO K3 = 1, 3, 1
          TEMP = TEMP + DFGRD1(K1,K3)*FIN(K3,K2)
        END DO
        DFGRD2(K1,K2) =  TEMP
      END DO
    END DO
C
C   JACOBIAN AND DISTORTION TENSOR
C
    DET1=DFGRD1(1, 1)*DFGRD1(2, 2)*DFGRD1(3, 3)
   1  -DFGRD1(1, 2)*DFGRD1(2, 1)*DFGRD1(3, 3)
    DET2=DFGRD2(1, 1)*DFGRD2(2, 2)*DFGRD2(3, 3)
   1  -DFGRD2(1, 2)*DFGRD2(2, 1)*DFGRD2(3, 3)
    IF(NSHR.EQ.3) THEN
     DET1=DET1+DFGRD1(1, 2)*DFGRD1(2, 3)*DFGRD1(3, 1)
   1       +DFGRD1(1, 3)*DFGRD1(3, 2)*DFGRD1(2, 1)
   2       -DFGRD1(1, 3)*DFGRD1(3,1)*DFGRD1(2, 2)
   3       -DFGRD1(2, 3)*DFGRD1(3, 2)*DFGRD1(1, 1)
     DET2=DET2+DFGRD2(1, 2)*DFGRD2(2, 3)*DFGRD2(3, 1)
   1       +DFGRD2(1, 3)*DFGRD2(3, 2)*DFGRD2(2, 1)
   2       -DFGRD2(1, 3)*DFGRD2(3,1)*DFGRD2(2, 2)
   3       -DFGRD2(2, 3)*DFGRD2(3, 2)*DFGRD2(1, 1)
    END IF
    STATEV(11) = DET1
    SCALE=DET1**(-ON/TH)
    SCALE2=DET2**(-ON/TH)
    DO K1=1, 3
     DO K2=1, 3
      FBAR1(K2, K1)=SCALE*DFGRD1(K2, K1)
      FBAR2(K2, K1)=SCALE2*DFGRD2(K2, K1)
     END DO
    END DO

C**********************************************************************
C   Now, we are finding the directions required for finding J1 and K1
C   for crystalline part which causes orthotropy
C   Directions are n(VECN) & m(VECM)
C        ***** verify  about (1) used in utility subroutine SPRIND
C        ***** (1) is for stress and (2) for strain tensor
C   CALCULATE LEFT CAUCHY-GREEN TENSOR
C
    BAMOR(1,1)=FBAR1(1, 1)**2+FBAR1(1, 2)**2+FBAR1(1, 3)**2
    BAMOR(2,2)=FBAR1(2, 1)**2+FBAR1(2, 2)**2+FBAR1(2, 3)**2
    BAMOR(3,3)=FBAR1(3, 3)**2+FBAR1(3, 1)**2+FBAR1(3, 2)**2
```

```
      BAMOR(1,2)=FBAR1(1, 1)*FBAR1(2, 1)+FBAR1(1, 2)*FBAR1(2, 2)
     1     +FBAR1(1, 3)*FBAR1(2, 3)

      BAMOR(2,1) = BAMOR(1,2)
      BCRY(1,1)=FBAR2(1, 1)**2+FBAR2(1, 2)**2+FBAR2(1, 3)**2
      BCRY(2,2)=FBAR2(2, 1)**2+FBAR2(2, 2)**2+FBAR2(2, 3)**2
      BCRY(3,3)=FBAR2(3, 3)**2+FBAR2(3, 1)**2+FBAR2(3, 2)**2
      BCRY(1,2)=FBAR2(1, 1)*FBAR2(2, 1)+FBAR2(1, 2)*FBAR2(2, 2)
     1     +FBAR2(1, 3)*FBAR2(2, 3)
      BCRY(2,1) = BCRY(1,2)
      BAMOR(1,3) = 0.D0
      BAMOR(2,3) = 0.D0
      BAMOR(3,1) = 0.D0
      BAMOR(3,2) = 0.D0
      BCRY(1,3) = 0.D0
      BCRY(2,3) = 0.D0
      BCRY(3,1) = 0.D0
      BCRY(3,2) = 0.D0
      IF(NSHR.EQ.3) THEN
       BAMOR(1,3)=FBAR1(1, 1)*FBAR1(3, 1)+FBAR1(1, 2)*FBAR1(3, 2)
      1      +FBAR1(1, 3)*FBAR1(3, 3)
       BAMOR(3,1) = BAMOR(1,3)
       BAMOR(2,3)=FBAR1(2, 1)*FBAR1(3, 1)+FBAR1(2, 2)*FBAR1(3, 2)
      1      +FBAR1(2, 3)*FBAR1(3, 3)
       BAMOR(3,2) = BAMOR(2,3)
       BCRY(1,3)=FBAR2(1, 1)*FBAR2(3, 1)+FBAR2(1, 2)*FBAR2(3, 2)
      1      +FBAR2(1, 3)*FBAR2(3, 3)
       BCRY(3,1) = BCRY(1,3)
       BCRY(2,3)=FBAR2(2, 1)*FBAR2(3, 1)+FBAR2(2, 2)*FBAR2(3, 2)
      1      +FBAR2(2, 3)*FBAR2(3, 3)
       BCRY(3,2) = BCRY(2,3)
      END IF

C
C*************************************************************
C   Calculating the CBAR2
      CBAR2(1,1)=FBAR2(1,1)**2+FBAR2(2,1)**2+FBAR2(3,1)**2
      CBAR2(2,2)=FBAR2(1,2)**2+FBAR2(2,2)**2+FBAR2(3,2)**2
      CBAR2(3,3)=FBAR2(1,3)**2+FBAR2(2,3)**2+FBAR2(3,3)**2
      CBAR2(1,2)=FBAR2(1,1)*FBAR2(1,2)+FBAR2(2,1)*FBAR2(2,2)
     1      +FBAR2(3, 1)*FBAR2(3, 2)
      CBAR2(2,1)= CBAR2(1,2)
      CBAR2(1,3) = 0.D0
      CBAR2(2,3) = 0.D0
      CBAR2(3,1) = 0.D0
      CBAR2(3,2) = 0.D0
      IF(NSHR.EQ.3) THEN
```

```
      CBAR2(1,3)=FBAR2(1,1)*FBAR2(1,3)+FBAR2(2,1)*FBAR2(2,3)
     1       +FBAR2(3, 1)*FBAR2(3, 3)
      CBAR2(3,1) = CBAR2(1,3)
      CBAR2(2,3)=FBAR2(1,2)*FBAR2(1,3)+FBAR2(2,2)*FBAR2(2,3)
     1       +FBAR2(3, 2)*FBAR2(3, 3)
      CBAR2(3,2) = CBAR2(2,3)
     END IF

C*********************************************************************

C*********************************************************************
C    Finding trace
     TRBAR1 = BAMOR(1,1) + BAMOR(2,2) + BAMOR(3,3)
     TRBAR2 = BCRY(1,1) + BCRY(2,2) + BCRY(3,3)

C*********************************************************************

C*********************************************************************
C
C   CALCULATE THE STRESS
C
     B1 = TW*C10/DET1
     B11 = TW*C20/DET2
     B2 = ( ((-TW*C10/TH)*TRBAR1/DET1) + ((TW/D1)*(DET1-ON)))
     B21 = ((-TW*C20/TH)*TRBAR2/DET2) + ((TW/D2)*(DET2-ON))
     B31 = FO*C201*(-ON)/DET2
     B41 = FO*C202*(-ON)/DET2
     DO K1=1,NDI
     R1=(ON-ALP)*(B1*BAMOR(K1,K1) + B2)
     R2=ALP*(B11*BCRY(K1,K1)+ B21)
     STRESS(K1) = R1 + R2

     END DO
     DO K1=NDI+1,NDI+NSHR
      IF (K1 .EQ. 4)THEN
         L1 = 1
         L2 = 2
      END IF
      IF (K1 .EQ. 5)THEN
         L1 = 1
         L2 = 3
      END IF
      IF (K1 .EQ. 6)THEN
         L1 = 2
         L2 = 3
      END IF
```

```
      R1=(ON-ALP)*(B1*BAMOR(L1,L2))
      R2= ALP*( B11*BCRY(L1,L2))

      STRESS(K1) = R1 + R2
      END DO
C
C     CALCULATE THE STIFFNESS
C*************************************************************************
C     Calculating required co-efficients
C     NOTE : A1 = B1 AND A11 = B11
      A2 = (-TW/TH)*B1
      A21 = (-TW/TH)*B11
      A3 = (TW/NI)*B1
      A31 = (TW/NI)*B11
      A4 = (TW/D1)*(TW*DET1-ON)
      A41 = (TW/D2)*(TW*DET2-ON)
      A5 = (-EI/TH)*C201*(-ON)/DET2
      A51 = (-EI/TH)*C202*(-ON)/DET2
      A7 = (-EI/TH)*C201*(-ON)/DET2
      A71 = (-EI/TH)*C202*(-ON)/DET2
      A8 = EI*C201/DET2
      A81 = EI*C202/DET2
      A10 = FO*C201*(-ON)/DET2
      A101 = FO*C202*(-ON)/DET2

C*************************************************************************
*
C     DESCRIBING THE REQUIRED MATRIX

      DO K1 = 1, NDI+1, 1
       IF (K1 .EQ. 1) THEN
         I = 1
         J = 1
       END IF
       IF (K1 .EQ. 2) THEN
         I = 2
         J = 2
       END IF
       IF (K1 .EQ. 3) THEN
         I = 3
         J = 3
       END IF
       IF (K1 .EQ. 4) THEN
         I = 1
         J = 2
       END IF
```

```
DO K2 = 1, NDI+1, 1
  IF (K2 .EQ. 1) THEN
    K = 1
    L = 1
  END IF
  IF (K2 .EQ. 2) THEN
    K = 2
    L = 2
  END IF
  IF (K2 .EQ. 3) THEN
    K = 3
    L = 3
  END IF
  IF (K2 .EQ. 4) THEN
    K = 1
    L = 2
  END IF
P1=( B1*(KRON(I,K)*BAMOR(L,J)+BAMOR(I,K)*KRON(J,L)) )
P2=(A2*(KRON(I,J)*BAMOR(K,L)) )
P3=(A2*(KRON(K,L)*BAMOR(I,J)) )
P4=(A3*(TRBAR1*KRON(K,L)*KRON(I,J)) )
P5=(A4*(KRON(K,L)*KRON(I,J)) )
P6=( B11*(KRON(I,K)*BCRY(L,J)+BCRY(I,K)*KRON(J,L)) )
P7=( A21*(KRON(I,J)*BCRY(K,L)) )
P8=( A21*(KRON(K,L)*BCRY(I,J)) )
P9=( A31*(TRBAR2*KRON(K,L)*KRON(I,J)) )
P10=( A41*(KRON(K,L)*KRON(I,J)) )

Q1 = (ON-ALP)*(P1+P2+P3+P4+P5) + ALP*(P6+P7+P8+P9+P10)
Q2 = Q1

C1(K1,K2) = Q1 + Q2

P1=( B1*(KRON(I,L)*BAMOR(K,J)+BAMOR(I,L)*KRON(J,K)) )
P2=(A2*(KRON(I,J)*BAMOR(L,K)) )
P3=(A2*(KRON(L,K)*BAMOR(I,J)) )
P4=(A3*(TRBAR1*KRON(L,K)*KRON(I,J)) )
P5=(A4*(KRON(L,K)*KRON(I,J)) )
P6=( B11*(KRON(I,L)*BCRY(K,J)+BCRY(I,L)*KRON(J,K)) )
P7=( A21*(KRON(I,J)*BCRY(L,K)) )
P8=( A21*(KRON(L,K)*BCRY(I,J)) )
P9=( A31*(TRBAR2*KRON(L,K)*KRON(I,J)) )
P10=( A41*(KRON(L,K)*KRON(I,J)) )

Q1 = (ON-ALP)*(P1+P2+P3+P4+P5) + ALP*(P6+P7+P8+P9+P10)
Q2 = Q1
```

```
 C2(K1,K2) = Q1 + Q2

DDSDDE(K1,K2) = (ON/TW)*(C1(K1,K2)+C2(K1,K2))
  END DO
END DO
IF (NSHR .EQ. 3) THEN
DO K1 = 1, NDI+1, 1
  IF (K1 .EQ. 1) THEN
    I = 1
    J = 1
  END IF
  IF (K1 .EQ. 2) THEN
    I = 2
    J = 2
  END IF
  IF (K1 .EQ. 3) THEN
    I = 3
    J = 3
  END IF
  IF (K1 .EQ. 4) THEN
    I = 1
    J = 2
  END IF
  DO K2 = NDI+NSHR-1, NDI+NSHR, 1
    IF (K2 .EQ. 5) THEN
      K = 1
      L = 3
    END IF
    IF (K2 .EQ. 6) THEN
      K = 2
      L = 3
    END IF
 P1=( B1*(KRON(I,K)*BAMOR(L,J)+BAMOR(I,K)*KRON(J,L)) )
 P2=(A2*(KRON(I,J)*BAMOR(K,L)) )
 P3=(A2*(KRON(K,L)*BAMOR(I,J)) )
 P4=(A3*(TRBAR1*KRON(K,L)*KRON(I,J)) )
 P5=(A4*(KRON(K,L)*KRON(I,J)) )
 P6=( B11*(KRON(I,K)*BCRY(L,J)+BCRY(I,K)*KRON(J,L)) )
 P7=( A21*(KRON(I,J)*BCRY(K,L)) )
 P8=( A21*(KRON(K,L)*BCRY(I,J)) )
 P9=( A31*(TRBAR2*KRON(K,L)*KRON(I,J)) )
 P10=( A41*(KRON(K,L)*KRON(I,J)) )

 Q1 = (ON-ALP)*(P1+P2+P3+P4+P5) + ALP*(P6+P7+P8+P9+P10)
 Q2 = Q1
```

```
C1(K1,K2) = Q1 + Q2

P1=( B1*(KRON(I,L)*BAMOR(K,J)+BAMOR(I,L)*KRON(J,K)) )
P2=(A2*(KRON(I,J)*BAMOR(L,K)) )
P3=(A2*(KRON(L,K)*BAMOR(I,J)) )
P4=(A3*(TRBAR1*KRON(L,K)*KRON(I,J)) )
P5=(A4*(KRON(L,K)*KRON(I,J)) )
P6=( B11*(KRON(I,L)*BCRY(K,J)+BCRY(I,L)*KRON(J,K)) )
P7=( A21*(KRON(I,J)*BCRY(L,K)) )
P8=( A21*(KRON(L,K)*BCRY(I,J)) )
P9=( A31*(TRBAR2*KRON(L,K)*KRON(I,J)) )
P10=( A41*(KRON(L,K)*KRON(I,J)) )

Q1 = (ON-ALP)*(P1+P2+P3+P4+P5) + ALP*(P6+P7+P8+P9+P10)
Q2 = Q1

C2(K1,K2) = Q1 + Q2

DDSDDE(K1,K2) = (ON/TW)*(C1(K1,K2)+C2(K1,K2))
 END DO
END DO
DO K1 = NDI+NSHR-1, NDI+NSHR, 1
  IF (K1 .EQ. 5) THEN
    I = 1
    J = 3
  END IF
  IF (K1 .EQ. 6) THEN
    I = 2
    J = 3
  END IF
  DO K2 = 1, NDI+NSHR, 1
    IF (K2 .EQ. 1) THEN
      K = 1
      L = 1
    END IF
    IF (K2 .EQ. 2) THEN
      K = 2
      L = 2
    END IF
    IF (K2 .EQ. 3) THEN
      K = 3
      L = 3
    END IF
    IF (K2 .EQ. 4) THEN
      K = 1
      L = 2
```

```
    END IF
    IF (K2 .EQ. 5) THEN
      K = 1
      L = 3
    END IF
    IF (K2 .EQ. 6) THEN
      K = 2
      L = 3
    END IF
P1=( B1*(KRON(I,K)*BAMOR(L,J)+BAMOR(I,K)*KRON(J,L)) )
P2=(A2*(KRON(I,J)*BAMOR(K,L)) )
P3=(A2*(KRON(K,L)*BAMOR(I,J)) )
P4=(A3*(TRBAR1*KRON(K,L)*KRON(I,J)) )
P5=(A4*(KRON(K,L)*KRON(I,J)) )
P6=( B11*(KRON(I,K)*BCRY(L,J)+BCRY(I,K)*KRON(J,L)) )
P7=( A21*(KRON(I,J)*BCRY(K,L)) )
P8=( A21*(KRON(K,L)*BCRY(I,J)) )
P9=( A31*(TRBAR2*KRON(K,L)*KRON(I,J)) )
P10=( A41*(KRON(K,L)*KRON(I,J)) )

Q1 = (ON-ALP)*(P1+P2+P3+P4+P5) + ALP*(P6+P7+P8+P9+P10)
Q2 = Q1

C1(K1,K2) = Q1 + Q2

P1=( B1*(KRON(I,L)*BAMOR(K,J)+BAMOR(I,L)*KRON(J,K)) )
P2=(A2*(KRON(I,J)*BAMOR(L,K)) )
P3=(A2*(KRON(L,K)*BAMOR(I,J)) )
P4=(A3*(TRBAR1*KRON(L,K)*KRON(I,J)) )
P5=(A4*(KRON(L,K)*KRON(I,J)) )
P6=( B11*(KRON(I,L)*BCRY(K,J)+BCRY(I,L)*KRON(J,K)) )
P7=( A21*(KRON(I,J)*BCRY(L,K)) )
P8=( A21*(KRON(L,K)*BCRY(I,J)) )
P9=( A31*(TRBAR2*KRON(L,K)*KRON(I,J)) )
P10=( A41*(KRON(L,K)*KRON(I,J)) )

Q1 = (ON-ALP)*(P1+P2+P3+P4+P5) + ALP*(P6+P7+P8+P9+P10)
Q2 = Q1

C2(K1,K2) = Q1 + Q2

DDSDDE(K1,K2) = (ON/TW)*(C1(K1,K2)+C2(K1,K2))
  END DO
END DO

END IF
```

```
      RETURN
      END
C*************************************************************************
C     Necessary Kronecker Delta function is defined below
      REAL FUNCTION KRON(P,Q)
      INTEGER P, Q
      IF (P .EQ. Q) THEN
      KRON = 1
      ELSE
      KRON = 0
      END IF
      RETURN
      END
```

APPENDIX B

MATERIAL MODULE

The following module is used with user subroutines given in Appendix A. Snapshots shown below are taken from ABAQUS/CAE window.

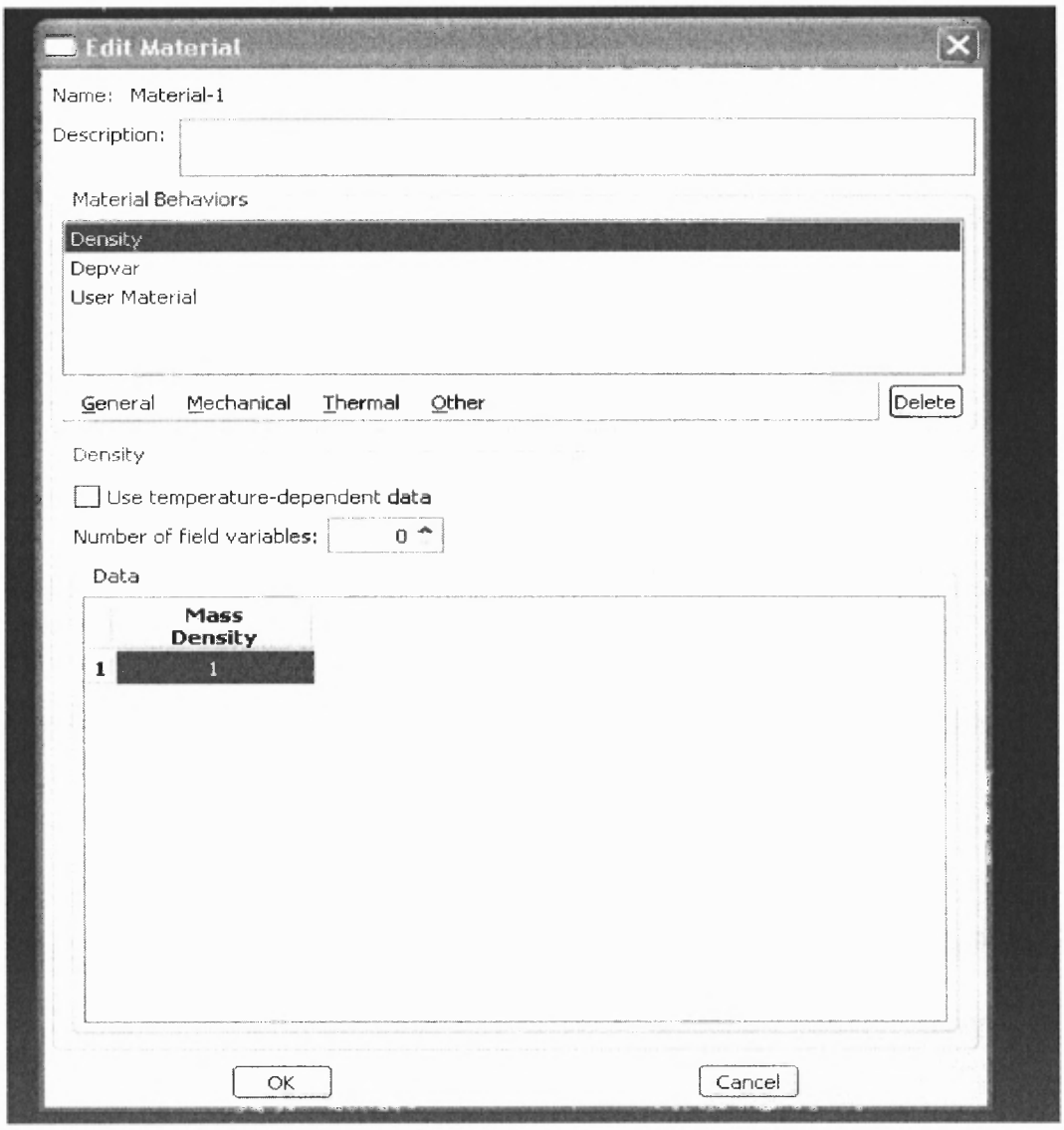

Figure B.1 Snap shots of the material module created in ABAQUS for simulating glassy shape memory polymers.

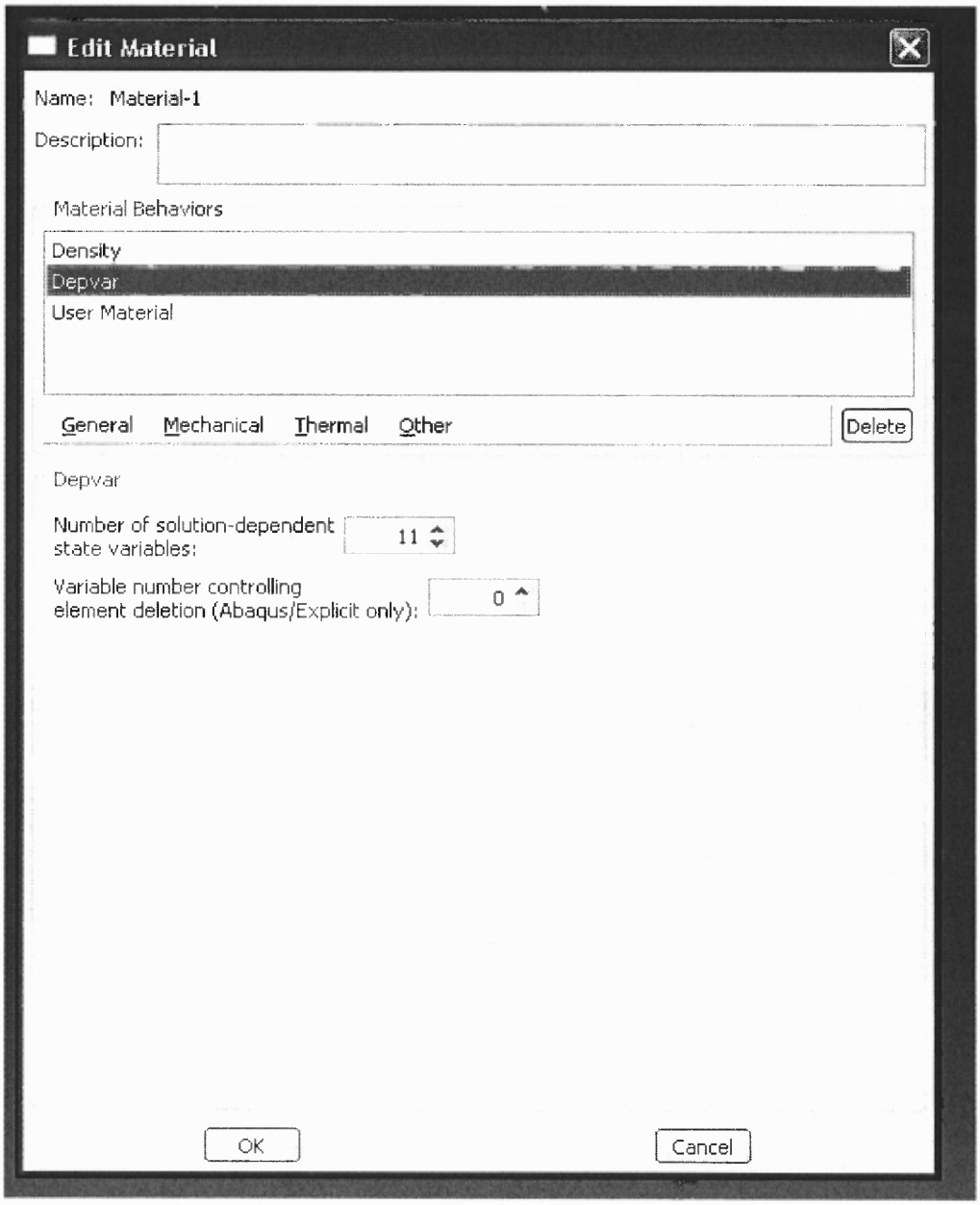

Figure B.2 Snap shots of the material module created in ABAQUS for simulating glassy shape memory polymers.

Figure B.3 Snap shots of the material module created in ABAQUS for simulating glassy shape memory polymers.

REFERENCES

1. Yiping Liu, Ken Gall, Martin Dunn, Alan Greenberg, Julie Diani, *Thermomechanics of shape memory polymers: uniaxial experiments and constitutive modeling,* International Journal of Plasticity, Volume 2, Issue 2, 2006, Pages 279-313.

2. P.C. Painter, M.M. Coleman, *Fundamentals of polymer science: an introductory text,* CRC Press, 1997.

3. N.G. McCrum, C.P Buckley and C.B Bucknall *Principles of polymer engineering,* Oxford University Press, 1997.

4. Qing-Qing Ni, Chun-sheng Zhang, Yaqin Fu, Guangze Dai, Teruo Kimura, *Shape memory effect and mechanical properties of carbon nanotube/shape memory polymer nanocomposites,* Composite Structures, Volume 81, Issue 2, 2007, Pages 174-184.

5. Gautam Barot, I.J. Rao, *Constitutive modeling and simulation of the thermo-mechanics associated with shape memory polymers,* Zeitschrift für Angewandte Mathematik und Physik (ZAMP), Volume 57, Issue 4, 2006, Pages 652-687.

6. Gautam Barot, I.J. Rao, K.R. Rajagopal, *A thermodynamic framework for the modeling of crystallizable shape memory polymers,* International Journal of Engineering Science Volume 46, Issue 4, 2008, Pages 325-351.

7. Yiping Liu, Ken Gall, Martin L. Dunn, Patrick McCluskey, *Thermomechanics of shape memory polymer nanocomposites,* Mechanics of Materials, Volume 36, Issue 10, 2004, Pages 929-940.

8. F. Li, W. Zhu, X. Zhang, C. Zhao, M. Xu, *Shape memory effect of ethylene–vinyl acetate copolymer*, Journal of Applied Polymer Science, Volume 71, Issue 7, 1999, Pages 1063-1070.

9. A. Lendlein, A.M. Schmidt, R. Langer, *AB-polymer networks based on oligo (epsilon-caprolactone) segments showing shape memory properties,* Proceedings of the National Academy of Sciences of the United States of America, Volume 98, Issue 3, 2001, Pages 842-847.

10. Ken Gall, Martin Mikulas, Naseem Munshi, Fred Beavers, *Carbon fiber reinforced shape memory polymer composites*, Journal of Intelligent Material Systems and Structures, Volume 11, Issue 11, 2000, Pages 877-886.

11. A.P. Lee, J.P. Fitch, *Micro devices using shape memory polymer patches for mated connections*, United States Patent 6,086,599, 2000,.

12. Erik Abrahamson, Mark Lake, Naseem Munshi, Ken Gall, *Shape memory mechanics of an elastic memory composite resin*, Journal of Intelligent Material Systems and Structures. Volume 14, Issue 10, 2003, Pages 623–632.

13. Annick Metcalfe, Anne-Cecile Desfaits, Igor Salazkin, L'Hocine Yahia, Witold Sokolowski, Jean Raymond, *Cold hibernated elastic memory foams for endovascular interventions*, Biomaterials, Volume 24, Issue 3, 2003, Pages 491-497.

14. Hisaaki Tobushi, Etsuko Yamada, Shunichi Hayashi, *Thermomechanical properties in a thin film of shape memory polymer of polyurethane series,* Journal of Smart Materials & Structures, Volume 5, Issue 4, 1996, Pages 483-490.

15. Hisaaki Tobushi, Takahiro Hashimoto, *Thermomechanical constitutive modeling in shape memory polymer of polyurethane series,* Journal of Intelligent Material Systems and Structures, Volume8, Issue 8, 1997, Pages 711-718.

16. Hisaaki Tobushi, Kayo Okumura, Shunichi Hayashi, *Thermomechanical constitutive model of shape memory polymer,* Journal of Mechanics of Materials, Volume 33, Issue 10, 2001, Pages 545-554.

17. Han Mo Jeong, *Shape memory polyurethane containing amorphous reversible phase,* Journal of Materials Science Volume 35, Issue 7, 2000, Pages 1579-1583.

18. Byung Kyu Kim, Sang Yup Lee, Mao Xu, *Polyurethanes having shape memory effects,* Polymer, Volume 37, Issue 26, 1996, Pages 5781-5793.

19. Byung Kyu Kim, Sang Yup Lee, Jeong Sam Lee, Sang Hyun Baek, Young Jin Choi, Jang Oo Lee, Mao Xu, *Polyurethane ionomers having shape memory effects,* Polymer, Volume 39, Issue 13, 1998, Pages 2803-2808.

20. Han Mo Jeong, Byoung Kun Ahn, Byung, *Miscibility and shape memory effect of thermoplastic polyurethane blends with phenoxy resin,* European Polymer Journal, Volume 37, Issue 11, 2001, Pages 2245-2252.

21. Seon Jeong Kim, Han Kim, Sang Jun Park, Sun Kim, *Shape change characteristics of polymer hydrogel based on polyacrylic acid/poly(vinyl sulfonic acid) in electric fields Sensors and Actuators,* A: Physical, Volume 115, Issue 1, 2004, Pages 146-150.

22. Andreas Lendlein, Robert Langer, *Biodegradable, elastic shape-memory polymers for potential biomedical applications,* Science 31, Volume 296, Issue 5573, 2002, Pages 1673-1676.

23. K.R. Rajagopal, A.R. Srinivasa, *Mechanics of the inelastic behavior of materials-part 1, theoretical underpinnings,* International Journal of Plasticity, Volume 14, Issues 10-11, 1998, Pages 945-967.

24. K.R. Rajagopal, A.R. Srinivasa, *Mechanics of the inelastic behavior of materials-part 1, inelastic response,* International Journal of Plasticity, Volume 14, Issues 10-11, 1998, Pages 965-995.

25. K.R. Rajagopal, *On a class of elastodynamic motions in a neo-hookean elastic solid,* International Journal of Non-Linear Mechanics, Volume 33, Issue 3, 1998, Pages 397-405.

26. K.R. Rajagopal, A.R. Srinivasa, *Inelastic behavior of materials. Part II. energetics associated with discontinuous deformation twinning,* International Journal of Plasticity, Volume 13, Issues 1-2, 1997, Pages 1-35.

27. K.R. Rajagopal, A.R. Srinivasa, *On the inelastic behavior of solids-Part 1: twinning,* International Journal of Plasticity, Volume 11, Issue 6, 1995, Pages 653-678.

28. K.R. Rajagopal, A.S. Wineman, *A constitutive equation for nonlinear solids which undergo deformation induced microstructural changes,* International Journal of Plasticity, Volume 8, Issue 4, 1992, Pages 385-395.

29. I.J. Rao, K.R. Rajagopal, *A thermodynamic framework for the study of crystallization in polymers,* Zeitschrift für Angewandte Mathematik und Physik (ZAMP), Volume 53, Issue 3, 2002, Pages 365-406.

30. K.R. Rajagopal, A.R. Srinivasa, *A thermodynamic framework for rate type fluid models*, Journal of Non-Newtonian Fluid Mechanics, Volume 88, Issue 3, 2000, Pages 207-227.

31. Ken Gall, Martin Dunn, Yiping Liu, Dudley Finch, Mark Lake and Naseem Munshi, *Shape memory polymer nanocomposites,* Acta Materialia, Volume 50, Issue 20, 2002, Pages 5115-5126.

32. Ken Gall, Christopher M. Yakacki , Yiping Liu , Robin Shandas , Nick Willett , Kristi Anseth, *Thermomechanics of the shape memory effect in polymers for biomedical applications,* Journal of Biomedical Materials Research Part A, Volume 73A, Issue 3 , 2005, Pages 339-348.

33. Takeru Ohki, Qing-Qing Ni, Norihito Ohsako, Masaharu Iwamoto, *Mechanical and shape memory behavior of composites with shape memory polymer,* Composites Part A: Applied Science and Manufacturing, Volume 35, Issue 9, 2004, Pages 1065-1073.

34. Marc Behl, Andreas Lendlein, *Shape memory polymers,* Materials Today, Volume 10, Issue 4, 2007, Pages 20-28.

35. S. Bhattacharya, K. Shinotani, C.P. Wong, R. Tummala, *Liquid crystal polymers (LCP) for high performance SOP applications,* Advanced Packaging Materials, 2002, Pages 249-253.

36. Eellen M. Arruda, Mary C. Boyce, *A three-dimensional constitutive model for the large stretch behavior of rubber elastic materials,* Journal of the Mechanics and Physics of Solids, vol. 41, issue 2, 1993, Pages 389-412.

37. O.A. Hasan, *A constitutive model for the nonlinear viscoelastic viscoplastic behavior of glassy polymers,* Polymer Engineering & Science Volume 35, Issue 4, 2004, Pages 331-344.

38. Ellen Arruda, Mary Boyce *Effects of strain rate, temperature and thermomechanical coupling on the finite strain deformation of glassy polymers,* Mechanics of Materials Volume 19, Issues 2-3, 1995, Pages 193-212.

39. Mary Boyce, *Constitutive model for the finite deformation stress-strain behavior of poly(ethylene terephthalate) above the glass transition* Polymer, Volume 41, Issue 6, 2000, Pages 2183-2201.

40. J.S. Bergstrom, S.M. Kurtz, C.M. Rimnac, A.A. Edidin, *Constitutive modeling of ultra-high molecular weight polyethylene under large deformation and cyclic loading conditions,* Biomaterials, Volume 23, Issue 11, 2002, Pages 2329-2343.

41. Ellen Arruda, Mary Boyce, Quintus Bosz, *Effects of initial anisotropy on the finite strain deformation behavior of glassy polymers,* International Journal of Plasticity, Volume 9, Issue 7, 1993, Pages 783-811.

42. J.S. Bergstrom, M.C. Boyce, *Constitutive modeling of the large strain time dependent behavior of elastomers,* Journal of the Mechanics and Physics of Solids, Volume 46, Issue 5, 1998, Pages 931-954.

43. Rebecca Dupaix, Mary Boyce, *Constitutive modeling of the finite strain behavior of amorphous polymers in and above the glass transition,* Mechanics of Materials Volume 39, Issue 1, 2007, Pages 39-52.

44. C. Liu, H. Qin, P.T. Mather, *Review of progress in shape-memory polymers,* Journal of Materials Chemistry, Volume 17, 2007, Pages 1543-1558.

45. C. Liang, C.A. Rogers, *One-dimensional thermomechanical constitutive relations for shape memory materials,* Journal of Intelligent Material Systems and Structures, Volume 1, Issue 2, 1990, Pages 207-234.

46. L.C. Brinson, *One-dimensional constitutive behavior of shape memory alloys: thermomechanical derivation with non-constant material functions and redefined martensite internal variable,* Journal of Intelligent Material Systems and Structures, Volume 4, Issue 2, 1993, Pages 229-242.

47. K. Tanaka, *Thermomechanical sketch of shape memory effect: one-dimensional tensile behavior,* Res Mech. Volume 18, Issue3, 1986, Pages 251-263.

48. Q.P. Sun, K.C. Hwang, *Micromechanics modelling for the constitutive behavior of polycrystalline shape memory alloys. I: derivation of general relations,* Journal of the Mechanics and Physics of Solids, Volume 41, Issue1, 1993, Pages 1-17.

49. L.C. Brinson, R. Lammering, *Finite element analysis of the behavior of shape memory alloys and their applications,* International Journal of Solids and Structures, Volume 30, Issue 23, 1993, Pages 3261-3280.

50. E.J. Graesser, F.A. Cozzarelli, *A proposed three-dimensional constitutive model for shape memory alloys,* Journal of Intelligent Material Systems and Structures, Volume 5, Issue 1, 1994, Pages 78-89.

51. Yefim Ivshin, Thomas Pence, *A thermomechanical model for a one variant shape memory material,* Journal of Intelligent Material Systems and Structures, Volume 5, Issue 4, 1994, Pages 455-473.

52. Dirk Helm, Peter Haupt, *Shape memory behaviour: modelling within continuum thermomechanics,* International Journal of Solids and Structures, Volume 40, Issue 4, 2003, Pages 827-849 .

53. Rohan Abeyaratne, Kim Sang-Joo, James Knowles, *A one-dimensional continuum model for shape-memory alloys,* International Journal of Solids and Structures Volume 31, Issue 16, 1994, Pages 2229-2249.

54. John Shaw, *A thermomechanical model for a one-dimensional shape memory alloy wire with propagating instabilities*, International Journal of Solids and Structures, Volume 39, Issue 5, 2002, Pages 1275-1305.

55. Sanjay Govindjee, Garret Hall, *A computational model for shape memory alloys,* International Journal of Solids and Structures, Volume 37, Issue 5, 2000, Pages 735-760.

56. Stefan Seleke, *Modeling the dynamic behavior of shape memory alloys,* International Journal of Non-Linear Mechanics, Volume 37, Issue 8, 2002, Pages 1363-1374.

57. Harsha Prahlad, Inderjit Chopra, *Comparative evaluation of shape memory alloy constitutive models with experimental data,* Journal of Intelligent Material Systems and Structures, Volume 12, Issue 6, 2001, Pages 383-395.

58. E. Patoor E, A. Eberhardt, M. Berveiller, *Micromechanical modelling of the shape memory behavior,* Mechanics of Phase Transformations and Shape Memory Alloys, Chicago, Illinois, USA, Volume 6, Issue 11, 1994, Pages 23-38.

59. F. Auricchio, E. Sacco, *A one-dimensional model for superelastic shape memory alloys with different elastic properties between austenite and martensite,* International Journal of Non Linear Mechanics, Volume 32, Issue 6, 1997, Pages 1101-1114.

60. Ireana Pawłow, *Three-dimensional model of thermomechanical evolution of shape memory materials,* Control and Cybernetics, Volume 29, Issue 1, 2000 Pages 341-365.

61. Z.M. Chen, K.H. Hoffman, *On a one-dimensional nonlinear thermoviscoelastic model for structural phase transitions in shape memory alloys,* Journal of Differential Equations, Volume 112, Issue 2, 1994, Pages 325-350.

62. J.G. Boyd, D.C. Lagoudas, *A constitutive model for simultaneous transformation and reorientation in shape memory materials,* Mechanics of Phase Transformations and Shape Memory Alloys, Volume 6, Issue 11, 1994, Pages 159-177.

63. D.J. Barrett, *A one-dimensional constitutive model for shape memory alloys,* Journal of Intelligent Material Systems and Structures, Volume 6, Issue 3, 1995, Pages 329-337.

64. Ferdinando Auricchio, Elio Sacco, *Thermomechanical modelling of a superelastic shape memory wire under cyclic stretching–bending loadings,* International Journal of Solids and Structures, Volume 38, Issues 34-35, August 2001, Pages 6123-6145.

65. Alberto Paiva, Marcelo Amorim Savi, Arthur Martins Barbosa Braga, Pedro Manuel Calas Lopes Pacheco, *A constitutive model for shape memory alloys considering tensile–compressive asymmetry and plasticity,* International Journal of Solids and Structures, Volume 42, Issues 11-12, 2005, Pages 3439-3457.

66. Muhammad Qidwai, Pavlin Entchev, *Modeling of the thermomechanical behavior of porous shape memory alloys,* International Journal of Solids and Structures, Volume 38, Issues 48-49, 2001, Pages 8653-8671.

67. V. Kafka, *Shape memory: a concept of explanation and of mathematical modelling,* Journal of Intelligent Material Systems and Structures, Volume 5, Issue 6, 1994, Pages 809-814.

68. Takeru Ohki, Qing-Qing Ni, Norihito Ohsak, Masaharu Iwamoto, *Mechanical and shape memory behavior of composites with shape memory polymer*, Composites Part A: Applied Science and Manufacturing, Volume 35, Issue 9, 2004, Pages 1065-1073.

69. Bo Sun Lee, Byoung Chul Chun, *Structure and thermomechanical properties of polyurethane block copolymers with shape memory effect macromolecules*, American Chemical Society, Volume 34, Issue 18, 2001, Pages 6431-6437.

70. S. Conti, M. Lenz, M. Rumpf, *Modeling and simulation of magnetic shape memory polymer composites,* Journal of the Mechanics and Physics of Solids, Volume 55, Issue 7, 2007, Pages 1462-1486.

71. Diego Mantovani, *Shape memory alloys: properties and biomedical applications,* Journal of the Minerals, Metals and Materials Society, Volume 52, Issue 10, 2000, Pages 6431-6437.

72. F. El-Feninat, G. Laroche, M. Fiset, D. Mantovani, *Shape memory materials for biomedical applications,* Advanced Engineering Materials, Volume 4, Issue 3, 2002, Pages 91-104.

73. Ken Gall, Christopher Yakacki, Yiping Liu, Robin Shandas, Nick Willett, Kristi Anseth, *Thermomechanics of the shape memory effect in polymers for biomedical applications,* Journal of Biomedical Materials Research Part A, Volume 73A, Issue 3, 2005, Pages 339-348.

74. Ken Gall, *Shape memory polymers for micro-electromechanical systems,* Journal of Micro-electromechanical Systems, Volume 13, Issue 3, 2004, Pages 472- 483.

75. Debdatta Ratna, J. Karger-Kocsis, *Recent advances in shape memory polymers and composites: a review*, Journal of Material Science, Volume 43, Issue 1, 2008, Pages 254-269.

76. Ken Gall, Martin Dunn, Yiping Liu, Goran Stefanic, Davor Balzar, *Internal stress storage in shape memory polymer nanocomposites,* Applied Physics Letters. Volume 85, Issue 2, 2004, Pages 1-3.